



Norwegian University of
Science and Technology

Piloted Protection Solutions For Distribution Networks With Integrated Distributed Energy Resources

Syed Hamza Hasan Kazmi

Wind Energy

Submission date: August 2017

Supervisor: Hans Kristian Høidalen, IEL

Co-supervisor: Marjan Popov, TU Delft
Jianping Wang, ABB Corporate Research

Norwegian University of Science and Technology
Department of Electric Power Engineering



PILOTED PROTECTION SOLUTIONS FOR DISTRIBUTION NETWORKS WITH INTEGRATED DISTRIBUTED ENERGY RESOURCES

Author: **Syed Hamza Hasan Kazmi**



MSc. Thesis report published in partial fulfillment of the requirements for the degree of
MSc. Electrical Engineering at Delft University of Technology
MSc. Technology in Wind Energy at Norwegian University of Science & Technology
under the European Wind Energy Master program.

The thesis is to be publicly defended on
25th August 2017 at NTNU, Trondheim

Supervisors

Dr. ir. Marjan Popov	(TU Delft)
Dr. Hans Kristian Høidalen	(NTNU)
Dr. Jianping Wang	(ABB – SECRC)
Dr. Youyi Li	(ABB – SECRC)



This page has been left blank intentionally.

Preface

This MSc. thesis report has been published by Syed Hamza Hasan Kazmi in partial fulfillment of the requirements for the degrees of:

- MSc. Electrical Engineering at Delft University of Technology
- MSc. Technology in Wind Energy at Norwegian University of Science & Technology

The author is a participant of European Wind Energy Master (EWEM) program with specialization in the Electrical Power Systems (EPS) track for the cohort 2015-17.

The master thesis is written at ABB Corporate Research Centre in Sweden (ABB SECRC) with the collaboration of NTNU and TU Delft. The daily supervision for the thesis is performed by the company supervisors:

- Dr. Jianping Wang (Senior Principal Scientist at ABB SECRC)
- Dr. Youyi Li (Senior Scientist at ABB SECRC)

Whereas, the academic supervision has been performed by:

- Dr. ir. Marjan Popov – TU Delft (Assoc. Prof. EEMCS Dept. – ESE IEPG research group)
- Dr. Hans Kristian Høidalen – NTNU (Prof. at EPE Department – Faculty of ITEE)

Besides the four supervisor, the thesis committee also includes Dr. Murari Mohan Saha (Assoc. Professor at the department of EPE at NTNU).

The thesis is to be publicly defended on 25th August 2017 at NTNU Gløshaugen Campus, Trondheim.

Abstract

The wide scale integration of distributed energy resources (DERs) in the distribution networks (LV/MV) over the last few decades has resulted in new challenges for the protection system. This thesis work explores the possibility to overcome challenges associated with overcurrent protection schemes, which are conventionally employed for distribution networks, by utilizing communication-based protection techniques, which are widely used in protection of HV transmission network. These techniques include piloted directional protection techniques based on conventional methods and transient signals. Moreover, current-based line differential protection is also investigated.

The individual algorithms for all these protection schemes used by relay manufacturers (including ABB, Siemens and SEL) are developed and tested. The test network, system parameters and performance criteria are developed in the PSCAD/EMTDC environment, whereas the individual algorithms are developed in MATLAB/Simulink. The system and performance parameters are carefully designed to reciprocate the performance of the modern distribution networks with weak sources replicating the performance of DERs during faults. Up to this point, the fault clearing time has not been critical for these networks but the integration of DERs has resulted in the additional requirement to fulfill the critical clearing time of each generator, therefore relay operating time is also considered in this study. However, the impacts of some real world imperfections including harmonics, measurement inaccuracies, communication noise and data loss etc. are ignored.

Different relay manufacturers propose using sequence components for different fault types. A directional algorithm combining the principles of all the conventional techniques based on different symmetrical components has been developed and tested. This algorithm responds to both the balanced and unbalanced faults, while overcoming the limitations of each individual technique. The test cases incorporate the weak network conditions in order to see the dependability of the protection functions.

The operating principles of investigated transient-based directional algorithms are fundamentally different. Therefore, each method is extensively tested and the results are compared. These techniques, also called ultra-high-speed directional methods, claim to fulfill the minimum operating time requirements without compromising the security or dependability of operation. Moreover, some less-explored but highly effective algorithms are also tested, which would be ideal in this case including current-only transient-based directional algorithms.

Line differential schemes based on dual slope current or charge comparison techniques are vulnerable to capacitive currents and saturation of CTs but their performance is ideal for weak networks, due to its selectivity as a unit protection. These schemes are included in the study to compare the performance with directional-based pilot protection schemes. The assessment is performed in both the current plane (operating and restraint current) and the polar plane for comparison.

Each of the tested algorithms has some inherent shortcomings. The ultimate goal is to identify these restrictions and suggest methods either to overcome them or to make relevant modifications. The communication-based limitations are investigated for each of the tested algorithm to assess the practicality of application, while the economic impacts of additional hardware to determine fault direction in the distribution network are also considered.

The above substantial assessment of all the piloted protection schemes to determine their feasibility for the protection of modern distribution networks has not been performed previously, which puts a rather unique perspective to this study.

Acknowledgements

First and foremost, to Dr. Jianping Wang for his mesmerizing supervision and to Dr. Youyi Li for his inspirational guidance, I am highly grateful to both of you.

To my academic supervisors Prof. Hans Kristian Høidalen at NTNU and Prof. Marjan Popov at TU Delft, this project could not have reached its final form without your efforts. I highly appreciate the valuable inputs and the critical feedback that both of you provided whenever I required. A big thank you to Dr. Murari Mohan Saha for his candid critical insights during our limited interaction.

Despite having multiple supervisors, the doors to each of their offices were always open whenever I ran into trouble. I was consistently motivated by Jianping to seek continuous inspirations, which allowed this report to be the true reflection of my own work. Thank you for steering me in the right direction whenever needed.

A very special gratitude goes out to everyone down at Corporate Research Centre at ABB: my managers Robert Saers, Linus Thrybom and Gargi Bag for initiating and approving this project. Monica Koerfer for her cheerfulness and the logistic support. Omer bhai, Saad bhai, Arif and Zulqarnain for the brotherly support during my period in Vasteras.

I would also like to mention my colleagues who accompanied me in this exciting journey of 2 years and 4 countries: Usman, Biran, Donny, Miguel, Ishwari, Amaia and Ryan.

Last but not the least, the most important people in my life: My parents, my sisters and my one true love. I could not have made it so far without the inspiration and pride of my father, without the prayers and never-ending care of my mother, without the love and tease of my sisters, and finally without my beautiful wife who always supported me, who trusted in my abilities more than I ever did and who loved me unconditionally despite the distance. I owe this to all of you.

I would also like to extend thanks to the Institute of Electrical and Electronics Engineers (IEEE) and International Electro technical Commission (IEC) for permitting to reproduce the relevant information from their database and the relevant international protection standards including IEC 61850. The information is the copyright of the respective owners and they are not responsible for the accuracy of the results of this publication.

Syed Hamza Hasan Kazmi

25 – Aug - 2017

Table of Contents

NOMENCLATURE.....	X
Table of Figures.....	XI
Chapter 1 - Introduction	1
1.1 Background	1
1.2 Overview of Transmission and Distribution line Protection schemes:	2
1.2.1 Non-Piloted Schemes:	3
1.2.2 Piloted Schemes:.....	4
1.3 Scope of Work and Research Objectives	7
1.4 Scientific Approach and Thesis Outline.....	8
Chapter 2 - Protection of Distribution Networks with DERs	10
2.1 LV Distribution Networks:.....	11
2.2 - MV Distribution Networks	12
2.3 Protection of DER infested Distribution Networks.....	13
2.4 Communication-based Protection	15
2.5 Directional Protection and Distributed Generation	16
Chapter 3 - Conventional Directional Element and Design	17
Principle of Operation	17
3.1 Phase Directional Element:	18
3.1.1 Cross Phase Quadrature Directional Element	18
3.1.2 Positive Sequence Directional Element.....	19
3.1.3 Negative Sequence Directional Element	20
3.2 - Ground Directional Element:	24
3.2.1 - Zero Sequence Directional Element.....	24
3.3 Practical Directional Element based on Preferred Order	25
Chapter 4 - High Speed Distance Protection and Directional Comparison based on Superimposed/Delta Quantities and Traveling Waves	26

4.1 Background	26
4.1.1 Operating Principle of the proposed scheme:	26
4.1.2 Brief History:	26
4.1.3 Superimposed Components / Delta Quantities:	27
4.2 Theoretical Analysis:	27
4.3 Steps of Operation	28
4.3.1 Detection of Fault	28
4.3.2 Loop Selection	29
4.3.3 Directional Element	30
4.3.4 Fault Location / Distance Element	31
4.4 Problems with superimposed/TWs based methods	34
4.5 Solution to these problems	34
Chapter 5 - Superimposed/Delta Quantities based Directional Protection	35
5.1 UHS Directional protection based on Transient Energy	35
5.1.1 - Salient Features and Limitations	36
5.2 - UHS Relay based on Replica Impedance	37
5.2.1 Salient Features and Limitations of Delta-Plane and tranjectory recognition	38
5.3 Compensated Current (MIMIC Filter) Approach	39
Salient Features and Limitations:	41
5.4 Positive Sequence Transient Impedance Method	42
5.4.1 Salient Features and Limitations:	44
5.5 Average of Superimposed Quantities:	45
5.5.1 Salient Features and Limitations:	45
Chapter 6 - Current-only Transient-based Directional Protection	47
6.1 Theoretical Analysis:	48
6.1.1 Internal Fault (F)	48
6.1.2 External Fault (F')	49

6.1.3 Reversal of Pre-fault Current Direction:	50
6.2 Relevant current-only directional algorithms:.....	51
6.2.1 Delta Phase Angle of post-fault and pre-fault currents:	52
6.2.2 Delta Phase Angle ($\Delta\theta$) comparison of Local and Remote Ends:	53
6.2.3 Post-fault current based method	55
Chapter 7 - Differential Line Protection	57
7.1 Salient Features of Line Differential Protection:	57
7.2 Operating Principle:	57
7.2.1 Operating and Restraining Quantities:	58
7.2.2 Operating and Restraining Range (For a Dual Slope Differential Relay)	59
7.3 Historical Development of Line Differential Relays:	59
7.4 Limitation of Conventional Line Differential Protection:.....	60
7.4.1 High Resistance Fault on the line:	61
7.4.2 Capacitive charging currents:	61
7.5 DATA Communication in Line Differential Protection	62
7.5.1 Communication Architecture:	62
7.5.2 Communication Delay Correction / Data Synchronization:	63
7.5.3 Communication Channels.....	64
7.6 Alternate Approaches for Line Differential Protection:.....	65
7.6.1 Polar Plane Approach for Phasor Comparison (SEL)	65
7.6.2 Phaselet & Variable Window Fourier Transform Approach by GE (1998):.....	68
Chapter 8 - Identification of Practical Constraints for Communication-based Protection and Tested Relays	71
8.1 Data Handling and Management.....	71
8.1.1 Protection constraints	72
8.1.2 Communication constraints	72
8.2 Data Synchronization	73

8.2.2 Data Synchronization using External Time Reference.....	75
8.3 Communication Channels and Multi-terminal Application:	76
8.4 Miscellaneous Issues:	77
Chapter 9 - Test System, Performance Parameters and Fundamental Blocks	78
9.1 Test Model.....	78
9.2 Performance Parameters:.....	79
9.3 Fundamental Blocks	81
9.3.1 Signal Processing and Filtering	82
9.3.2 Analog to Digital Conversion (ADC – Sampling Block).....	84
9.3.3 Discrete Fourier Transform Block.....	85
9.3.4 Sequence Component Extraction.....	86
Chapter 10 - Conventional Directional Protection Model and Performance Evaluation	87
10.1 Comprehensive Model	87
10.2 Test Results	88
10.2.1 Unbalanced Faults	88
10.2.2 Balanced Faults.....	90
10.2.3 Extensive Test Results.....	91
Chapter 11 - Transient-based Directional Protection Models and Performance Evaluation .	94
11.1 Fundamental Blocks.....	95
11.1.1 Delta Filter.....	95
11.1.2 Fault Detection Block.....	96
11.2 Directional Element.....	98
11.2.1 Energy-based Algorithm (ASEA-RALDA)	99
11.2.2 Replica Impedance and Compensated Current Model (SEL & Siemens).....	101
11.2.3 Positive Sequence Transient Impedance (ΔZ_1) Model	104
11.2.4 Average of Superimposed Quantities (sliding window method).....	106
11.2.5 Current-only Directional Algorithms	110

Chapter 12 - Line Differential Protection Models and Verification	115
12.1 PSCAD/EMTDC Model	115
12.1.1 Signal Processing & Communication.....	116
12.1.2 Differential and Inrush Restraint Blocks	118
12.2 Relay Settings.....	119
12.3 Test Results and Discussion.....	120
12.4 Polar Plane Analysis and Discussion	122
Chapter 13 – Discussion and Performance Comparison of Pilot Protection Schemes (Line Differential, Conventional and Transient-based Directional Protection)	126
13.1 Practicality of implementation (Current and Voltage information).....	126
13.2 Communication Channel:.....	126
13.3 Data Management and Synchronization:	127
13.4 Data Transmission Delay:	127
13.5 Parallel and Double Circuit Lines:	127
13.6 Series Compensated Lines:	128
13.7 High Impedance Faults:	128
13.8 Charging Current and Phase Shift Correction:.....	128
13.9 Saturation of Current Transformers:	128
13.10 Impact of Source Strength (DG integration) and fault locations:	129
13.11 Impacts of System Grounding:.....	129
Conclusive Remarks.....	130
Future Work.....	131
References.....	132
APPENDIX A.....	136
APPENDIX B.....	137
APPENDIX C.....	139

NOMENCLATURE

UHSD	Ultra High Speed Distance
OHL	Over Head Line
TWs	Traveling Waves
BBC	Brown Boveri & Company
ABB	Asea Brown Boveri
SEL	Schweitzer Engineering Laboratories
DERs	Distributed Energy Resources
DNs	Distribution Networks
CB	Circuit Breaker
WPP	Wind Power Plant
PSCAD	Power System Computer Aided Design
EMTDC	Electro Magnetic Transient Design and Control
WT	Wind Turbine
WAM	Wide Area Monitoring
WAP	Wide Area Protection
PMU	Phasor Monitoring Units
MTA	Maximum Torque Angle
CT	Current Transformer
VT	Voltage Transformer
OC	Over Current
PSFC	Positive Sequence Fault Component
SONET	Synchronous Optical Networking
SDH	Synchronous Digital Hierarchy
GPS	Global Positioning System
ZOH	Zero Order Hold
CCT	Critical Clearing Time (Fault)
OC	Over Current

TABLE OF FIGURES

FIGURE 1.1 CLASSIFICATION OF LINE PROTECTION SCHEMES	3
FIGURE 1.2 METHODOLOGY OF PILOTED PROTECTION SCHEME.....	4
FIGURE 1.3 ZONES FOR DISTANCE PROTECTION SCHEMES	5
FIGURE 2.1 CONTRIBUTION OF RENEWABLES IN ENERGY GENERATION [51]	10
FIGURE 2.2 TYPICAL LAYOUT OF AL MICROGRID	12
FIGURE 2.3 EXAMPLE OF FALSE TRIPPING.....	13
FIGURE 2.4 EXAMPLE OF PROTECTION BLINDING	13
FIGURE 2.5 EXAMPLE OF WIDE AREA PROTECTION	14
FIGURE 2.6 COMMUNICATION-BASED DIRECTIONAL PROTECTION	15
FIGURE 3.1 CONVENTIONAL DIRECTIONAL PROTECTION (OPERATING PRINCIPLE)	18
FIGURE 3.2 NEGATIVE SEQUENCE QUANTITIES FOR FORWARD FAULTS UNDER NO-LOAD CONDITION	21
FIGURE 3.3 SEQUENCE DIAGRAM FOR PHASE-GROUND FAULT.....	22
FIGURE 3.4 SETTINGS FOR NEGATIVE SEQ. IMPEDANCE DIRECTIONAL ELEMENT	23
FIGURE 3.5 SETTINGS FOR NEG. SEQUENCE IMPEDANCE RELAY.	23
FIGURE 4.1. SCHEMATIC REPRESENTATION OF ELECTRICAL CIRCUIT STRUCTURE CHANGE AFTER FAULT.....	27
FIGURE 4.2. SCHEMATIC REPRESENTATION OF AN ELECTRICAL CIRCUIT IN THE FORM OF PRE AND POST-FAULT ..	28
FIGURE 4.3. ELECTRICAL QUANTITIES DURING FAULT EVENT:	29
FIGURE 4.4 VOLTAGE CRITERION FOR PHASE SELECTION.....	30
FIGURE 4.5 POST-FAULT CIRCUIT (INTERNAL FAULT)	30
FIGURE 4.6 POST-FAULT CIRCUIT (EXTERNAL FAULT).....	31
FIGURE 4.7 INTERNAL FAULT CONDITION	32
FIGURE 4.8 SUPERPOSITION PRINCIPLE: PRE-FAULT CIRCUIT (LEFT) POST-FAULT CIRCUIT (RIGHT).....	32
FIGURE 4.9 PHASOR REPRESENTATION OF VOLTAGES (LOCAL, REMOTE, FAULT POINT & RELAY REACH POINT)...	33
FIGURE 5.1 PRINCIPLE OF REPLICA IMPEDANCE COMPARISON (INTERNAL FAULT - LEFT)	37
FIGURE 5.2 TRAJECTORY OF COMPENSATED DELTA CURRENT ON THE DELTA PLANE.....	37
FIGURE 5.3 STABILIZATION INTEGRAL DESCRIPTION.....	39
FIGURE 5.4 STABILIZATION INTEGRAL RESPONSE	39
FIGURE 5.5 BLOCK DIAGRAM FOR COMPENSATED CURRENT APPROACH IN THE TIME DOMAIN (SEL) [30].....	41
FIGURE 5.6 BLOCK DIAGRAM OF COMPENSATED CURRENT APPROACH IN FREQUENCY DOMAIN.....	42
FIGURE 5.7 POSITIVE SEQ. PREFault CIRCUIT (SUPERPOSITION PRINCIPLE)	43
FIGURE 5.8 POSITIVE SEQ. PURE-FAULT CIRCUIT (LEFT: INTERNAL FAULT) (RIGHT: EXTERNAL FAULT).....	43
FIGURE 5.9 FORWARD AND REVERSE FAULT OPERATING REGIONS FOR POSITIVE SEQ. APPROACH	43
FIGURE 5.10 SYSTEMIC PROCESS FOR POSITIVE SEQUENCE TRANSIENT IMPEDANCE METHOD.....	44
FIGURE 5.11 FLOWCHART FOR AVERAGE WINDOW BASED TRANSIENT ENERGY DIRECTIONAL PROTECTION [21]	46
FIGURE 6.1 FORWARD AND REVERSE FAULT CONDITION IN A BIDIRECTIONAL FEEDER	47
FIGURE 6.2 PHASE CHANGE OF CURRENT DURING FORWARD (F2) AND REVERSE FAULT (F1) BUS M.....	47
FIGURE 6.3 PHYSICAL SETUP OF THE CURRENT-ONLY DIRECTIONAL PROTECTION.....	48
FIGURE 6.4 APPLICATION OF SUPERPOSITION PRINCIPLE FOR INTERNAL FAULT CONDITION	48
FIGURE 6.5 VARIATION IN CURRENT PHASOR FOR LOCAL (1) AND REMOTE (2) ENDS DURING INTERNAL FAULT ...	49

FIGURE 6.6 APPLICATION OF SUPERPOSITION PRINCIPLE FOR EXTERNAL FAULT CONDITION	49
FIGURE 6.7 VARIATION IN CURRENT PHASOR FOR LOCAL (1) AND REMOTE (2) ENDS DURING EXTERNAL FAULT ..	50
FIGURE 6.8 VARIATION IN CURRENT PHASE FOR LOCAL (1) AND REMOTE (2)	51
FIGURE 6.9 CURRENT-ONLY DIRECTIONAL PROTECTION ALGORITHM [54-56]	53
FIGURE 6.10 SYSTEM DESCRIPTION OF DELTA-PHASE-ANGLE COMPARISON METHOD FOR CURRENT-ONLY N.....	54
FIGURE 6.11 FLOWCHART FOR CURRENT-ONLY METHOD UNDER DISCUSSION [61]	54
FIGURE 6.12 OPERATING REGIONS FOR FORWARD AND REVERSE FAULTS [57]	55
FIGURE 6.13 FLOWCHART FOR POST-FAULT CURRENT BASED DIRECTIONAL PROTECTION	56
FIGURE 7.1 SIMPLE REPRESENTATION OF DIFFERENTIAL PROTECTION	58
FIGURE 7.2 COMPARISON OF LOCAL AND REMOTE CURRENTS (LEFT: EXTERNAL FAULT), (RIGHT: INTERNAL	58
FIGURE 7.3 DUAL SLOPE OPERATING CHARACTERISTICS OF DIFFERENTIAL PROTECTION	59
FIGURE 7.4 INDICATION OF CAPACITIVE CHARGING CURRENT IN A MEDIUM LENGTH TRANSMISSION LINE	62
FIGURE 7.5 TWO TERMINAL MASTER-MASTER CONFIGURATION FOR LINE DIFFERENTIAL PROTECTION	63
FIGURE 7.6 MULTI TERMINAL CONFIGURATION (LEFT: MASTER-MASTER), (RIGHT: MASTER-REMOTE)	63
FIGURE 7.7 PING-PONG METHOD FOR COMMUNICATION DELAY CORRECTION	64
FIGURE 7.8 EXAMPLE OF SWITCHED MICROWAVE SYSTEMS	64
FIGURE 7.9 EXAMPLE OF DATA PACKET TRANSFERRED BETWEEN LOCAL AND REMOTE RELAYS.....	65
FIGURE 7.10 OPERATING TRAJECTORIES IN POLAR PLANE FOR DIFFERENT RESTRAIN CURRENTS	66
FIGURE 7.11 RESTRAIN AND OPERATING REGION FOR IDEAL CONDITIONS (POLAR PLANE ANALYSIS)	67
FIGURE 7.12 RESTRAIN AND OPERATING REGION FOR NON-IDEAL CONDITIONS (POLAR PLANE ANALYSIS)	67
FIGURE 7.13 PROPOSED OPERATING CHARACTERISTICS OF LINE DIFFERENTIAL PROTECTION IN POLAR PLANE ..	67
FIGURE 7.14 COMPARISON OF PROPOSED SCHEME WITH CIRCULAR RESTRAIN CHARACTERISTICS	68
FIGURE 7.15 FIXED WINDOW APPROACH (LEFT: TIME VARYING SIGNAL) (RIGHT: FIXED WINDOW INTEGRATION) ..	68
FIGURE 7.16 VARIABLE WINDOW APPROACH (LEFT: TIME VARYING SIGNAL)	69
FIGURE 7.17 DOTTED: SAMPLE SIGNAL, BOLD: RECONSTRUCTED SINE SIGNAL	69
FIGURE 7.18 POLAR PLANE ANALYSIS (LEFT: STATIC RESTRAINT SIGNAL, MIDDLE: DYNAMIC RESTRAINT SIGNAL, RIGHT: DYNAMIC ELLIPTICAL RESTRAINT SIGNAL)	70
FIGURE 8.1 OFFSET TIME DETERMINATION FOR CHANNEL-BASE DATA SYNCHRONIZATION (PROPOSED)	74
FIGURE 8.2 DATA SYNCHRONIZATION USING EXTERNAL TIME REFERENCE	75
FIGURE 8.3 MULTIPLEXED COMMUNICATION TECHNIQUE BASED ON SONET/SDH	77
FIGURE 9.1 TEST POWER SYSTEM	78
FIGURE 9.2 INTERNAL AND EXTERNAL FAULT CONDITION FOR TEST SYSTEM.....	78
FIGURE 9.3 PROPOSED PILOTTED PROTECTION SCHEME.....	82
FIGURE 9.4 SIGNAL PROCESSING SEQUENCE FOR MODERN NUMERICAL RELAYS	82
FIGURE 9.5 MAGNITUDE RESPONSE OF ANTI-ALIASING FILTER (BUTTERWORTH - 2ND ORDER, FC = 1KHZ).....	83
FIGURE 9.6 OUTPUT OF SAMPLING BLOCK (TOP), OUTPUT OF DIGITAL FILTER (BOTTOM).....	83
FIGURE 9.7 PROPOSED SAMPLING BLOCK FOR PSCAD/EMTDC BASED MODELS.....	84
FIGURE 9.8 SAMPLED SIGNAL (TOP) AND SAMPLING PULSE (BOTTOM) - FS = 20 SAMPLES PER CYCLE	85
FIGURE 9.9 SYMMETRICAL COMPONENTS FOR A THREE PHASE SYSTEM	86
FIGURE 10.1 DESCRIPTION OF STEPS FOR COMBINED CONVENTIONAL DIRECTIONAL PROTECTION	87

FIGURE 10.2 L-G FAULT (FORWARD). SEQUENCE CURRENTS (TOP-LEFT), NEGATIVE SEQUENCE IMPEDANCE (BOTTOM-LEFT), POSITIVE SEQUENCE TORQUE (TOP-RIGHT), NEGATIVE AND ZERO SEQUENCE TORQUES . 88

FIGURE 10.3 L-G FAULT (REVERSE). SEQUENCE CURRENTS (TOP-LEFT), NEGATIVE SEQUENCE IMPEDANCE (BOTTOM-LEFT), POSITIVE SEQUENCE TORQUE (TOP-RIGHT), NEGATIVE AND ZERO SEQUENCE TORQUES . 89

FIGURE 10.4 L-L FAULT (FORWARD). SEQUENCE CURRENTS (TOP-LEFT), NEGATIVE SEQUENCE IMPEDANCE (BOTTOM-LEFT), POSITIVE SEQUENCE TORQUE (TOP-RIGHT), NEGATIVE AND ZERO SEQUENCE TORQUES . 89

FIGURE 10.5 L-L FAULT (REVERSE). SEQUENCE CURRENTS (TOP-LEFT), NEGATIVE SEQUENCE IMPEDANCE (BOTTOM-LEFT), POSITIVE SEQUENCE TORQUE (TOP-RIGHT), NEGATIVE AND ZERO SEQUENCE TORQUES . 90

FIGURE 10.6 L-L-L FAULT (FORWARD). SEQUENCE CURRENTS (TOP-LEFT), NEGATIVE SEQUENCE IMPEDANCE (BOTTOM-LEFT), POSITIVE SEQUENCE TORQUE (TOP-RIGHT), NEGATIVE AND ZERO SEQUENCE TORQUES . 90

FIGURE 10.7 L-L-L FAULT (REVERSE). SEQUENCE CURRENTS (TOP-LEFT), NEGATIVE SEQUENCE IMPEDANCE (BOTTOM-LEFT), POSITIVE SEQUENCE TORQUE (TOP-RIGHT), NEGATIVE AND ZERO SEQUENCE TORQUES . 91

FIGURE 11.1 SIMULINK BLOCK DIAGRAM FOR TRANSIENT-BASED DIRECTIONAL PROTECTION..... 95

FIGURE 11.2 L-G FAULT (TOP: THREE PHASE SIGNALS) (BOTTOM: THREE PHASE DELTA QUANTITIES) FAULT ... 95

FIGURE 11.3 IMPACT OF POWER SWINGS ON THREE PHASE CURRENT (TOP) AND THREE PHASE VOLTAGE 96

FIGURE 11.4 L-G FAULT WITH POWER SWINGS (TOP: THREE PHASE SIGNALS) (BOTTOM: THREE PHASE DELTA 96

FIGURE 11.5 L-G FAULT (TOP: REAL TIME CURRENT AND THRESHOLD CURRENT) (BOTTOM: DIFFERENCE BETWEEN THRESHOLD AND REAL-TIME CURRENT)..... 97

FIGURE 11.6 POWER SWINGS, NO FAULT (TOP: REAL TIME CURRENT AND THRESHOLD CURRENT) (BOTTOM: DIFFERENCE BETWEEN THRESHOLD AND REAL-TIME CURRENT) 98

FIGURE 11.7 POWER SWINGS, L-G FAULT (TOP: REAL TIME CURRENT AND THRESHOLD CURRENT) (BOTTOM: DIFFERENCE BETWEEN THRESHOLD AND REAL-TIME CURRENT) 98

FIGURE 11.8 PROPOSED ALGORITHM FOR TRANSIENT ENERGY BASED METHOD 99

FIGURE 11.9 L-G FAULT (LEFT: FORWARD FAULT) (RIGHT: REVERSE FAULT)..... 100

FIGURE 11.10 OUTPUT OF DISCRETE TIME INTEGRATOR (TOP) LEFT: FORWARD FAULT , RIGHT:REV FAULT . 102

FIGURE 11.11 OUTPUT OF DISCRETE TIME INTEGRATOR DURING POWER SWINGS 103

FIGURE 11.12 PHASE ANGLE OF ΔZ_1 FOR L-G FAULT (LEFT: FORWARD FAULT) (RIGHT: REVERSE FAULT)..... 104

FIGURE 11.13 COMPARISON OF DELTA FILTER OUTPUT WITH AVERAGE INTEGRAL FILTER OUTPUT TOP: 3-PHASE QUANTITIES, 3-PHASE CONVENTIONAL DELTA FILTER OUTPUT, 3-PHASE AVERAGE INTEGRAL OUTPUT ... 107

FIGURE 11.14 COMPARISON OF DELTA FILTER OUTPUT WITH AVERAGE INTEGRAL FILTER OUTPUT (L-L-L FAULT) TOP: 3-PHASE QUANTITIES,3-PHASE CONVENTIONAL DELTA FILTER OUTPUT, AVERAGE INTEGRAL 107

FIGURE 11.15 L-G FAULT (LEFT: FORWARD FAULT, RIGHT: REVERSE FAULT) TOP: 3-PHASE VOLTAGE AVERAGE, MIDDLE: 3-PHASE CURRENT AVERAGE, BOTTOM: CR (PRODUCT OF POST-FAULT AVERAGE QTY.) 108

FIGURE 11.16 AVERAGE OF SUPERIMPOSED COMPONENTS FOR ZERO DC FAULT COMPONENT 110

FIGURE 11.17 VARIATION IN CURRENT PHASE ANGLE - FORWARD POWER FLOW W.R.T LOCAL RELAY 110

FIGURE 11.18 VARIATION IN CURRENT PHASE ANGLE - REVERSE POWERFLOW W.R.T LOCAL RELAY EVERSE ... 111

FIGURE 11.19 IMPACT OF ± 180 DEGREE LIMIT ON VARIATION OF CURRENT PHASE ANGLE - FORWARD POWERFLOW W.R.T LOCAL RELAY (LEFT: FORWARD FAULT) (RIGHT: REVERSE FAULT)..... 111

FIGURE 11.20 FORWARD POWER FLOW W.R.T LOCAL RELAY (LEFT: INTERNAL FAULT) (RIGHT: EXT FAULT).... 113

FIGURE 11.21 REVERSE POWER FLOW W.R.T LOCAL RELAY (LEFT: INTERNAL FAULT) (EXTERNAL FAULT)' 113

FIGURE 11.22 FORWARD POWER FLOW (LEFT: FORWARD FAULT) (RIGHT: REVERSE FAULT) TOP: PHASE ANGLES,
MIDDLE: PHASE ANGLE OF I_{REF} , BOTTOM: DELTA ANGLE 114

FIGURE 11.23 REVERSE POWER FLOW (LEFT: FORWARD FAULT) (RIGHT: REVERSE FAULT) TOP: PHASE ANGLES,
MIDDLE: PHASE ANGLE OF I_{REF} , BOTTOM: DELTA ANGLE 114

FIGURE 12.1 CLASSIFICATION OF BLOCKS IN PSCAD/EMTDC MODEL FOR LINE DIFFERENTIAL PROTECTION . 116

FIGURE 12.2 STEPS OF OPERATION FOR THE TESTED PSCAD/EMTDC MODEL 116

FIGURE 12.3 MECHANISM OF DATA TRANSMISSION FOR TESTED RELAYS 118

FIGURE 12.4 TESTED OPERATING CHARACTERISTICS OF ABB RED 615/670 RELAY 118

FIGURE 12.5 THREE PHASE DIFFERENTIAL AND RESTRAIN CURRENTS FOR INTERNAL FAULTS 120

FIGURE 12.6 THREE PHASE DIFFERENTIAL AND RESTRAIN CURRENTS FOR EXTERNAL FAULTS 121

FIGURE 12.7 THREE PHASE DIFFERENTIAL AND RESTRAIN CURRENTS FOR 200 OHM A-G FAULTS 121

FIGURE 12.8 NOMINAL LOAD CONDITION INCLUDING VOLTAGE BUILDUP PERIOD 123

FIGURE 12.9 EXTERNAL FAULT TRAJECTORY IN THE POLAR PLANE (LEFT: L-G FAULT, RIGHT: L-L-L FAULT) 124

FIGURE 12.10 INTERNAL FAULT TRAJECTORY IN THE POLAR PLANE (LEFT: L-G FAULT, RIGHT: L-L-L) 124

FIGURE 12.11 NOMINAL LOAD CONDITION INCLUDING VOLTAGE BUILDUP PERIOD (LEFT: FS = 0.5 KHZ, 125

Chapter 1 - Introduction

1.1 Background

Transmission and distribution systems are considered to be two essential subsystems of an electrical power system. Transmission grids supply the electric energy generated by the generation unit to the sub-transmission and distribution grids connected to the respective consumers. Since the core responsibility of the entire electrical power system is to ensure reliable supply of electricity to the consumers, the role of transmission and distribution grids is quintessential. [5-6]

Transmission and distribution lines serve as the primary mode of fulfilling the operative demands of their respective grids. These lines are most commonly found in the form of overhead lines (OHL). However, the promotion of idea to preserve the aesthetic nature of the environment in recent times and long-distance offshore energy transfer due to development of large offshore windfarms has increased the employment of underground and undersea cables. The more common method of electricity transfer includes a combination of both OHL and cables. [2-7].

The exposure of transmission and distribution lines to the environment makes them susceptible to highest fault incidence fault rates in the electrical network. These faults do not originate only due to the natural phenomena like lightning strikes, storms, breakage of OHL conductors due to icing and intrusion of vegetation, but can also arrive as a result of human negligence [26]. In order to ensure reliable operation of the entire power system and minimal equipment damage, these faults must be accurately detected, isolated and cleared within a short period. Failure to which can result in stability issues, especially in transmission grids, which can even lead to total system blackout in the worst case [19]

The protection relays installed at each end of transmission/distribution lines can generally be classified into 2 categories: piloted (communication-based) and non-piloted [1]. Communication-based protection schemes provide high-speed, reliable and simultaneous clearing of faults along the entire line [29]. According to an IEEE survey [2], directional comparison distance protection schemes, which utilized both current and voltage information, were considered to be the most widely employed communication-based transmission line protection scheme in North America until the late 1980's. This trend slowly shifted towards other methodologies including phase-comparison and conventional current-differential

schemes with the developments in the field of communication systems and hardware processing speeds [26]. Over the last two decades, the protection of high-voltage transmission lines has been performed by simultaneously using multiple relaying principles to ensure secure and reliable operation of power systems [29].

The performance of piloted protection schemes severely depends upon the execution of the communication system and the employed methodology. Current-based line differential protection or phase comparison methods, although more accurate than the distance protection, are greatly influenced by the performance of communication system such as channel asymmetry, data insecurity and latency, since these schemes require transfer of actual phasor quantities. [28]

The directional comparison scheme, which is apparently less-dependent on communication system performance, has evolved significantly since the 1980's due to development of ultra-high speed protection (UHSD) [26]. The protection of transmission and distribution lines require quick fault detection, while accurate and fast distance and direction estimation are also essential in modern relays. The principle of operation of modern directional digital relays can usually be classified into two categories [29, 23]:

- Power frequency components based methods; this method has been widely used in traditional protection practices including voltage-based, sequence current components-based, distance approximation based principles, etc.
- Transient signals-based methods utilized by UHSD protection, either based on travelling waves (TWs) or superimposed components-based methods.

1.2 Overview of Transmission and Distribution line Protection schemes:

The development of protection schemes for transmission and distribution lines began more than a hundred years ago, with voltage restrained time over current relay (1921) being one of the more prominent attempts in history. However, phase and neutral overcurrent protection, in its simplest forms, offered a significant disadvantage for line protection because its fault coverage of the protected circuit is dependent on source impedance variations [Ref E4]. Since then, the line protection schemes have faced undeterred evolution. [3-6] provides a rather simplistic classification of line protection schemes available today, which is presented in the Fig. 1.1

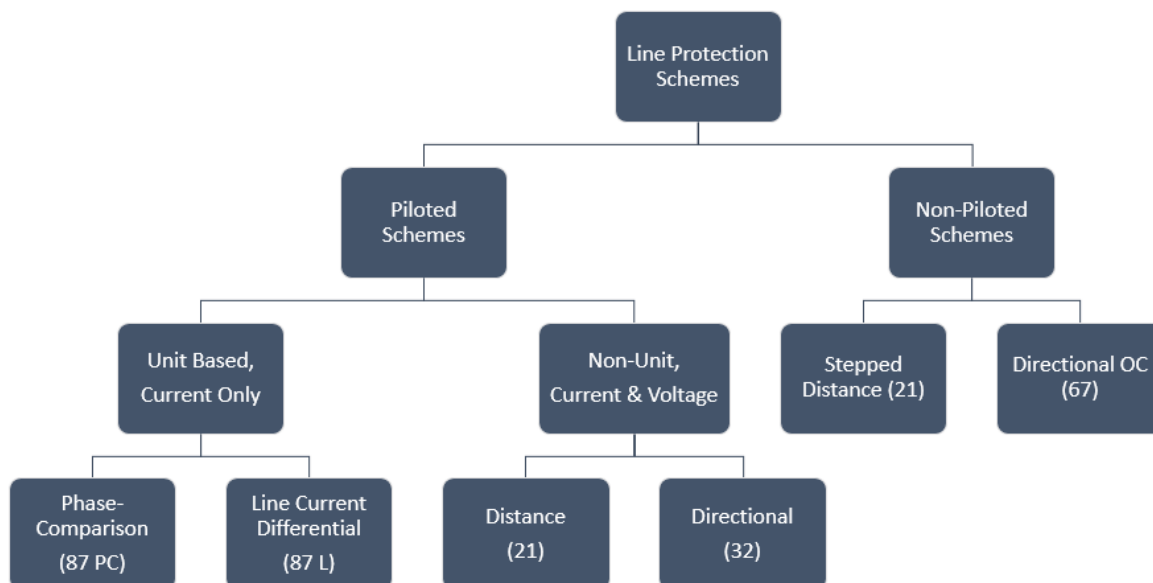


Figure 1.1 Classification of Line Protection Schemes

The protection schemes, as described in [1, 3] can essentially be classified in to two categories

- **Piloted Schemes:** The schemes which are based on communication between 2 or more relays, and the relaying decision is based on the mutual decision of these relays are referred as piloted schemes. In the most simplistic case, each end of the transmission/distribution line is equipped with a relay. Therefore, each end has one local relay that communicates with at least one remote relay.
- **Unpiloted Schemes:** These schemes do not require communication between the relays on each end of the protected line and the relaying decision is based solely on system measurements made by the local relay of each end.

Piloted protection schemes offer significant improvement in performance in terms of speed, security, and selectivity, which advocates the employment of these schemes for critical HV and EHV long transmission lines. The only restrictions are limited to communication issues including channel asymmetry, communication latency and data insecurity.

1.2.1 Non-Piloted Schemes:

These schemes are widely used for short and medium transmission lines and for distribution networks. The stepped distance protection and direction over-current schemes are the core members of this class.

1.2.2 Piloted Schemes:

These schemes are widely employed in protection of long lines because the complexity of non-piloted protection schemes, which is required to offer reliable operation for long lines, restricted their application. Whereas, availability of information from all line terminals allows pilot protection scheme to perform high-speed simultaneous fault clearing [6]. Fig. 1.2 presents the scheme's methodology in its simplest form.

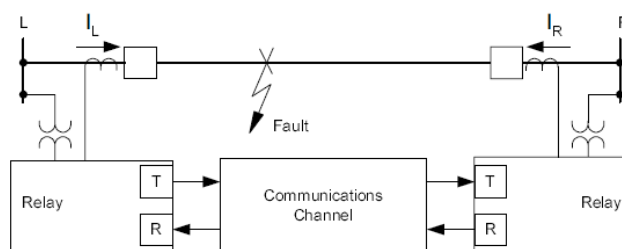


Figure 1.2 Methodology of Piloted Protection Scheme

Traditionally, pilot wires, power line conductors and microwave radio channels have served as the communication channels for piloted schemes [6]. The emergence of fiber-optics in late 1980's revolutionized the market for this scheme because of its inherent broad bandwidth, high signal to noise ratio (SNR), minimal electrical induction and no electrical insulation problems [29]. The recent researches are evaluating the feasibility of using long-distance wireless communication channels. The data that is transferred over the communication path might be real-time sampled values, phasors or logical decisions [5].

Piloted Schemes can further be divided in to 2 categories:

- 1) **Non-Unit Based, Current and Voltage protection schemes:** As the term non-unit suggests, these schemes do not require comparison of the locally and remotely measured quantities before reaching a decision. The only data that is transferred over the channel is discrete and logical, usually trip and block commands or fault direction. Reference [6] uses the terms 'state-comparison protection scheme' and 'open system' for this scheme. It must be noted that the relays based on this scheme always require the complete terminal information (i.e. current and voltage) before reaching the relevant decision [29]
- 2) **Unit Based, Current only protection schemes:** These schemes perform actual comparison of the measured quantities (usually amplitude, phase of current or complete current phasors) of the local and remote ends before a relevant decision has been reached. The logical decision achieved by each local relay may or may not be

transferred to the respective remote relay. These schemes often require only the current information to reach the correct decision.

I. Non-Unit Based, Current and Voltage protection Schemes:

- a) **Distance Protection Schemes (21):** These schemes improve the non-piloted distance protection and eliminates the inherent time delays associated with it by allowing permissive tripping or blocking signals to the subsequent relays. The concept is called permissive transfer tripping (under and over reach) and blocking. This allows instantaneous detection and communication of faults in Zone 2 and 3 of Fig 1.3. However, the application is limited to fault detection only because the actual clearance of zone 2 and 3 is performed unless the fault time equals the zone time settings, in order to ensure system selectivity [4, 6].

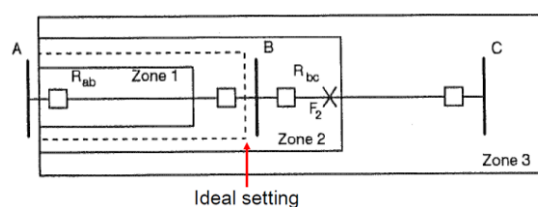


Figure 1.3 Zones for Distance Protection Schemes [5]

- b) **Directional Protection Schemes (32):** These schemes utilize both the current and voltage information of the local terminal to detect the fault and determine its direction. The direction is then transmitted to the remote terminal which then compares it with the direction of fault determined by its own relay and takes necessary measures.

These schemes have been the most widely used pilot protection scheme (especially 32) [2], particularly because of following reasons:

- Limited channel requirement: The transferred data is usually discrete and logical which limits the required channel bandwidth (BW).
- Inherent redundancy of directional (32) and distance (21) protections.
- Fault resistance coverage is better [29]
- Channel delay/asymmetry etc. are not as critical (as compared to unit based schemes)
- Offers better tolerance against CT Saturation

However, following critical restrictions must be acknowledged:

- This scheme requires voltage information of each terminal, which restricts its application in distribution and even some sub-transmission networks.

- Problems associated with voltage transformers (VTs): loss of potential for close-in faults and other problems such as blown potential fuses, Ferro resonance in VTs and transients in CVTs)
- Sensitivity of 21 and 32 may be limited because of system unbalance and CT/VT errors.

II. Unit Based, Current Only Protection Schemes:

These schemes are essentially based on differential protection principle. The tripping action is performed if the differential value of the compared quantity (current magnitude or phasors) crosses the set threshold. In order to perform this comparison the real time sampled values of the respective quantities are transferred over the channel; which signifies the importance of sizable communication channels [29, 4]

Line Current Differential Protection (87 L): This scheme follows the conventional differential protection principle which is based on Kirchhoff's current law and compares the amplitude of the terminal currents.

- a) **Phase Comparison Schemes (87 PC):** The current phasors of the remote and local terminals are compared in these schemes. These schemes are discussed in detail in Chapter 4.

Following advantages should be noted:

- Better performance for complex faults (evolving, cross-country and inter circuit faults)
- Less affected by variation in line loading [5]
- Better performance than non-unit based protection for series-compensated lines, power swings, current reversals, zero sequence mutual induction effects, multi terminal operation, short transmission lines etc. [14 – 17, 5]
- Doesn't require voltage (therefore all VT related problems resolved)
- Extremely sensitive in detecting earth faults, advantage over distance protection, especially for short lines [29]
- Immune to series compensation related applications.

Following prominent drawbacks are vital for discussion:

- Exchanges digital info (phasor, Fourier coefficients etc.) which increases the BW requirement of the communication path [29].
- Data alignment/synchronization of measured signals is required.
- Causes of false differential current in line differential application [15, 5]
 - i. Line Charging current (cables and long OHL) and Tapped load
 - ii. Channel time-delay
 - iii. CT saturation

It must be noted that a reliable communication path is extremely critical for proper operation of current based differential protection schemes, and redundant solutions must always be present (E.g. Distance Relays, which would require Potential Transformer)

1.3 Scope of Work and Research Objectives

The protection scheme employed to protect transmission and distribution lines must satisfy the basic characteristics of electrical system protection. Therefore, it should be selective, dependable, fast, secure and sensitive.

Fault clearing time is extremely critical for HV and EHV transmission lines because the amount of energy drained by the faults is directly proportional to it. This energy is provided by the system by losing the kinetic energy of the generation sources resulting in deceleration. This can cause stability issues in the system and can even lead to system blackout [20].

However, the scope of this thesis work is limited to distribution networks only, for which the fault clearing time has been more flexible. The integration of DERs has resulted in the additional requirement to fulfill the critical clearing time of each generator, therefore relay operating time is also considered. The ultimate goal of the thesis is to assess the feasibility of employment of directional-based pilot protection and line differential protection in future distribution networks with large-scale integration of distributed energy resources (DERs).

Several well-established solutions utilized by prominent relay manufacturers (including Siemens, ABB, SEL etc.) for conventional directional, transient-based directional and line differential protection are reviewed, reconstructed and tested for predefined test conditions. These test conditions take into account the modifications of distribution networks due to integrated DERs. Moreover, some less-explored but highly effective algorithms are also tested which would be ideal for protection of these networks.

Decades of research has pinpointed the short-comings of each of these methods. For e.g. the performance of UHSD protection based on travelling waves is not ideal when faults are close to the relaying point, for faults with small inception angle and the fault resistance coverage is also limited [26]. In fact, the requirement of large processing speed halted the development of these schemes initially but this is not necessarily a problem in modern digital relays.

Ultimately, all the available piloted methods have some inherent disadvantages. The purpose of this review is to discuss the principle of operation of these methods, highlight the drawbacks

associated with each and mention the available algorithms, which were developed to resolve one or more of these problems.

The extensive research work carried out for this project has resulted in development of an original piloted directional scheme based on current information only, which makes it ideal for the protection of distribution networks. However, the invention has only been disclosed to the relevant authorities at ABB and is currently under review. Therefore, no further information would be revealed about the possible invention in this report.

1.4 Scientific Approach and Thesis Outline

Each of the piloted protection schemes under discussion have been extensively tested by their relevant manufacturers mostly for applications associated with transmission networks, but a similar study has seldom appeared for MV and LV distribution networks. Although the development of microgrids has significantly increased the focus on these issue, but in order to assess the feasibility of application of these schemes for modern distribution networks, the associated problems must be identified and a convoluted test criteria must be defined before these algorithms can be tested. Hence, this project uses the following approach to meet these intricate requirements:

- Identification of major challenges associated with protection of distribution networks with integrated DERs and their possible solutions.
- Theoretical review of piloted protection algorithms that are currently available in the market.
- Development of a simplistic distribution system that closely represent a modern MV network with sufficient complexity and DERs.
- Defining the testing criteria and system parameters to validate the performance of all the tested algorithms.
- Discussion and Comparison of the test results.

Chapter 2 mentions the recent trends in development of modern distribution networks and the future protection challenges associated with this development. Moreover, the widely explored solutions for these problems are also briefly mentioned.

Chapters 3 through 6 discusses the theoretical background of proclaimed conventional and transient-based directional protection algorithms. While chapter 7 presents the conjectures for line differential protection. This review is based on extensive literature study of both classified

and publicly available documents of famous relay manufacturers; therefore, the discussion is extremely relevant for the project. Moreover, this theoretical review also serves as the basis for development and testing of relevant models in the subsequent chapters. The theoretical background for current-only transient based methods has been discussed in detail because these options are relatively less explored and has the potential to provide adequate protection for modern distribution networks.

Chapter 8 mentions the practical hurdles that had to be resolved before the communication-based protection algorithms could be tested. These hurdles are mostly relevant for the tested line differential protection relays.

The test system representing a modern distribution network has been defined in chapter 9. In order to represent a DER infested distribution network, small-scale weak sources are installed at different locations. Moreover, the test parameters necessary to assess the performance of each of the algorithms are also structured in this chapter. Finally, the fundamental blocks associated with all the relays and test models under discussion are also defined in this chapter.

Chapter 10 through 12 present the test results for all the piloted protection methods based on the discussion of the preceding chapters. These results are elaborately discussed and a critical review is provided for each algorithm's weaknesses that are identified on the basis of predefined performance criteria.

Finally, chapter 13 compares the performance of all the tested algorithms based on the discussion of chapters 8 through 12.

Chapter 2 - Protection of Distribution Networks with Distributed Energy Resources (DERs)

The blatant rise in renewable-based generation began in the start of the 21st century in order to reduce the carbon footprints and to prevent further environmental damage [37]. According to the Global Status Report for Renewables (2016) [51], 23.7% of the entire global electricity production was based on renewable generation by the end of 2015; with Hydro, Wind and PV being the major contributors (Fig. 2.1). Strictly discussing the status of renewable integration in Europe, the share of renewable-based electricity generation increased from 24% to a massive 44% in the first decade and a half of this century, which advertently crossed the 50% mark last year. The addition of new generation sources in European electricity market is clearly overshadowed by these sources since renewable-based generation collaborated to 77% of the newly added generation in EU and surpassed the conventional sources for the 8th year in consecution [51]. This trend is going to peak soon, especially in light of the Paris Agreement of 2015.

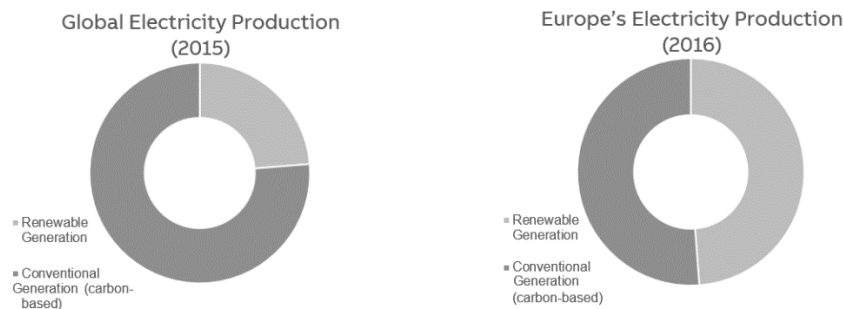


Figure 2.1 Contribution of Renewables in Energy Generation [51]

Ever since the early 1970's, Type I and II wind turbines were the most commonly employed ones and utilized Induction generators directly connected to the grid. In early 1980's, type III wind turbines were introduced which took over the industry in less than a decade. These wind turbines utilized Doubly Fed Induction Generators (DFIGs) and were rated between 6 to 8 MW; while the respective Power Electronic (PE) converters were rated up to 30% of these ratings [21]. Nowadays, type IV WTs with full scale back to back converters rated at 100% power rating of the turbine and directly connected to the grid are widely used and currently hold 80% of the entire market [18].

As a result, complex WPP structures with multiple WTs connected to a Point of Common Coupling (PCC) are present in the distribution network. These windfarms are connected

through MV cables, subsea cables (for offshore windfarms) and often result in limited fault currents due to the presence of PE based converters.

A traditional distribution network is designed to carry power from higher voltage level to the lower ones. The direction of flow of fault currents follows the same principle. These distributed energy resources (DERs) have primarily been integrated in the distribution network [46], which has introduced new challenges for the protection of the distribution system [35-38]. The major challenges include:

1. Variation in fault current level with the varying operating conditions of the DER. The operating conditions depend on a number of variables including weather conditions, network demand etc.
2. Variation in direction of power flow in the network, which depends upon the location of the fault.

If the system employs only the overcurrent protection without directional discrimination, these challenges would result in reduced sensitivity and selectivity. Currently, the primary protection schemes for LV distribution networks rely on non-piloted and non-directional overcurrent protection; while the MV distribution systems employ numerous piloted and non-piloted methods including distance protection without directional supervision and differential protection [37].

This section further elaborates the status of LV and MV distribution systems and the developing challenges in the respective networks.

2.1 LV Distribution Networks:

Besides the integration of PV, small-scale wind turbines and Bio-fuel in LV distribution networks, there is a growing trend of employing Microgrids. Microgrids, as defined in [52], are LV (< 1kV) distribution systems with intermittent micro-sources (PV, wind etc.) and controllable loads distributed across the network; and are capable to operate both in grid-connected (dependent) and islanded (independent) states. A typical layout of a microgrid is given in Fig. 2.2, where small-scale DERs and controllable loads are located close to each other. The discussion on benefits of such a system is beyond the scope of this work.

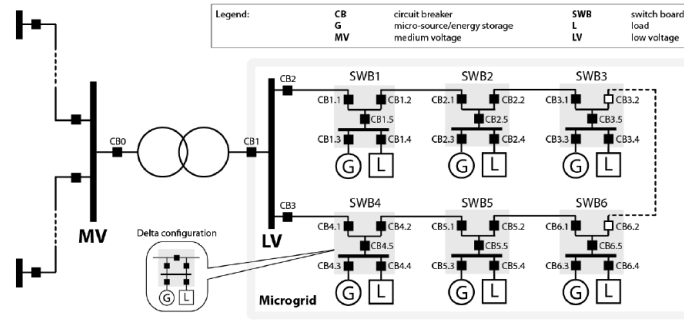


Figure 2.2 Typical layout of a Microgrid [41]

Following observations have been listed about such systems in the References [38 -41]:

1. Since a great number of LV distribution systems (including Microgrids) are designed to operate in the radial fashion, the protection system follows the same protocol.
2. Historically, such systems have been protected using non-directional overcurrent (OC) relays, which may result in non-selective operation in case of bidirectional power flow. Moreover, the short-circuit level used to parameterize OC relays depends abundantly on the position of the micro-sources and their operating condition, especially in case of wind and PV based DGs.
3. The ability of such DER infested systems to operate in both the grid-connected and islanded mode results in large variation in short circuit levels, which when accompanied by fault current variation due to changing operating conditions of the DERs create sensitivity issues for the traditional OC protection. The sensitivity issues are prevalent during islanded operation, because of limited short-circuit level of Power Electronics (PE) interfaced DERs.
4. Such networks would require transmission of auxiliary reactive power through the network, thereby increasing the sensitivity and selectivity challenges for the protection system.
5. Lastly, the network topologies of such systems are bound to change regularly for economic and operational reasons, which would result in relay-coordination issues.

2.2 - MV Distribution Networks

Like LV networks, most of the MV distribution networks are designed to operate in a radial fashion. The transition of vertically operated MV distribution network to a horizontal one due to the influence of distributed generation has created problems for the protection of future MV grids. The problems associated with DER integration in MV grids strongly depend on the

characteristics of the distributed generator (including type of generator, PE interface etc.) and on the grid characteristics as well (Underground cables - UGCs, Overhead Lines- OHLs etc.). References [38, 44-45] highlight major concerns in protection of DERs infested MV Distribution Networks as summarized below:

1. The contribution of DERs situated on a healthy feeder during fault on an adjacent feeder may cause false tripping of the healthy feeder if only non-directional overcurrent protection is employed (Fig. 2.3). This is prevalent in distribution systems using a combination of UGCs and OHLs.

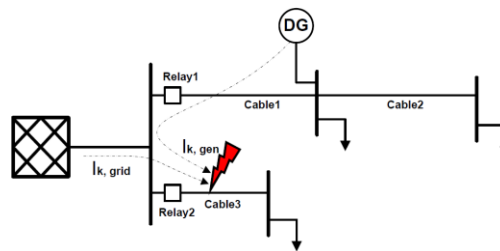


Figure 2.3 Example of False Tripping [45]

2. The position of DER in the network may result in protection blinding and similar selectivity and sensitivity issues if the fault pickup current of protection relay, as shown in Fig. 2.4, is set to max SC level of the grid. The relay may fail to detect the fault if DG is connected and contributes significantly to the fault current; thereby reducing the contribution of fault current by the grid.

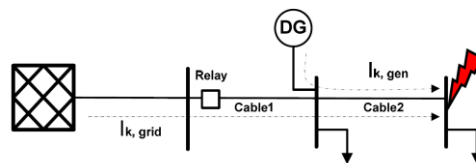


Figure 2.4 Example of protection blinding [45]

3. Automatic reclosing feature (normally employed with OHL protection) can be incompatible with the DER and utilizing this feature without synchronization with the DER may cause extensive damage to the generator as well.

2.3 Protection of DER infested Distribution Networks

So far, the problems identified earlier have been dealt with, by employing current-based time-graded relays and by disconnecting the DERs from the network during faults by using under

voltage or similar protections [47 – 48]. This, however, cannot be allowed with the increasing penetration of DERs in order to prevent total system collapse. Therefore, the national and international grid codes have been revised to introduce *Fault-Ride-Through* (FRT) characteristics for DERs, which prevents large-scale disconnection of these distributed sources in case of network disturbances (including faults).

In case of FRT operation, the Critical Clearing Time (CCT) for the distribution network fault must be less than the CCT of the associated DERs. This has to be done to not only limit the overall system damage, but to ensure the stability (rotor-angle) of the DERs as well [46 - 47, 53]. Several approaches have been proposed over the years to deal with this particular problem, some of which have been listed below:

1. Adaptive overcurrent protection scheme [41]
2. Multi-agent approach for relay coordination (Adaptive and Non-Adaptive)
3. Piloted directional protection (Conventional and transient-based)
4. Line differential protection

Besides the inherent challenges, the modern electrical system also brings new opportunities that can be used for the development of protection measures necessary to tackle these challenges. One of these opportunities is the deployment of wide-area protection (WAP) and wide-area monitoring (WAM), shown in Fig. 2.5, based on Phasor Measurement Unit (PMU) [39-40]. The technological advancement in microprocessor design and communication systems along with the wide-scale adoption of WAP has allowed researchers to investigate the possibility of adaptive protection schemes.

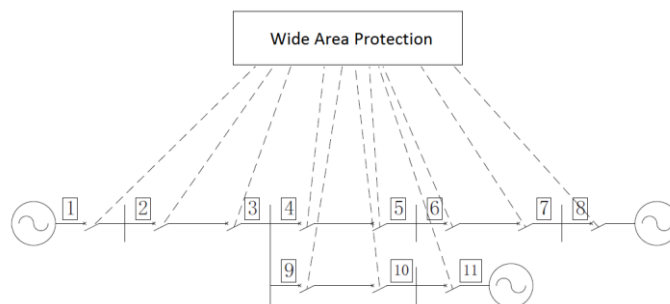


Figure 2.5 Example of Wide Area Protection

These adaptive schemes focus primarily on conforming the pickup settings for fault detection by continuously monitoring the systemic changes in the network to improve protection sensitivity [41]. The employment of directional element with or without adaptive protection

schemes is extremely crucial to keep the protection sensitive for both the MV and LV distribution networks with integrated DERs.

Another opportunity, which is comparatively simpler but equally effective, utilizes relay-to-relay communication to overcome the challenges mentioned earlier. The protection techniques that utilize this sort of communication include Line Differential protection and Directional protection (conventional and transient-based). This thesis discusses the sought after communication-based protection schemes that are currently available in the market.

2.4 Communication-based Protection

The idea to employ Piloted-protection for distributed generation systems is an extension of WAM that utilizes the already-established features of modern microprocessor relays currently available in the market [46]. The communication channel transfers either the actual real-time data or only the trip supervision signals between the local and remote relays, as shown in Fig. 2.6. The concept is prevalent in transmission lines protection and even MV distribution system protection; but the extension of these plans to LV/MV distribution networks of the future is the way forward.

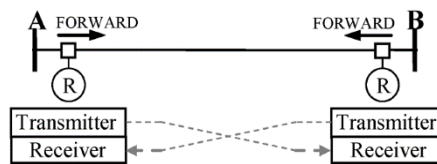


Figure 2.6 Communication-based Directional protection

However, this kind of protection does offer some bottlenecks, if based on current wireless communication technology, which include:

1. As mentioned earlier, the time to clear the faults in future distribution networks must be as low as possible.
2. Based on the protection algorithm, the extensive communication channel width might be required.

Chapter 8 sheds more light on IEC 61850 standard for communication-based protection of the future distribution networks with modern substation-oriented infrastructure using wireless communication.

2.5 Directional Protection and Distributed Generation

Directional elements are extremely critical for a secure and selective protection scheme involving DERs, especially in case of remote faults. Besides determining the direction of fault, the main applications of this element range from supervising distance element and controlling the OC element to developing quadrilateral characteristics of these relays [28 - 32].

Almost all the directional elements require both the voltage and current measurements to detect the direction of power flow during faults [48]. The directional elements when employed in communication-based protection can detect if the fault is in the protected zone (forward fault for both the remote and local relays) or not (reverse fault for at least one of the relays).

The importance of such directional protection schemes holds ground for secure operation of future networks due to high penetration of renewable distributed generation in the distribution feeders [35 – 37]. As discussed earlier, the emergence of bidirectional flow of power in future grids has left conventional non-directional protection futile [37]. Moreover, the multi-terminal condition introduced by these connections of DGs also favors the addition of directional elements to pre-existing protection schemes.

Chapter 3 - Conventional Directional Element and Design

Directional relays have been around for several decades. Initially, the employment of this element was restricted to crucial HV transmission lines; however, with the advent of numerical relays, the applications extended to the protection of distribution network as well [26]. The extensive rise in integration of renewable distributed generation and microgrids in the distribution network has made this element a paramount component of the protection system. [35-37]

Directional element can be used as the primary component of transmission and distribution line's protection in case of piloted directional protection. On the other hand, the directional element can also serve as supervision for overcurrent protection [55].

Principle of Operation

Conventionally, the numerical relays determine the direction of fault by either calculating torque like quantities or by deducing the impedance measurement based on sequence components [28].

- a) **Torque-like quantity:** Directional elements, based on this principle, determine the phase-shift between a *polarizing quantity* and an *operating quantity*. Either of these quantities have several possible combinations ranging from phase voltages and currents to their phase-to-phase equivalents. Moreover, the possibility of using symmetrical sequence components has made this element more secure and sensitive, especially in case of complex faults.
- b) **Sequence Impedance:** This approach also determines the phase shift between two quantities; the quantities being sequence voltages and currents. By determining the ratio between these quantities, the equivalent sequence impedance is calculated. The polarity of this impedance regulates the direction of fault in the system.

The basic operating principle can be reviewed using a simplistic example of Fig. 3.1. The polarizing quantity (phase voltage V) leads the operating quantity (phase current I of the fault loop) by the impedance angle of the faulted loop (θ_F) for Forward faults; whereas the same polarizing quantity lags behind the faulted phase current by angle θ_R (which is equal to 180 minus the Impedance angle of the faulted loop).

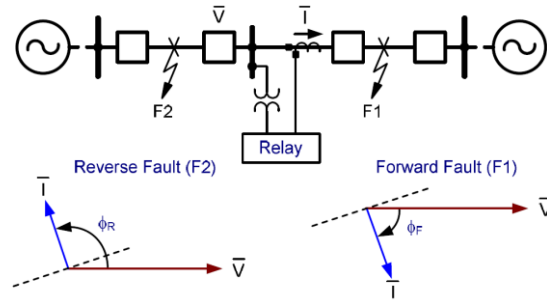


Figure 3.1 Conventional Directional protection (operating principle)

This chapter explores and evaluates the performance of several approaches for determining fault direction in case of complex fault conditions. Finally, a comprehensive algorithm utilizing multiple directional elements is presented.

3.1 Phase Directional Element:

3.1.1 Cross Phase Quadrature Directional Element

The most commonly employed phase directional element, as suggested by Sonnemann in 1950 [49], was later transformed in to quadrature directional relay (Eq. 3.1) for improved performance.

$$T32P = |V_{LL}| |I_L| \cos(\beta - 90) \tag{3.1}$$

Where,

- T32P = Torque based element for directional power protection
- V_{LL} = Phase to Phase voltage of unprotected phases (polarizing quantity)
- I_L = Phase Current of protected phase (operating quantity)
- β = angle between V_{LL} and I_L

The sign of T32P determines the direction of faults.

Table 3-1 presents the polarizing and operating quantities for each protected phase.

Table 3-1 Typical polarizing and operating quantities for T32P

Phase	Operating Quantity (I_{OP})	Polarizing Quantity (V_{POL})
A	I_A	$V_{POLA} = V_{BC}$
B	I_B	$V_{POLB} = V_{CA}$
C	I_C	$V_{POLC} = V_{AB}$

Although this technique is one of the widely used directional element and fulfills the operation requirement for most faults (including three-phase faults), there is an inherent security flaw.

This shortcoming was initially identified by Warrington [32]; which suggests the failure to determine the correct fault direction in case of Reverse (out of section) Phase to ground faults in case of short or medium lines. This inaccuracy is primarily due to incorrect direction determined by directional element of unaffected phases [28]. Several solutions to this problem have been suggested and summarized in Table 3-2 [27-32]

Table 3-2 Proposed solutions to resolve shortcoming of conventional T32P

	Solutions	Advantage	Drawback
1	Seek agreement of all three phases before determining final fault direction	Satisfactory operation during SLG fault	Blocks operation during Phase-Phase fault, therefore separate directional element needed
2	Supervise each phase with Phase-Phase overcurrent element (because this current is zero for SLG fault)	Satisfactory operation for Numerical Relays	Impractical for Electromechanical Relays
3	Use Positive Sequence Directional Element (T32P)	Satisfactory operation for Balanced Faults	1. Unbalanced fault detection require a separate directional element 2. Doesn't give any output for SLG faults 3. Out of Section P-P fault can adversely affect T32P

3.1.2 Positive Sequence Directional Element

Instead of using three separate directional element for each phase, it is a popular option to switch to symmetrical-sequence based quantities. The possibility of using positive sequence quantities for determining fault direction offers a unique advantage in case of balanced three-phase fault detection. Neither negative sequence nor zero sequence quantities are ideally present in this fault condition. The operating principle is based on Eq. 3.2

$$T32P = |3V_1| |3I_1| \cos(\angle V_1 - (\angle I_1 + \angle Z_{L1})) \quad (3.2)$$

Where,

V_1 = Positive Seq. Voltage (polarizing quantity)

I_1 = Positive Seq. Current (operating quantity)

Z_{L1} = Positive Seq. Impedance of the protected line

The performance of positive sequence directional element has been widely investigated in references [27-29]. The shortcomings of this technique and the relevant solutions have been listed in Table 4-3

Table 3-3 Problems with Positive Seq. Directional Element and Relevant Solutions

Type of Fault	Problem Description	Relevant Solution
Single Phase to Ground Fault	For reverse SLG faults, the operating quantity might be too small resulting in sensitivity issues	Zero or Negative Sequence directional elements
Zero Voltage, Three Phase Fault	For close-in faults with low three-phase voltages	Employing memory storage to use pre-fault voltages as polarizing quantities instead
Phase-Phase faults	In case of heavy load conditions (similar load current and fault current magnitudes)	Negative Sequence directional element

Since the focus of this section is phase directional element, the problem associated with phase-phase faults is resolved first.

3.1.3 Negative Sequence Directional Element

Besides positive sequence quantities, only the negative sequence counter parts exist for both unbalanced phase fault condition (L-L and L-L-G faults) which makes the negative sequence directional Element an automatic replacement for the problems associated with previous option [28]. The operating principle is based on Eq. 3.3 below:

$$T32Q = |3V_2| |3I_2| \cos(\angle -V_2 - (\angle I_2 + \angle Z_{L1})) \quad (3.3)$$

Where,

$-V_2$ = Negative Seq. Voltage (polarizing quantity) rotated by 180°

I_2 = Negative Seq. Current (operating quantity)

Z_{L1} = Positive Seq. Impedance of the protected line

The angle of positive sequence impedance of the protected line gives the maximum torque angle (MTA) in this case. The polarity of T32Q determines the direction of fault; where as a positive value of T32Q represents forward fault condition. The negative sequence quantities along with phase equivalents for a forward fault in case of no load condition is given in Fig. 3.2

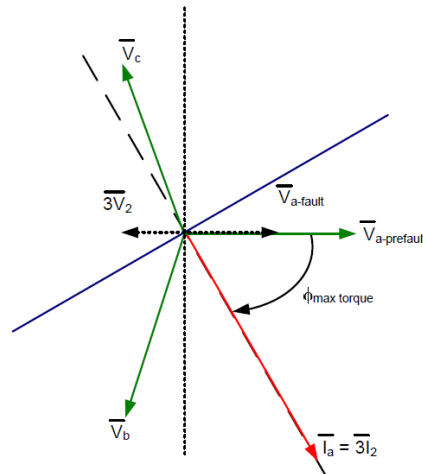


Figure 3.2 Negative Sequence quantities for forward faults under no-load condition

Inherently, negative sequence directional element offers two distinctive advantages:

- These symmetrical components determine the amount of unbalance in the system, therefore they are basically zero under perfectly balanced conditions but increase dramatically in case of unbalanced loads or faults which make them ideal for Phase fault detection (Phase-Phase faults) [33]
- Negative sequence directional element can serve as a backup for Zero Sequence element in case of unbalanced faults involving ground (Phase-Ground and Phase-Phase-Ground) [32]

Ever since the advent of modern numerical relays, the directional element based on T32Q of Eq. 3.3 has successfully been employed for several years. However, the performance of this algorithm extensively depends on the strength of the source. For strong sources with low impedance, the negative sequence voltage produced in case of unbalanced faults is significantly low; thereby affecting the sensitivity of the relay, especially for high resistance faults [32-33].

In 1993, Schweitzer Engineering Laboratories (SEL) first addressed this limitation in the SEL-321 Relay [50]. The solution is based on the ratio of negative sequence voltage and current, resulting in the corresponding impedance. Eq. 3.4 gives the simplified version of these calculations:

$$z_2 = \frac{v_2}{i_2} = \frac{\text{Re} [V_2 \cdot I_2 < Z_{L1}]}{|I_2^2|} \quad (3.4)$$

The polarity of this impedance determines the direction of fault, where negative impedance phasor represents a forward fault. The principle of operation of this relay can be explained

using the sequence components diagram in case of L-G fault in Fig. 3.3. In case of forward faults, the calculated impedance is equivalent to *negative* of the negative-sequence impedance of the source behind the relay; whereas reverse faults result in calculating the sum of line impedance and source impedance of the remote end. Therefore, by comparing the calculated impedance with predefined thresholds, correct directional decision can be taken.

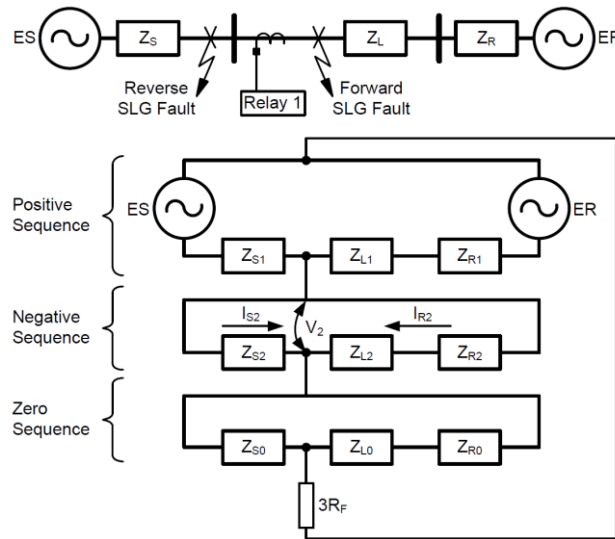


Figure 3.3 Sequence Diagram for Phase-Ground Fault [71]

The setting of these relays require determining following 5 thresholds:

1. Z_{2F} = Z_2 threshold for Forward faults
2. Z_{2R} = Z_2 threshold for Reverse faults
3. $50Q_F$ = Instantaneous Overcurrent threshold for Forward Faults
4. $50Q_R$ = Instantaneous Overcurrent threshold for Reverse Faults
5. a_2 = Current Restraint factor (I_2/I_1)

These settings can be explained by representing the characteristics on the polar plane, as shown in Fig. 3.4, $50Q_F$ and $50Q_R$ are used as fault detectors and determine the minimum negative sequence current required to trigger this element, while a_2 prevents the negative sequence element from operating in case of balanced faults (three-phase). The principal settings of this directional element (Z_{2F} and Z_{2R}) are based on the fact that the calculated impedance is essentially negative for forward faults and positive for reverse faults.

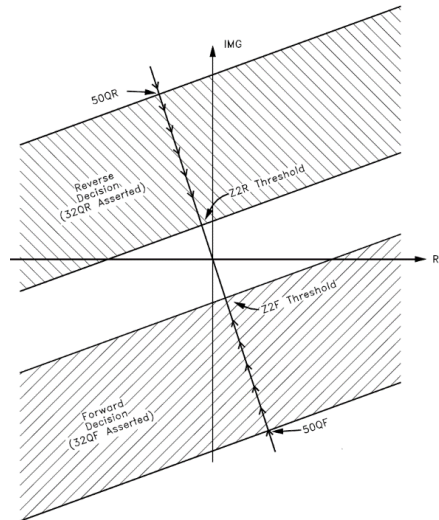


Figure 3.4 Settings for Negative Seq. Impedance Directional Element [28]

In the presence of strong sources resulting in low negative sequence voltage, the calculated impedance can still be used to determine the fault direction, resulting in significantly improved sensitivity. This has been discussed extensively in references [28-33]. The setting of Z_{2F} and Z_{2R} , in this case, depends on the *location of the strong source with respect to the relay position*. For forward fault, V_2 is inversely proportional to the strength of source behind the relay; whereas the same V_2 is affected by the strength of the source on the remote end in case of reverse faults. Therefore, based on this theory, V_2 (and consequently Z_2) would almost be zero in case of a forward fault only if the source behind it is strong. Similar comprehensions can be deduced for reverse faults. Fig. 3.5 presents the two possible conditions that can occur and the relevant settings for Z_{2F} and Z_{2R} in each case, where the left figure mentions the more common condition.

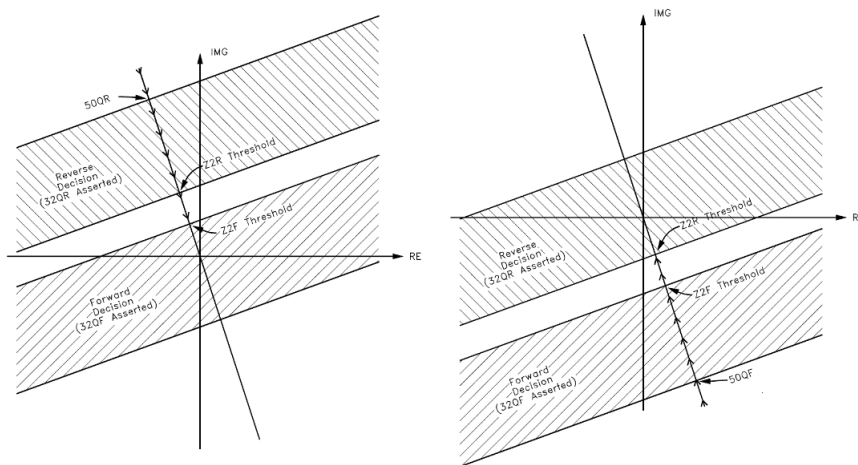


Figure 3.5 Settings for Neg. Sequence Impedance relay. [28]
 Left: Strong Source behind the relay. Right: Strong Source in front of the relay

3.2 - Ground Directional Element:

This element primarily resolves directional issues for L-G and L-L-G faults. The symmetrical component analysis reveals the presence of all three-sequence components during these faults. The heavy dependence of positive sequence components on load condition leaves only zero and negative sequence components for ground directional element design.

3.2.1 - Zero Sequence Directional Element

This directional element can be employed using three methods, as listed in Table 3-4

Table 3-4 Zero Sequence Directional Element (Operating Principle)

Name	Operating Equation	Polarizing Qty.
Voltage Polarized	$T_{32V} = 3V_0 3I_0 \cos(\angle -V_0 - (\angle I_0 + \angle Z_{L0}))$	Zero Seq. Voltage
Current Polarized	$T_{32I} = 3I_1 3I_0 \cos(\angle I_1 - (\angle I_0))$	Pos. Seq. Current
Dual Polarized	T32VI	Combined

Practically, the zero sequence directional element is susceptible to grounding errors of VTs and incorrect polarity identification of neutral CTs. The dual polarized zero sequence directional element provides a more flexible solution to drawbacks offered by the remaining methods in case of weak zero sequence voltage source and absence of zero sequence current sources (e.g. grounded transformers) during faults. However, this element still exhibits two inherent limitations:

1. The zero-sequence mutual coupling of parallel lines can affect the directional decision
2. The strength of zero sequence source adversely affects the polarizing quantities in each case.

Based on this analysis, the **negative sequence directional element** based on impedance calculations offer distinctive advantages for ground fault detection. However, if the local generation is not directly connected to the protected system (E.g. using Wye-grounded transformer), I_2 would be insufficient to determine the correct fault direction because of pure zero-sequence source which is present behind the relay. In such case, Zero sequence directional element determines the correct direction [32].

3.3 Practical Directional Element based on Preferred Order

The extensive review of all the available directional techniques suggests that no particular method is suitable to perfectly determine the direction of all the faults under all circumstances. However, careful analysis of the protected system allows the user to determine the order in which each directional technique can complement each other. The possible selection order includes following options:

1. Negative Sequence Impedance element (Z_{2Q}) and negative sequence torque based element (T32Q) for all unbalanced faults
2. Voltage polarized zero sequence element (T32V) for unbalanced ground faults
3. Current polarized zero sequence element (T32I) for unbalanced ground faults
4. Positive sequence directional element (T32P) for balanced Faults

The final decision regarding the fault direction is based either on the high priority element (depending on the chosen order) or on the complementary decision of each priority element. The process may result in slight delay of the directional decision (1.5-2 cycles), but the delay is well within the prescribed decision period length for distribution networks.

Summarizing the contents of this section, a more secure and sensitive directional element can be devised using negative-sequence, positive-sequence and zero-sequence elements. The shortcomings of each of these elements including mutual coupling impacts on zero-sequence element and inaccurate operation of positive-sequence element for three phase faults near the relay location are resolved using the proposed directional scheme. Negative-sequence element plays the most significant role for all unbalanced faults, which account for 95% of all the faults associated with transmission/distribution lines [2]. The independence of this element from varying load condition and insufficient negative-sequence voltage makes it ideal for protecting systems involving large integration of renewable DERs.

The applications of such directional element can be extended for series-compensated lines by manipulating the setting references for negative-sequence impedance thresholds. While, maloperation due to unbalanced loads can be avoided using OC supervision.

Chapter 4 - High Speed Distance Protection and Directional Comparison based on Superimposed/Delta Quantities and Traveling Waves

4.1 Background

The inherent drawbacks of conventional distance protection listed below resulted in development of this method.

- The process of impedance measurement using conventional methods results in delayed operation because of filter length, which can severely influence the system in case of faults, especially for HV and UHV systems [19].
- Poor fault resistance coverage of conventional distance protection (applicable to mho-type only)
- Power swings at frequencies significantly lower than fundamental frequency can cause mal-operation. This problem is resolved by bypassing distance protection as long as heavy power swings persist in the system, which leaves the affected line unprotected during this period. [21]

4.1.1 Operating Principle of the proposed scheme: When a fault occurs at a certain position it results in instantaneous change in the current and voltage of that point. The instantaneous changes in these quantities produces traveling waves (TWs) which propagate away from the location of the fault [22]. These instantaneous changes in voltage/current and the propagation of TWs can be utilized to detect the fault, determine the faulted loop, analyze the direction of fault and acquire the actual distance of the fault from the relay point as well [18, 21].

4.1.2 Brief History: The protection schemes that are based on this principle are extremely fast and have the ability to accurately detect faults in a few milliseconds [21-22]. The utilization of TWs for UHSD protection of EHV/UHV transmission lines was initially proposed by ASEA in 1978. The accuracy offered by these relays is contradictory to the common belief that protection system's speed and security are antagonistic properties but a detailed review of this contradiction is provided in [20].

Ultra high-speed distance (UHSD) protection based on travelling wave estimation is a well-versed topic, which has been scrutinized since the publication of reference [20] and several improvements to the original method have been proposed up until reference [23]. As stated

earlier, reference [26] mentions that the shortcomings of UHSD protection based on travelling waves in case of close-in faults, faults with small inception angle and the fault resistance coverage is also limited.

The idea of monitoring real time changes in the power system (superimposed quantities) is relatively new, which emerged with the publication [11] in 1988 and has been built upon, ever since. Several publications based on this concept [18-24] proposed minor or major changes to the algorithm in order to resolve one or more limitations of the original concept. Development in microprocessor technology and digital relays, has allowed this approach to become top-contender for line protection especially with rise in applications of WAM and PMUs.

4.1.3 Superimposed Components / Delta Quantities: Superimposed components / delta quantities are instantaneous changes in voltage and current quantities (either phase to phase or phase to ground). Eq. 4.1 and 4.2 define the delta quantities for voltage and current respectively.

$$\Delta U_a(t) = U_a(t) - U_A(t - T) \quad (4.1)$$

$$\Delta I_a(t) = I_a(t) - I_A(t - T) \quad (4.2)$$

Here the subscript ‘a’ refers to phase-A and the respective quantities are phase-ground. While ‘T’ represents one cycle period which is 20 ms for a 50 Hz AC power system.

4.2 Theoretical Analysis:

The proposed scheme can be analyzed using superposition principle, which is presented in the schematic diagrams of Fig. 4.1 and 4.2

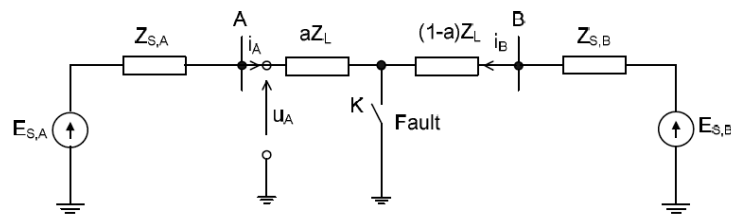


Figure 4.1. Schematic representation of electrical circuit structure change after fault on the line

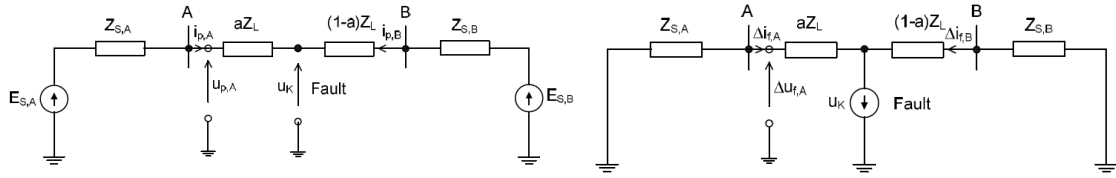


Figure 4.2. Schematic representation of an electrical circuit in the form of pre-fault and delta quantities

According to the superposition principle, following equations are obtained:

$$U_a(t) = U_{P,A} + \Delta U_{f,A}(t) \quad (4.3)$$

$$I_a(t) = I_{P,A} + \Delta I_{f,A}(t) \quad (4.4)$$

Where $\Delta U_{f,A}(t)$ and $\Delta I_{f,A}(t)$ represent the delta component for phase-A voltage and current (as shown in Fig. 4.2 and defined in Eq. 4.1 and 4.2)

4.3 Steps of Operation

4.3.1 Detection of Fault

The fault is detected when delta quantities change to a non-zero value (as shown in Fig. 4.3). The delta quantities appear to be zero under stable operation and become non-zero in case of a disturbance. These disturbances can range from normal load changes to low-frequency power swings and fault conditions. A simplistic fault detection method evaluates ΔI using Eq. 4.2 and continuously compares it with a fixed threshold like Eq. 4.5

$$\Delta I_{th} = KI_N \quad (4.5)$$

Reference [18] suggests an adaptive threshold for phase-to-phase delta currents to avoid mal-operation of the transient-based protection during load changes and power swings. This adaptive threshold is defined by Eq. 4.6. The impacts of power swings and load changes on the delta quantities and the effectiveness of adaptive -threshold fault detection method are simulated in Chapter 8

$$\Delta I_{th} = A. |\Delta I_{p-p}(t - T)| + KI_N \quad (4.6)$$

Where the weighing factors A and K determine the adaptability and sensitivity of fault detection algorithm.

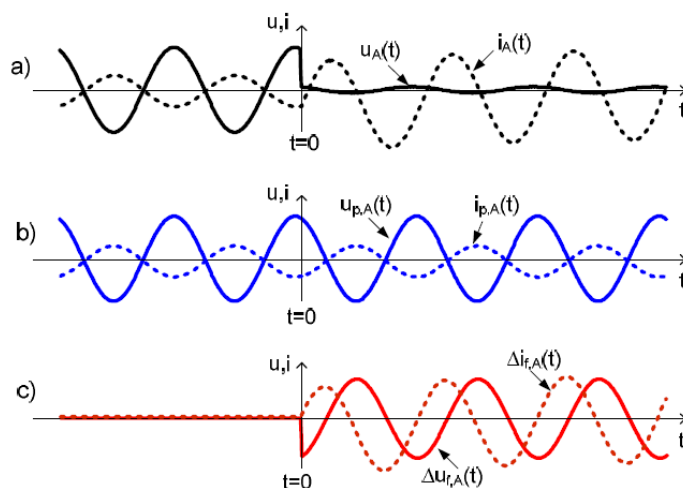


Figure 4.3. Electrical quantities during fault event:
 a) voltage and current before and after short circuit;
 b) voltage and current without short circuit;
 c) delta-voltage and delta-current.

4.3.2 Loop Selection

Selection of faulted phase is extremely important for the protection of transmission network because of following reasons:

- To isolate faulted phase if single pole operation is available [5]
- To employ the relevant distance protection algorithm, if required. [5-6]
- To allow single phase automatic reclosing to ensure system stability in case of transient faults [21]

These reasons are not necessarily as important for the distribution network. The phase selection criteria has been summarized in the Table 4-1 [18-19]. It must be noted that both the current and voltage criterion must be satisfied before a final decision is reached to avoid malfunction. The voltage criterion can also be reviewed in the Fig. 4.4

Table 4-1 Current and Voltage Criteria for Phase Selection

Fault Type	Current Criteria	Voltage Criteria
For a single-phase fault	Delta-phase-phase current of the healthy phases is close to zero.	The ratio between the delta-voltage in the faulted phase and the delta-phase-to-phase voltage in the healthy phases is high.
For a phase-to-phase fault	Delta-phase-phase current of the faulted phases is much larger than the other delta-phase-phase currents.	The ratio between the faulted phase-to-phase delta-voltage and the delta-voltage of the non-faulted phase is high.
For a three phase fault	All delta-phase-phase currents are equal to each other.	All delta-phase-phase voltages are equal to each other.

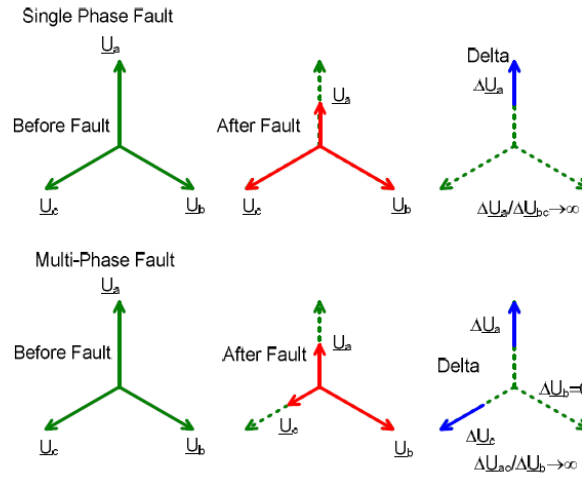


Figure 4.4 Voltage Criterion for Phase Selection [19]

4.3.3 Directional Element

The equivalent circuit diagram of the post-fault condition with superimposed fault voltage source are given in Fig 4.5 and 4.6 for both internal and external faults; while Eq. 4.7 and 4.8 respectively describe the measured delta voltage at End A in each condition. During forward faults, the relay at point A determines the superimposed delta voltage across source impedance of A and is opposite to the direction of superimposed current component. Whereas, during reverse (external) faults, the delta voltage is consequently obtained across the sum of line impedance and impedance of the remote-end source [18-19].

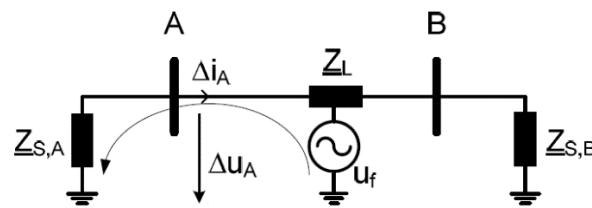


Figure 4.5 Post-fault Circuit (Internal fault)

$$\Delta u_A(t) = -Z_{s,A} \cdot \Delta i_A(t) \quad (4.7)$$

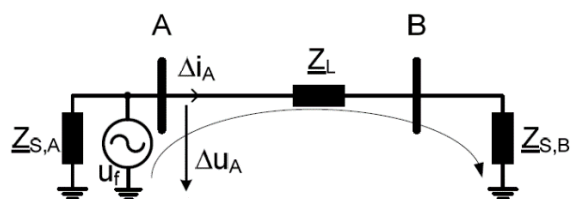


Figure 4.6 Post-fault Circuit (External Fault)

$$\Delta u_A(t) = (Z_{S,B} + Z_L) \cdot \Delta i_A(t) \quad (4.8)$$

This unique difference between the superimposed delta voltage and currents for forward and reverse faults has been extensively used to determine fault direction. The actual method to obtain this relation may vary from method to method but the ultimate result follows the principles of Eq. 4.7 and 4.8. The algorithms

1. Energy-Based Algorithms

- Asea's approach (RALDA – 1978)

2. Impedance-Based Algorithms

- **Brown Boveri & Company's** Replica Impedance approach (IV Quadrants – later modified by **Siemens**)
- Compensated Current (MIMIC Filter) approach (**SEL** and **Siemens**)
- Positive Sequence Impedance Method

3. Alternate Methods with improved performance and wide-scale applications

- Average of superimposed quantities (sliding window method)
- Current-only method

Detailed description of relevant algorithms along with their respective limitations have been provided in Chapter 5.

4.3.4 Fault Location / Distance Element

The distance element basis its decision on the evaluation of two quantities:

- Pre fault reference voltage at the exact reach point of the relay
- Post fault delta voltage at the exact reach point of the relay

Fig. 4.7 presents the internal fault condition, while Fig. 4.8 applies the superposition principle on the same internal fault. Z_{HSD} represents the impedance of reach point and U_{HSD} represents the post fault voltage of reach point.

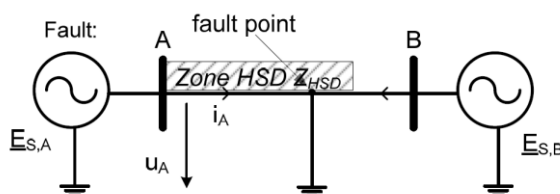


Figure 4.7 Internal Fault Condition [18]

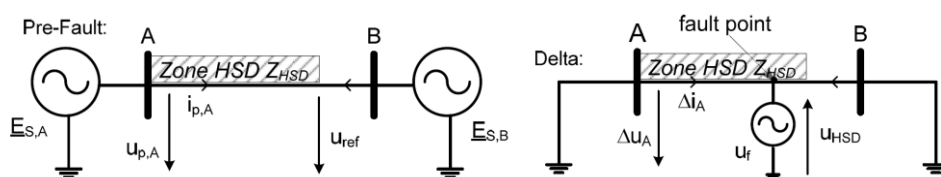


Figure 4.8 Superposition principle: Pre-fault Circuit (Left) Post-fault circuit (Right)

The possible outcomes are listed in the Table 4-2

Table 4-2 Fault Location Determination Principle

Delta Voltage > Reference Voltage at Reach point	Fault is Internal
Delta Voltage < Reference Voltage at Reach point	Fault is External
Delta Voltage = Reference Voltage at Reach point	Fault is exactly at the zone limit

Since primary detection of fault location in piloted protection is performed by the directional element, Distance element would serve as back up in this case.

I. Discrepancies with Distance Element

Reference [24] lists the major discrepancies with the distance element operation proposed in previous section. Referring to Fig. 4.9, the phasor representation of the criteria defined earlier is given by Eq. 4.9

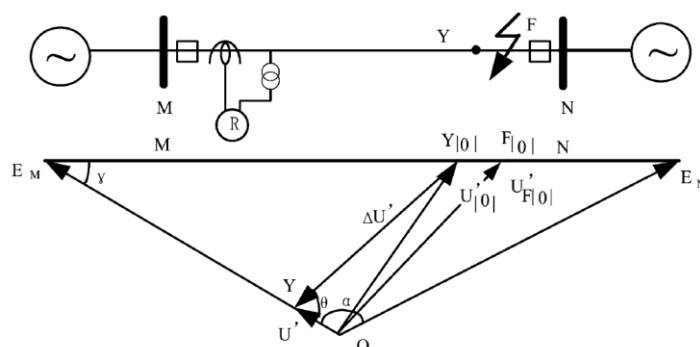


Figure 4.9 Phasor Representation of Voltages (local, remote, fault point & relay reach point) [24]

$$|U' - U'_{|0|}| > U'_{|0|} \text{ or } \Delta U' > U'_{|0|} \quad (4.9)$$

Where ‘Y’ represents relay reach point and ‘F’ represents fault location. M and N are respective buses operating at voltages separated by angle α , which suggests the direction of power flow. The symbol $U'_{|0|}$ represents the pre-fault voltage at reach point Y, while symbol $U'_{F|0|}$ represents pre-fault voltage at fault point. Finally the symbols U' and $\Delta U'$ represent postfault and delta voltages at relay reach point, while angle Θ represents the angular shift in voltage of reach point and depends upon the fault location, fault resistance and the type of fault. Based on this analysis, reference [24] mentions possibility of mal-operation of the presented scheme under following conditions:

- a) Development of external fault during power swings resulting in large Alpha
- b) Removal of external faults resulting in power swings (large Alpha)
- c) Grid splitting due to power swings

These shortcomings have so far been met using solutions listed in [12] and [18 – 19]. Each of the solution and its performance is listed in Table 4-3.

Table 4-3. Counter measures for resolving Distance-Element shortcomings

Countermeasure			Advantages	Drawbacks
No.	Title	Description		
1	Fixed Threshold Criterion	Reach point Reference voltage is fixed to last pre-fault value	Resolves problem 'a'	Fails to resolve problems 'b' and 'c'
2	Floating Threshold Criterion	Reach point Reference voltage is not fixed	Resolves problems 'a' and 'b'	Fails to resolve 'c' and operating region is severely reduced resulting in low dependability
3	Mutual Tripping Scheme	Mutual tripping signal by Conventional distance and superimposed distance relays	Resolves all inherent problems	High fault detection and clearance time
4	Adaptive Threshold Criterion	Selects between 1 and 2, depending upon the value of Alpha	Resolves all inherent problems	Requires PMU/WAM application to determine angle Alpha
5	Average Rectified Values and adaptive threshold	Combines the properties of 2 and 5 while averaging over the moving window of a half cycle	Resolves all inherent problems	Complicated Algorithm May require PMU/WAM

4.4 Problems with superimposed/TWs based methods

- a) Require high sampling frequency, which is significantly higher than most conventional relays [25] for traveling waves-based applications.
- b) Sensitive to heavy load conditions
- c) Mal-operation in case of removal of external faults, power swings resulting in large delta angles between 2 ends of the lines and grid splitting. These problems are usually observed in power-frequency superimposed component based distance protection, proposed in [10].
- d) Transients component based approach (especially for TWs) offers extremely high speed but may result in mal-operation because of inaccurate extraction of transient components during faults [24, 8].
- e) Complications in measurement of superimposed quantities due to limitation in Bandwidth of CTs and VTs [21].
- f) Positive-sequence superimposed components is relatively fast, offers high reliability and offers high sensitivity, which makes it ideal. However, the evaluation of criteria over the entire post-fault cycle can result in relatively longer time delays.
- g) Performance of RALDA and similar relays is inferior to conventional directional relays for close in faults [26, 20].

4.5 Solution to these problems

- a) Can be resolved using technique proposed in reference [21]
- b) Resolved using superimposed currents for phase comparison protection, proposed in reference [5]
- c) Most of these problems are resolved by the adaptive criterion proposed in reference [24] which requires real time phasor information of each end (possible to obtain in case of WAM and PMU utilization)

Chapter 5 - Superimposed/Delta Quantities based Directional Protection

The directional algorithms based on Superimposed (Delta) quantities mentioned in Chapter 4 are broadly discussed in this chapter. The extensive review of relevant literature and testing under predefined circumstances has helped in identifying the pros and cons of each approach.

5.1 UHS Directional protection based on Transient Energy

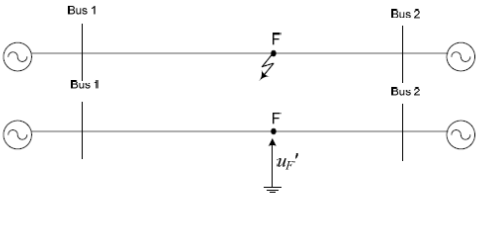
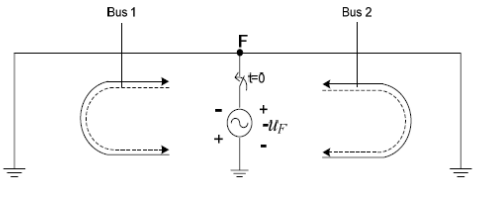
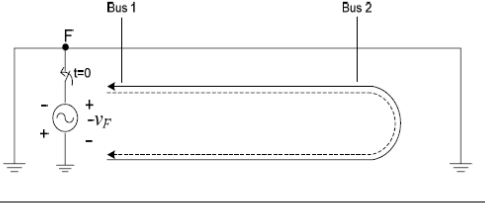
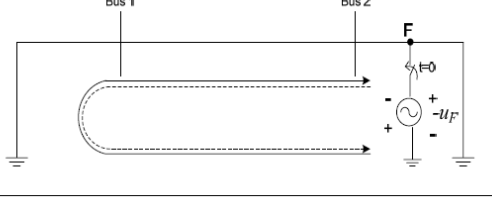
This principle was first implemented in **ASEA RALDA Relay (1978)**

The voltage and current waves produced by the inception of fault travel from the fault point towards each relay point (A and B). According to reference [20], with the help of post-fault circuit diagram following observations are noted:

- The imaginary source ' u_f ' produces a negative voltage wave towards each end; which is clear because the voltage tends to be zero or at least reduces at the fault point.
- The same source produces a positive current wave towards each end; which is because this fictitious source tends to draw current from both ends (in case of infeed from both ends)

Table 5-1 from reference [20] perfectly sums up the complete scenario for both internal and external faults, which concludes that internal faults result in opposite polarities for current and voltage changes: while external faults cause similar polarities. This distinctive property can be used to detect fault direction [18-20].

Table 5-1. Determination of direction based on ASEA publication [20]

Type of the fault	Polarity of u_F'	Bus no.				
		1		2		
		Δi	Δu	Δi	Δu	
Internal	+	+	-	+	-	
	-	-	+	-	+	
External to Bus 1	+	-	-	+	-	
	-	+	+	-	+	
External to Bus 2	+	+	-	-	-	
	-	-	+	+	+	

5.1.1 - Salient Features and Limitations

1. Provides extremely fast fault and directional detection (referred as Ultra High Speed - UHS Relay)
2. Since it is based on information contained in both steady state and transient changes, therefore does not require extensive filtering due to fault transients, which could limit the speed of operation.
3. The same reason also reveals that the transients produced by instrument transformers during the inception of fault do not affect the operation. This observation resolves following issues:
 - a. Bandwidth requirements of CT/VT are minimized because the relay is not exclusively dependent on high frequency components, which may have been lost due to limited BW of CT/VT.
 - b. Risk of dead-zones for particular faults is limited.
4. The principle can be employed on distribution networks as well, if relevant hardware requirements are met.
5. Both the speed and security criteria of an ideal protection system are satisfied.

- This method offers one noteworthy limitation due to its utilization of both the current and voltage information to determine correct fault direction. The unavailability of voltage transformers on both the remote and local buses in the distribution network makes this approach practically irrelevant for directional protection of distribution lines.

5.2 - UHS Relay based on Replica Impedance

This principle was initially developed by Brown Boveri & Company and the theoretical model was proposed in 1980. This method employs the use of replica impedance (Z_R) to predict the direction of voltage induced by the superimposed current component. As shown in Fig. 5.1, the polarity of this predicted induced voltage ($\Delta U_R = \Delta i \cdot Z_R$) is then compared with the superimposed voltage measured by the VT and the decision is based on Table 5-2 [18].

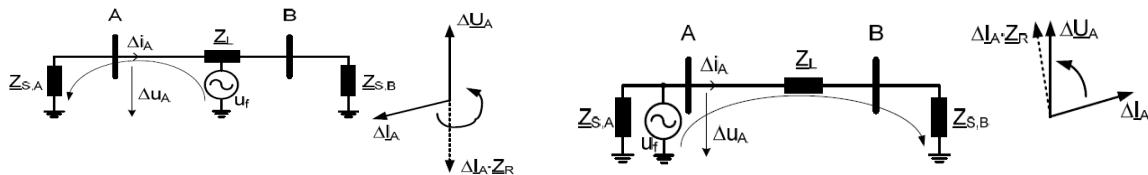


Figure 5.1 Principle of Replica Impedance Comparison (Internal Fault - left) (External fault - right) [18]

Table 5-2. Relation between superimposed components of induced and measured voltages at point A for forward and reverse faults

polarity of half-cycle	Fault Direction			
	Forward		Reverse	
	Δu_A	$\Delta i_A \cdot Z_R$	Δu_A	$\Delta i_A \cdot Z_R$
positive	-	+	-	-
negative	+	-	+	+

The replica impedance should be chosen such that it is close to the source impedance of each point, i.e. Z_{SA} for point A and Z_{SB} for point B relay [19, 12]. The original idea was based on determining the trajectories of both the voltages in a delta-plane, shown in Fig. 5.2 below.

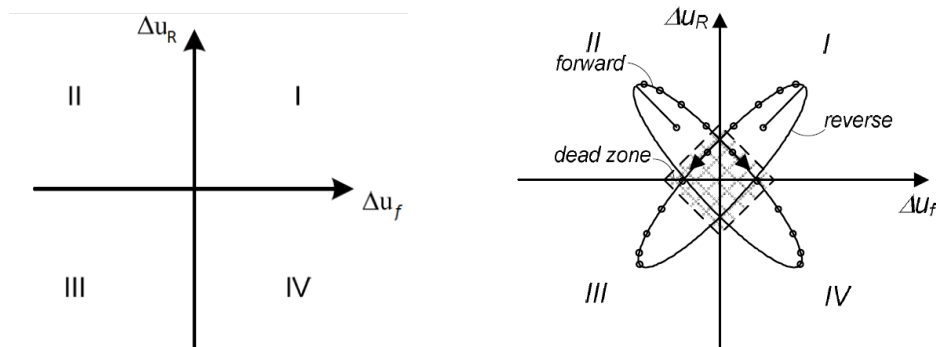


Figure 5.2 Trajectory of compensated delta current on the Delta plane [19]

5.2.1 Salient Features and Limitations of Delta-Plane and trajectory recognition

1. The quadrants acquired by trajectories for forward and reverse faults are coherent with Table 5-2.
2. The circulation of trajectories are positive clockwise for forward faults and negative or counter-clockwise for reverse faults [19]
3. Ideally the shape of trajectory should be a straight line with slope of +1 or -1 for reverse and forward faults respectively if the replica impedance and the actual impedance have the exact same angle (for straight line) and even same magnitude (for slope ± 1). Nevertheless, the elliptical shape arrives due to mismatch between the replica impedance and actual Delta impedance [19], which could have been calculated using Eq. (5.1) below.

$$\Delta Z = \frac{f_{\cos} [\Delta u_{A,f}] + j \cdot f_{\sin} [\Delta u_{A,f}]}{f_{\cos} [\Delta i_{A,f}] + j \cdot f_{\sin} [\Delta i_{A,f}]} \quad (5.1)$$

4. Dead zones are introduced to eliminate the possible mal-operation of relays in case of uncertainty in delta quantities (due to measurement error, etc.), thereby reducing the sensitivity of this method.
5. The necessity to employ potential transformers on relevant nodes in the distribution network makes this approach uneconomical, therefore practically infeasible for directional protection of distribution lines.

I. Stabilization integral

The sensitivity issue can be resolved using a stabilizing integral similar to that of Eq. (5.2). A detailed review of selection of relevant replica impedance is given in [19] and [11]

$$F(\tau) = \int_0^{\tau} \Delta u_f(t) \cdot \Delta u_R(t) dt \quad (5.2)$$

Fig. 5.3 and 5.4 present the description and response of this stabilization integral during forward and reverse faults. The stable variation of this integral in both the positive and negative direction for the respective reverse and forward faults allow this method to determine fault direction within the first cycle (<20ms for 50 Hz) of fault inception.

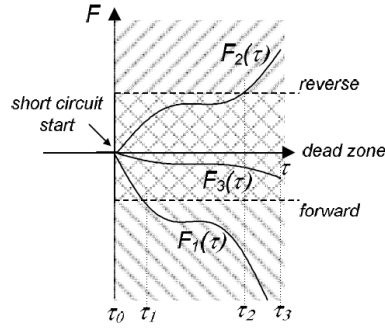


Figure 5.3 Stabilization Integral description [22]

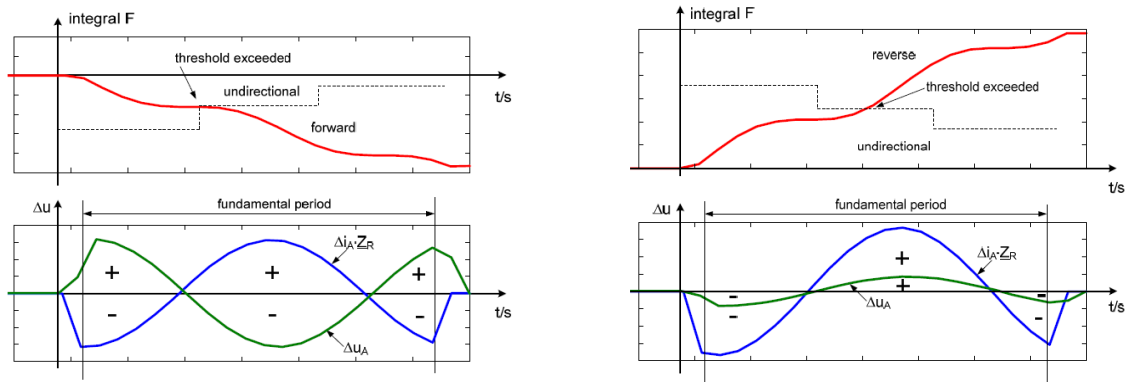


Figure 5.4 Stabilization Integral Response (Forward Fault - left) (Reverse Fault - right)

5.3 Compensated Current (MIMIC Filter) Approach

This method has been discussed extensively by Schweitzer Engineering Laboratories (SEL) in numerous literatures. The accuracy of the replica impedance method, as discussed earlier, depends upon the choice of this replica impedance (ΔZ_R).

Reference [19] and [30] perform a detail sequence-based analysis for conventional shunt faults by calculating the Transient (Delta) Impedances based on phase-ground, phase-phase and positive sequence fault components of the voltage and current. This analysis proves that, ideally, the transient (delta) Impedance calculated using phase-phase and positive sequence fault components correspond to the positive sequence impedance of the source behind the relay (Z_{S1}). Conclusively, in order to improve the performance of the Replica Impedance Method in terms of sensitivity and accuracy, ΔZ_R must coincide with $-Z_{S1}$, as shown in Eq. (5.3)

$$\Delta Z_R = \frac{\Delta V_R}{\Delta I_R} = -Z_{S1} \quad (5.3)$$

The method introduced by SEL is based on the decision of Eq. 5.4 which obtains the compensated current (ΔI_{RC}), given by Eq. 5.5. This relation between the phasor of ΔV_R and the

dot product of the phasors ΔI_R & $(-Z_{S1})$ can be exploited to determine fault direction. A simpler method of representing this relationship is provided in Eq. 5.6, which results in a negative value for reverse faults and positive for forward faults.

$$\frac{\Delta V_R}{\Delta I_R \cdot (-Z_{S1})} = 1 \quad (5.4)$$

$$\Delta I_{RC} = \Delta I_R \cdot (-Z_{S1}) \quad (5.5)$$

$$\text{real} [\Delta V_R \cdot \text{conj}(\Delta I_{RC})] = \Delta v_R \Delta i_R z_{S1} \quad (5.6)$$

The compensated current, which includes the impact of angle of Z_{S1} on the fault component of the current phasor, is obtained in the time domain by using a **MIMIC** (High Pass) filter (tuned to fundamental frequency), with following order:

$$K (1 + s \tau) \quad (5.7)$$

Where, the gain K is chosen such that the overall gain is equal to '1' at 50 Hz while τ determines the filter time constant. The block diagram, presented in Fig. 5.5, reveals the time domain implementation of this method. According to reference [30], the real time current and voltage samples are allowed to pass through a low pass filter (tuned at 50 Hz) to remove noise and other high frequency disturbances which are used to obtain the respective delta components.

The MIMIC Filter consecutively performs two relevant tasks:

- The delay introduced by the MIMIC corresponds to multiplying the current with unit source impedance behind the relay, which fulfills the requirement of Eq. 5.5.
- It also removes any dc offset in the current waveform. The frequency and time domain response of the filter are recorded in Chapter 11.

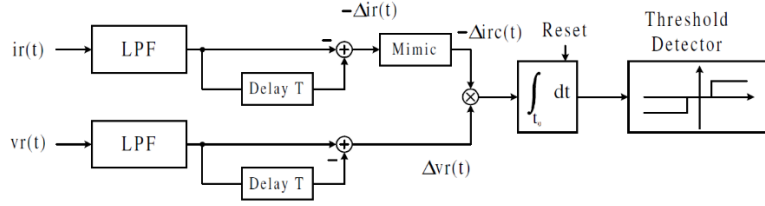


Figure 5.5 Block diagram for Compensated Current Approach in the time domain (SEL) [30]

The integrator and the threshold detector serve as **phase angle comparators** for delta voltage and compensated delta current [63]. The output of the integrator, given by Eq. 5.8, results in a positive value if the ΔV_R & ΔI_{RC} are within $\pm 90^\circ$ of each other. The ‘Reset’ signal is received when the Fault is detected by the fault detection block (t_0), which is later explained in Chapter 11. Therefore, the cumulative output of the integrator after the fault is either positive (for forward faults) or negative (for reverse faults).

$$\int_{t_0}^{t'} \Delta V_R \cdot (\Delta I_{RC}) dt \tag{5.8}$$

Salient Features and Limitations:

- One of the critical decisions for the implementation of this algorithm is to determine the correct current and voltage quantities as I_R and V_R . These quantities should be chosen such that the transient impedance (ΔZ_R) is equal to $-Z_{S1}$ (as explained in Eq. 5.3 earlier). Table 5-3 presents the relevant quantities (either phase-phase, phase-ground or positive sequence) which would satisfy this requirement [30]. It is clear that both the phase-phase and the positive sequence delta quantities fulfill the criteria under all types of faults. However, only phase-phase quantities are chosen for this report and the equivalent simulation results are provided in Chapter 11.

Table 5-3 Transient Impedance corresponding to $-Z_{S1}$ during certain fault conditions

Fault Type	Incremental Impedances
A-G	$\Delta Z_{ab}, \Delta Z_{ca}, \Delta Z_1$
B-C	$\Delta Z_b, \Delta Z_c, \Delta Z_{ab}, \Delta Z_{bc}, \Delta Z_{ca}, \Delta Z_1$
BC-G	$\Delta Z_{ab}, \Delta Z_{bc}, \Delta Z_{ca}, \Delta Z_1$
ABC	$\Delta Z_a, \Delta Z_b, \Delta Z_c, \Delta Z_{ab}, \Delta Z_{bc}, \Delta Z_{ca}, \Delta Z_1$

- In the frequency-domain, the same algorithm can be represented by the block diagram of Fig 5.6.

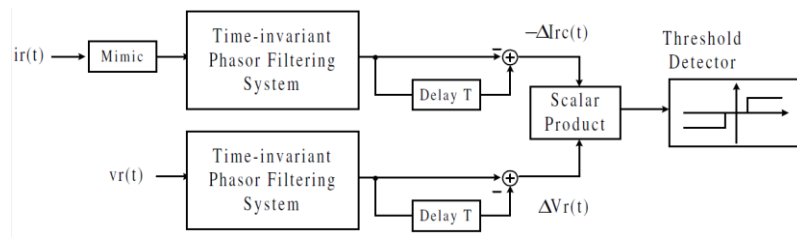


Figure 5.6 Block Diagram of Compensated Current Approach in frequency domain

- The calculations hold strong for parallel lines as well. The phase angle of transient impedance corresponds with $-Z_{S1}$
- One of the limitations of this method is its application for series compensated lines, especially if the capacitors is located behind the relay and its corresponding impedance is larger than the positive sequence impedance of the local source, resulting in inaccurate directional decision [32]. This, however, is not a problem for the distribution network.
- When using phase-phase quantities as I_R and V_R , it is possible to determine the faulted phase, which can be used for single pole tripping. This is not completely relevant for current distribution systems.

5.4 Positive Sequence Transient Impedance Method

The idea to use positive sequence fault components (PSFC) for fault direction determination offers unique advantages over the methods discussed earlier, which were primarily dependent on fundamental-frequency components [8]. Some of these advantages include:

1. Unlike negative and zero sequence components, PSFC exist for all types of faults
2. Although the positive sequence components are highly influenced by changing loads, PSFC are independent of load conditions.
3. The most important advantage is the phase relationship between the voltage and current PSFC, which is fundamentally influenced by the positive sequence impedance between the relay point and the neutral point of the system.

The positive sequence components for voltage and current are used to obtain the pre-fault positive sequence network and the positive sequence fault component (PSFC) network of Fig. 5.7 for both the internal and external fault conditions.

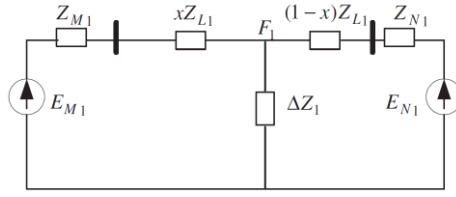


Figure 5.7 Positive Seq. Prefault Circuit (Superposition Principle) [8]

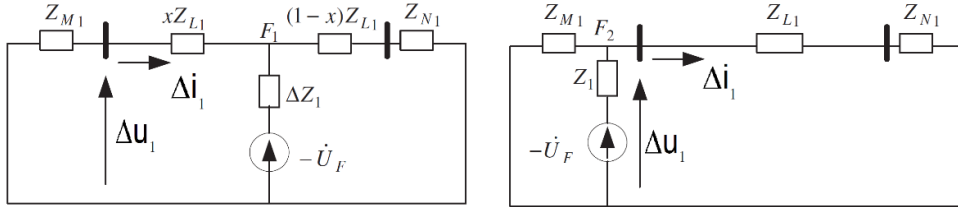


Figure 5.8 Positive Seq. Pure-fault Circuit (Left: Internal fault) (Right: External fault) [8]

The relationship between the voltage and current PSFC for forward and reverse faults are given by Equations 5.9 and 5.10

$$\Delta U_1 = -\Delta I_1 \cdot Z_{M1} \tag{5.9}$$

$$\Delta U_1 = \Delta I_1 (Z_{L1} + Z_{N1}) \tag{5.10}$$

There are a number of available methods to exploit these relationships for fault direction determination; phase-relationship being one of the simpler ones. The essential basis of this method is given by Eq. 5.11, while Fig. 5.9 presents the operating and blocking regions of the PSFC phase relation method.

$$\arg \frac{U_1}{I_1} = \left\{ \begin{array}{l} -90^\circ \text{ or } 270^\circ \text{ for forward fault} \\ 90^\circ \text{ for backward fault} \end{array} \right\} \tag{5.11}$$

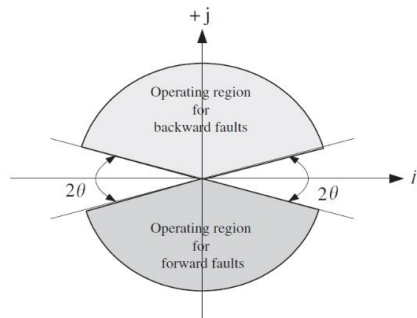


Figure 5.9 Forward and Reverse fault operating regions for Positive Seq. Approach

Fig. 5.10 gives the systematic process for this approach. The magnitude of PSFC calculated after reconstructing the signal using DFT is used to detect fault condition based on Adaptive

Threshold technique mentioned earlier. Whereas, the phase angles of both the voltage and current PSFC determines fault direction.

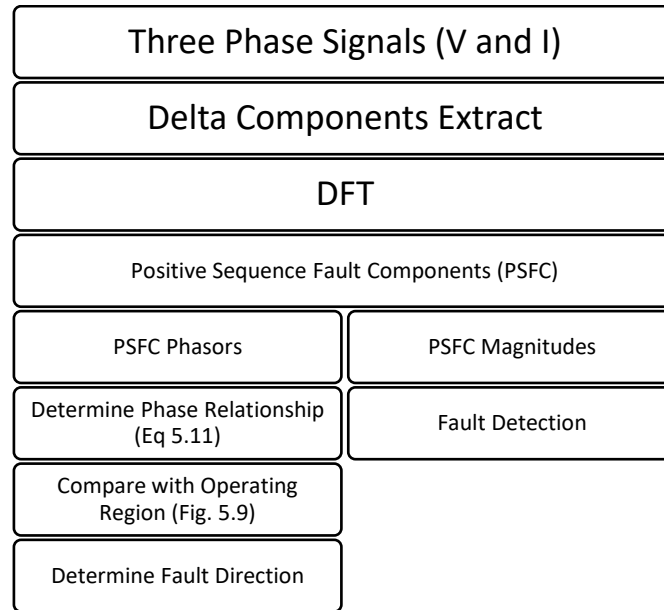


Figure 5.10 Systemic process for Positive Sequence Transient Impedance method

5.4.1 Salient Features and Limitations:

1. Satisfactory operation for all types of faults
2. Insignificant impact of load variation
3. Good fault resistance coverage
4. There are no dead zones observed due to insignificant voltage for close-in faults
5. The directional decision is held stably.
6. The DFT block requires one complete cycle's information after the fault to correctly determine the fault direction
7. Following limitations have been listed in Reference [8] and observed in simulations as well:
 - a. Source strength results in sensitivity issues. For e.g. for a strong local source with fault near the remote end, the voltage PSFC might be negligible and may result in inaccurate decision. Similar observations have been recorded for weak local source and remote end faults (with high resistance) resulting in insignificant current PSFC
 - b. Large fault resistance results in sensitivity and dependability issues.

8. These problems can be resolved using compensated voltage techniques discussed in references [8] and [24].

5.5 Average of Superimposed Quantities:

In order to reduce the number of samples and processing requirements, an alternative method is proposed in [21], which determines the direction of fault by averaging the superimposed quantities over one cycle. Ideally, the average of sinusoidal voltage and current signals are equal to zero under steady state conditions given by Eq. 5.12

$$\langle v_{\text{postfault}}(t) \rangle = \langle v_{\text{prefault}}(t) \rangle + \langle \Delta v(t) \rangle = \langle \Delta v(t) \rangle \quad (5.12)$$

Therefore, a non-zero value or a value above a certain threshold suggests a faulted condition. The averaging filter is based on Eq. 5.13, the data window slides from sample to sample.

$$\langle x[n] \rangle = \frac{1}{N} \sum_{n=1}^N x[n] \quad (5.13)$$

Reference [21] suggests that the averaging filter brings an inherent problem, which increases the error in detecting correct polarities of superimposed voltages and currents within certain windows. However, these errors can be minimized by simple mathematical modifications as proposed in [21].

5.5.1 Salient Features and Limitations:

1. Sampling rate of 64 samples per cycle (3.2 kHz for 50 Hz system) is enough and fault is detected using 8 consecutive superimposed cycles (therefore with 1/8th period of a cycle)
2. Phase selection is rather simple and simple overcurrent settings approach can be used to detect faulted phase(s).
3. The proposed flowchart for determining fault direction is presented below. Fault is detected when C_r crosses a threshold, while positive C_r suggests reverse fault and vice versa.

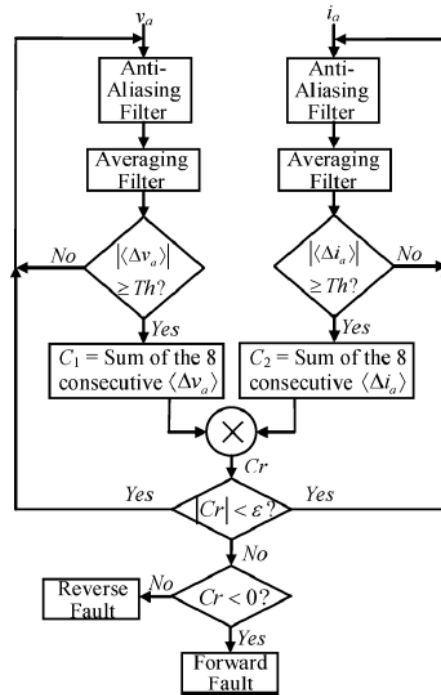


Figure 5.11 Flowchart for Average Window based Transient Energy directional protection [21]

4. Simulations performed in [21] suggest:
 - a. Excellent fault resistance coverage.
 - b. Fault location does not affect the operation of the relay
 - c. DC component present in delta quantities depends heavily on the fault inception angle. Simulations suggest complete coverage from 0 to 360 degrees of fault inception angle and the maximum detection delay is found to be 10 mS.
 - d. The performance of algorithm for IEEE PSRC proposed system is satisfactory for operation of double-circuit lines, multi-terminal lines, power-swings and series compensated lines.
5. Extensive tests performed in Chapter 11 reveal that this method is quite sensitive to power swings and may result in insecure operation under such circumstances.

Unavailability of voltage information for all the relevant nodes in the distribution network limits the practical application of this method.

Chapter 6 - Current-only Transient-based Directional Protection

The protection challenges associated with active distribution networks have been drawn up in detail in Chapter 02. One of the explored solutions to these problems is employment of directional supervision or piloted directional protection. Such directional elements require both the current and voltage information for accurate operation [46]. In order to keep the protection schemes economic while ensuring security and dependability, the directional protection algorithms proposed for future distribution networks must avoid wide-scale installation of voltage transformers (VTs). Therefore determining the direction of fault based on current information only is a necessity [57 – 62].

Among other methods, current-only directional relays determine fault direction on the basis of *phase-change* between the post-fault and pre-fault currents. Referring to Fig 6.1 and 6.2, the difference between current phase change in case of forward (F2) and reverse (F1) faults, as seen by the relay, can be used to discriminate between forward and reverse faults [56 – 58].

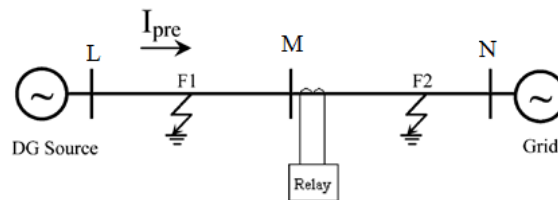


Figure 6.1 Forward and Reverse Fault Condition in a bidirectional feeder

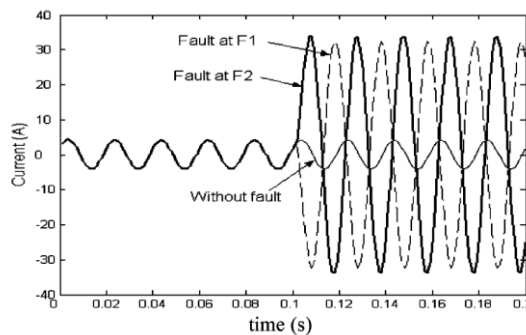


Figure 6.2 Phase change of current during forward (F2) and reverse fault (F1) for relay after bus M

This method is ideal for directional protection of radial unidirectional feeders and the phase-change of either the positive sequence currents or each of the three phases can be used for this purpose [56].

6.1 Theoretical Analysis:

The sources 1 and 2 in Fig 6.3 represent two separate distribution networks consisting of DERs and relevant strong grids on either end. The initial power flow direction is given by P, while I_{pre} represents the pre-fault current in the network. F and F' represent the internal and external faults respectively.

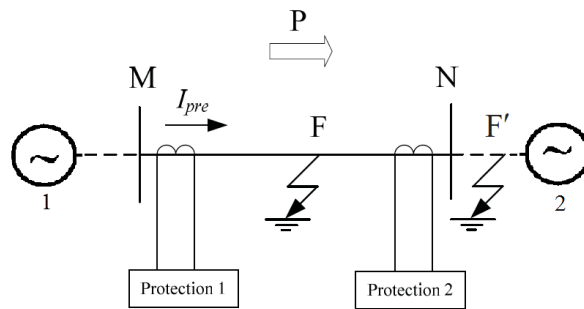


Figure 6.3 Physical setup of the current-only directional protection with internal fault (F) and external fault (F')

6.1.1 Internal Fault (F)

The pre-fault and post-fault circuits, based on superposition principle, are given in Fig 6.4 for internal fault condition. According to Fig. 6.3, the prefault current is given by Eq. 6.1

$$I_{pre} = \frac{U_M - U_N}{Z_{MN}} \tag{6.1}$$

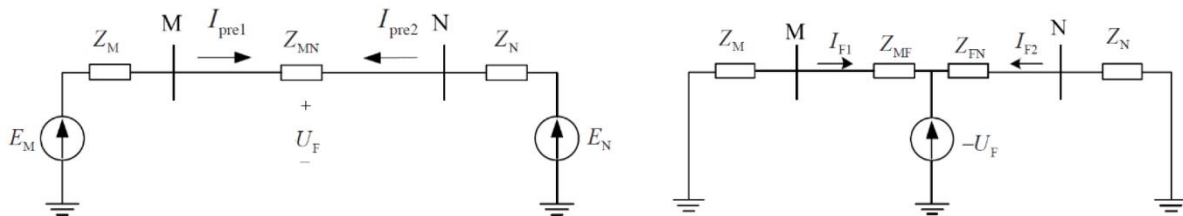


Figure 6.4 Application of superposition principle for internal fault condition

Therefore, the currents I_{pre1} is equal to I_{pre} while I_{pre2} is equal in magnitude but opposite in direction to the pre-fault current mentioned in Eq. 6.1. If Z_M and Z_N are the system impedance

for 1 and 2 respectively and U_F represents the fault point pre-fault voltage, then the delta post-fault currents I_{F1} and I_{F2} for bolted fault condition are given by Eq. 6.2 and 6.3 respectively.

$$I_{F1} = - \frac{- U_F}{Z_M + Z_{MF}} = \frac{U_F}{Z_M + Z_{MF}} \quad (6.2)$$

$$I_{F2} = - \frac{- U_F}{Z_{FN} + Z_N} = \frac{U_F}{Z_{FN} + Z_N} \quad (6.3)$$

The voltage and current phasor diagram given in Fig 6.5 represents the change in current phase angle for both the remote and local ends in case of internal fault condition. The total postfault currents of each end are the sum of respective pre-fault and postfault-delta currents (superimposition principle). This internal fault is to be considered as forward fault for both the protection 1 and 2.

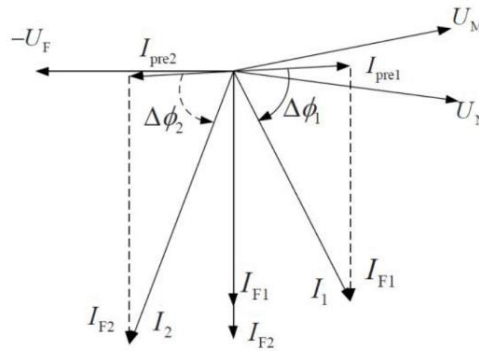


Figure 6.5 Variation in current phasor for local (1) and remote (2) ends during internal fault condition

6.1.2 External Fault (F')

Fig 6.6 gives the superimposed pre-fault and post-fault circuits for external fault condition. The delta-post-fault currents (Eq. 6.4 and 6.5) are used to plot the current phasor diagram of Fig 6.7. The external fault is considered to be forward fault by the relay at bus M and reverse by the relay at bus N. The difference in signs of Eq. 6.4 and 6.5 correspond with this observation.

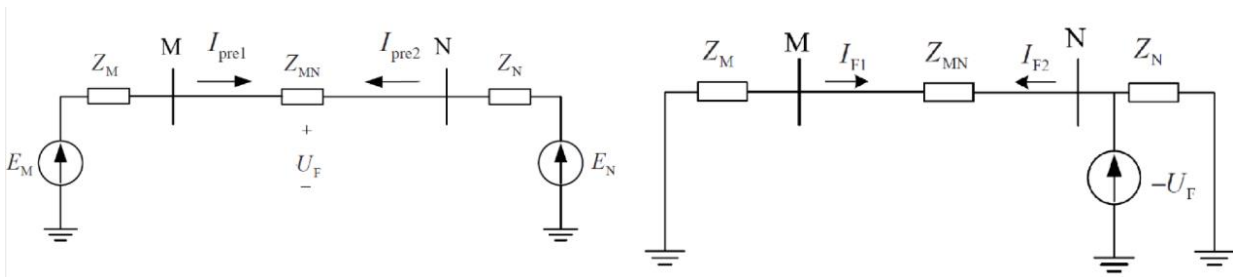


Figure 6.6 Application of Superposition principle for external fault condition

$$I_{F1} = - \frac{-U_F}{Z_M + Z_{MN}} = \frac{U_F}{Z_M + Z_{MN}} \quad (6.4)$$

$$I_{F2} = - \frac{-U_F}{Z_M + Z_{MN}} = - \frac{U_F}{Z_{FN} + Z_N} \quad (6.5)$$

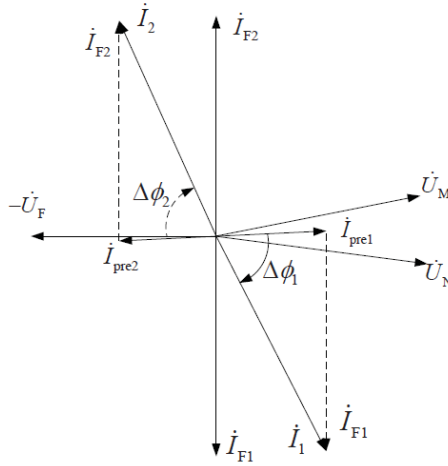


Figure 6.7 Variation in current phasor for local (1) and remote (2) ends during external fault condition

6.1.3 Reversal of Pre-fault Current Direction:

Fig. 6.8 gives the current and voltage phasors in case of internal and external fault condition, if the pre-fault current direction is reversed. It must be noted that the current phase change for each end is opposite in polarity to the previous case, which means that the definition of forward and reverse current would vary with the variation in powerflow direction variation. This is the potential drawback that current-only directional protection algorithms based on pre-fault and post-fault delta currents carry.

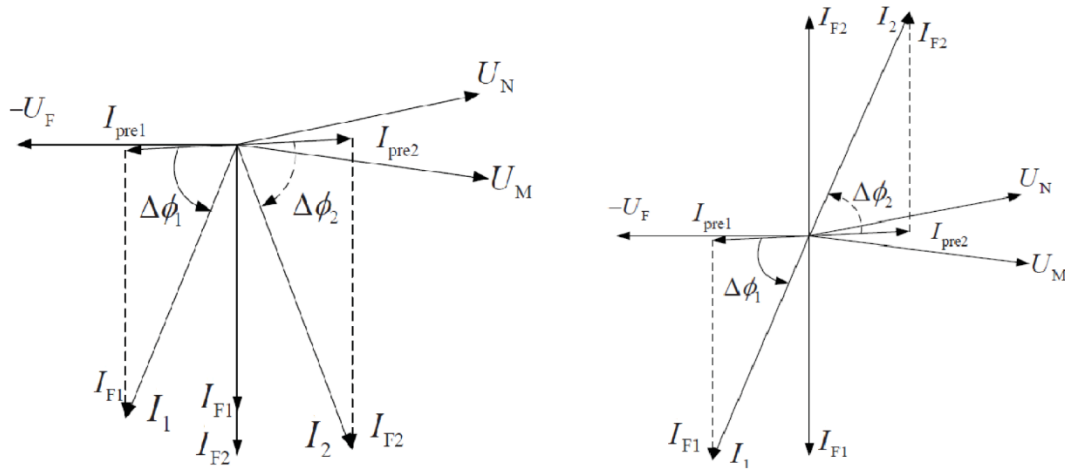


Figure 6.8 Variation in current phase for local (1) and remote (2) ends during internal fault (left) and external fault (right) condition during reversed power flow

6.2 Relevant current-only directional algorithms:

The distinctive difference in current phase change for forward and reverse faults can be utilized as the means to determine fault direction. A contented research reveals that current-based directional algorithms have been extensively studied since the 1990s. Some of the methods have been listed below:

- Delta Phase Angle of the Negative Sequence Current (**Pradhan and Jena**) [56]
- Modal Transformation method for ground faults (**Popov and Xyngi**) [47]
- Phase Angle Difference of Parallel feeders currents (**Youyi**) [55]
- Delta Phase Angle of the Positive Sequence Current (**Pradhan**) [54, 56]
- Delta Phase Angle of each of the three Phase Currents (**Abhishek**) [58-59]
- Post fault current based method (**Jalilian and Tarafdar**) [57]

Table 6-1 summarizes the salient features and limitations of each of these methods. References [54-62] can be examined for further elaboration on each method. The theoretical analysis and a substantial part of the discussion would be focused on Pradhan's [56], Abhishek's [58-59], Jalilian's [57] and Xinyue's [61] work.

In order to ensure correct operation, the phase angle obtained using one of the Fourier transform methods must lie within the $-\pi < \phi < +\pi$ range for each of these current-only methods.

Table 6-1 Reviewed current-only transient-based piloted directional protection schemes

Method	Salient Features	Limitations
Phase Change in Positive Seq. Current [54, 56]	a. Utilizes fault and pre-fault phasors of Positive Sequence Currents b. Applicable to Distribution Networks with large DG penetration	a. Requires Pre-fault Power Flow Direction (only Suitable for Radial Networks) b. Sensitive to Noise (depends on filtering technique) c. Sensitive to frequency deviation, system unbalance and measurement errors
Phase Change in Negative Seq. Current [56]	a. Utilizes fault and pre-fault phasors of Positive Sequence Currents	a. Requires Power Flow Direction b. Sensitive to Noise c. Only valid for unbalanced faults d. Susceptible to unbalanced load condition (common in Distribution Network)
Modal & Wavelet Transformation Method [47]	a. Novel Transient based method b. Applicable to Distribution Networks with large DG penetration c. Doesn't require extensive communication or initial power flow direction	a. Requires Multiple Parallel branches to determine fault direction b. Sensitive to frequency deviation, system unbalance and measurement errors
Phase Angle Difference of Parallel line currents [55]	a. Doesn't require initial power flow direction b. Not Sensitive to Noise	a. Requires Multiple Parallel lines to determine fault direction
Delta Phase Angle of each Phase [58-59]	a. Utilizes fault and pre-fault phasors of each phase current	a. Requires Pre-fault Power Flow Direction b. Sensitivity depends on Sampling Frequency c. Sensitive to frequency deviation, system unbalance, measurement errors and noise
Post-fault current derivative method [57]	a. Derivate the post fault current to obtain the polarizing quantity which is then compared with the phase of original post-fault current b. Doesn't require pre-fault current's information	a. Blind spots at certain fault inception angles b. Requires directional supervision c. Sensitive to sampling frequency, measurement errors and noise

6.2.1 Delta Phase Angle of post-fault and pre-fault currents:

Referring to Fig. 6.1 and 6.2, Pradhan and Abhishek define the basis to determine fault current direction. The simplistic algorithm to obtain $\Delta\theta$ is presented in Fig 6.9 and the basis for directional decision is summarized in Table 6-2. It is clear that this approach would require the pre-fault current's direction for accurate operation because the phase change is dependent on both the fault location and the pre-fault current's direction [58]. The current ' I ' can be either the phase currents of each phase or the positive sequence current of the three-phase network. The application of such algorithms would be economical and fairly accurate for radial networks with vertically integrated power flow. However, with the increase in DG integration in the distribution networks additional hardware and directional supervision would be required. Moreover, the limitations listed in Table 6-1 are also relevant.

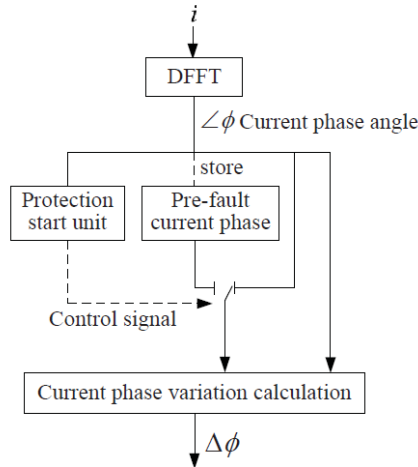


Figure 6.9 Current-only directional protection algorithm [54-56]

Table 6-2 Decision mechanism for current-only directional protection [54 - 56]

Fault Location	Phase Change
Fault in direction of pre-fault current	Negative
Fault opposite to pre-fault current's direction	Positive

6.2.2 Delta Phase Angle ($\Delta\theta$) comparison of Local and Remote Ends:

The method developed in reference [61] utilizes the information mentioned in Table 6-2 and determines the fault direction by means of communication. Referring to the current phasors plot of Figures 6.5, 6.7 and 6.8, one can easily identify a pattern in current phase change for internal and external faults as seen by the local and remote end relays. The approach is rather simplistic and Table 6-3 elaborates it further.

Table 6-3 Operating principle for delta phase angle comparison of local and remote end currents [61]

Current Phase Change ($\Delta\theta$)		Fault Decision
Remote End	Local End	
Positive	Positive	External
Positive	Negative	Internal
Negative	Negative	External
Negative	Positive	Internal

The phasor diagrams of Figures 6.5, 6.7 and 6.8 have been drawn for a purely inductive line whose impedance angle aligns with the source impedance. Moreover, the practical errors

involved in calculating the current phasors tend to reduce the accuracy of such methods. This, however, can be resolved by adding a block angle (Θ) which separates the two operating regions, thereby changing the operating criteria from positive and negative current delta phase angle ($\Delta\theta$) to $\Theta < \Delta\theta < \pi - \Theta$ and $-\pi + \Theta < \Delta\theta < -\Theta$ respectively. The overall system is given in Fig 6.10, while the algorithm is provided in Fig 6.11

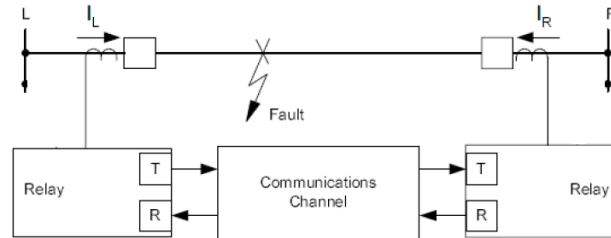


Figure 6.10 System description of delta-phase-angle comparison method for current-only piloted directional protection

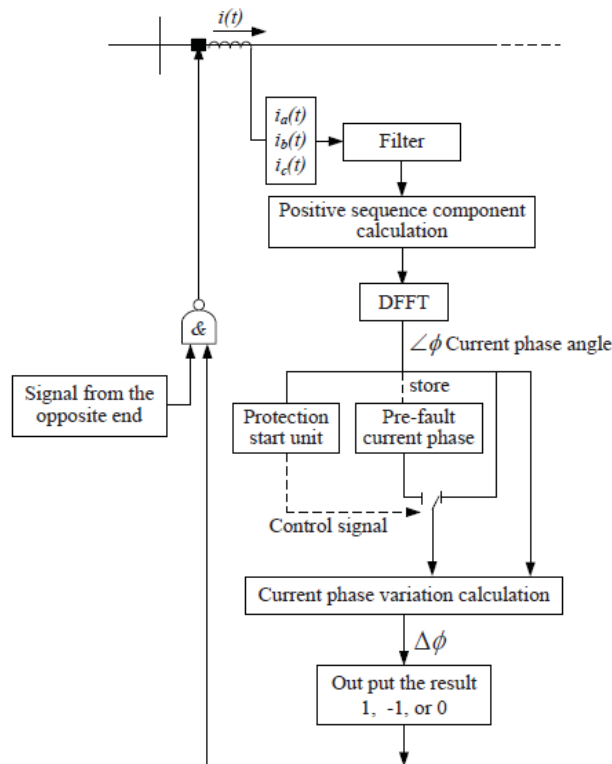


Figure 6.11 Flowchart for current-only method under discussion [61]

I. Limitations:

The algorithm proposed in [61] results in dependability issues when used for protection of lines with multiple branches. Therefore, faults on networks with integrated DGs may result in

inaccurate operation. Similar problems have been observed for small load angle (low load) conditions.

6.2.3 Post-fault current based method

Reference [57] presents a unique method to determine fault current direction based on post-fault current information only. The positive and negative derivatives of the post-fault current phasor are obtained according to Equations 6.6 and 6.7. These derivatives are used to obtain the operating quantity (I_{ref}) which is then compared with the polarizing quantity which is the post fault current itself. The difference between the phase angles of I_{ref} and post fault currents is then used to determine the fault direction on the basis of Fig. 6.12

$$+i'[k] = \frac{1}{2 \omega \Delta T} (i[k + 1] - i[k - 1]) \quad (6.6)$$

$$-i'[k] = \frac{1}{2 \omega \Delta T} (i[k - 1] - i[k + 1]) \quad (6.7)$$

Where ω represents the electrical frequency in rad/s and ΔT is the sampling time in seconds, while k represents the sample number.

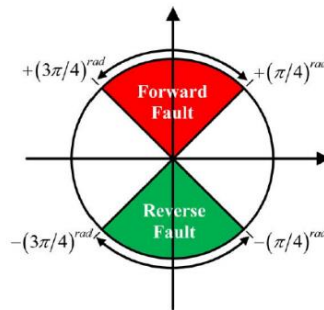


Figure 6.12 Operating regions for forward and reverse faults [57]

An important feature of this method is its independence of the power flow direction. The directional decision is not affected by bidirectional power flow operation, which makes it extremely relevant for the protection of modern distribution networks. A detailed flowchart description of this method has been provided in Fig 6.13. The detection of fault is based on the adaptable threshold method (Eq. 4.6). This algorithm has been critically reviewed and several observations, shortcomings and improvement have been listed in Chapter 11 after extensive testing. Reference [57] can be reviewed for further information on this approach.

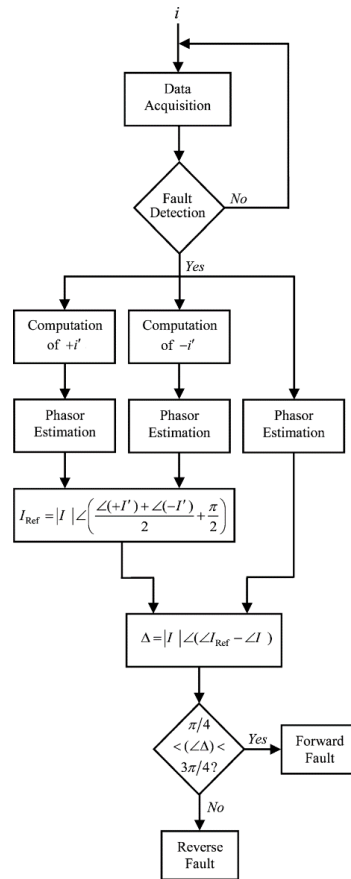


Figure 6.13 Flowchart for post-fault current based directional protection

I. Limitations:

The employment of Fourier Transform to obtain current phasors delays the correct fault direction definition by one electrical cycle. This delay, however, is not a matter of concern for distribution networks protection. Extensive testing reveals that the algorithm fails to determine the actual fault direction at certain pre-fault current phase angles. Among other things, these phase angles depend upon the line and source impedance angles along with the fault inception instant/angle. The pre-fault current phase angles at which correct fault direction is obtained for forward and reverse power flow are listed in Table 6-4; rest of the angles can be called *blind spots* of the algorithm. However, these *blind spots* can be removed by employing power flow direction supervision and using adaptive direction threshold. Chapter 11 further presents the performance and limitations of this method. However, the impact of power flow direction supervision and adaptive direction threshold are not presented in this report because of the originality of suggested improvements.

Table 6-4 Pre-fault current's phase angle range for accurate operation of algorithm of Reference [57]

Forward Power Flow	
Fault Direction	Pre-fault Current Phase Angle Range (Degrees)
Forward	-150 to +150
Reverse	+150 to -150

Reverse Power Flow	
Fault Direction	Pre-fault Current Phase Angle Range (Degrees)
Forward	+150 to -150
Reverse	-150 to +150

Chapter 7 - Differential Line Protection

7.1 Salient Features of Line Differential Protection:

The idea to protection transmission lines using well established differential protection method has been around for ages. The popularity of this scheme is based on following distinct advantages:

- Selective (operates for intended faults only).
- Secure (doesn't operate for faults that it is not intended for).
- Performance is good for evolving/cross country faults [29].
- Immunity against power swings, mutual coupling & series impedance unbalance (series compensated lines) [5, 15].
- Data sampling principle in numerical differential protection can be used for harmonic evaluation and sequence components [5].
- Since this scheme is primarily a part of current-only unit based protection, following inherent features are listed:
 - No Potential Transformer required (therefore relief from Fuse Failure, transients, CCVT & Power swings).
 - Extremely sensitive in detecting earth faults, advantage over distance protection, especially for short lines.
 - Segregated phase protection possible (therefore good for evolving, cross country faults, single pole tripping and series compensated lines).
- Causes of false differential current include:
 - Line charging current (cables and long OHL) and Tapped load (Both Resolved by Phase differential element with high minimum pickup or use extremely sensitive negative sequence differential for unbalanced faults which is sensitive because low negative sequence charging current).
 - Channel time-delay.
 - CT saturation during external faults (both these errors are resolved by careful selection of operating characteristics).

7.2 Operating Principle:

The operating principle of line differential protection is essentially the same as other differential protection schemes and a simplistic representation is given in Fig. 7.1.

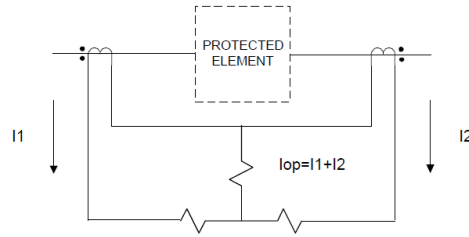


Figure 7.1 Simple representation of Differential Protection

For a single slope differential relay, following criteria must be met for relay operation:

$$I_{OP} \geq K \cdot I_{RT} + K_0 \quad (7.1)$$

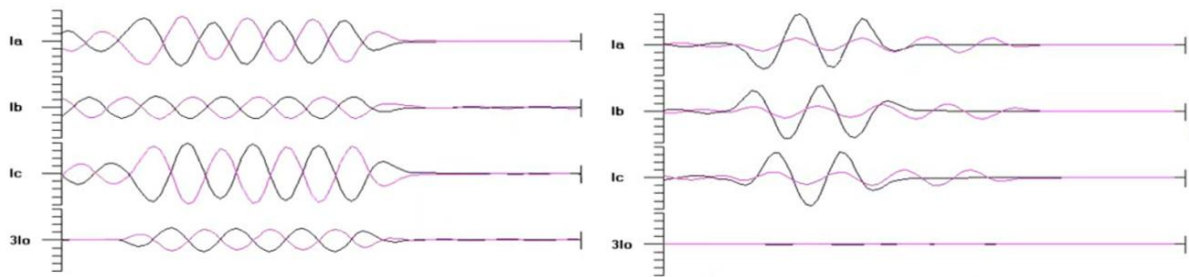


Figure 7.2 Comparison of local and remote currents (Left: External Fault), (Right: Internal Fault)

Where current transformer readings of local and remote ends of the lines are represented by black and pink colors respectively.

7.2.1 Operating and Restraining Quantities:

In order to prevent certain inherent differential protection issues like CT mismatch, saturation, capacitive leakage currents, pilot wire capacitive mismatch etc., a restraining region is usually defined. Restraining current can be any arbitrary function of either components of the differential currents and depends on the relay design and manufacturer [5]. A number of commonly used restraining quantities are listed in [29] and [5]

$$I_{RT} = k |I_L - I_R| \quad (7.2)$$

$$I_{RT} = k (|I_L| + |I_R|) \quad (7.3)$$

$$I_{RT} = \text{Max}(|I_L| \cdot |I_R|) \quad (7.4)$$

$$I_{RT} = \sqrt{|I_L| \cdot |I_R| \cos\theta} \quad (7.5)$$

Whereas operating current is always the sum of local and remote currents

$$I_{OP} = |I_L + I_R| \quad (7.6)$$

7.2.2 Operating and Restraining Range (For a Dual Slope Differential Relay)

The dual slope characteristic ensures secure performance in case of external faults by introducing adaptive restraint regions.

- Region 1: Slope = 0, where current flow is very small, therefore the performance of CTs on each end is similar and mismatch is low. Also CT saturation is not an issue in this region.
- Region 2: Through-current (might be by external faults) is larger than region1 (3.5 to 5 pu), slope $K1 > 0$. Since restraining current which directly represents load current in most conditions is higher therefore CT mismatch might be an issue.
- Region 3 represents heavy line loading as a result of which one of the CTs might saturate earlier than the other therefore slope is set even higher than $K1$; hence restraining region is more significant in this case to avoid malfunctioning or mal-operation.

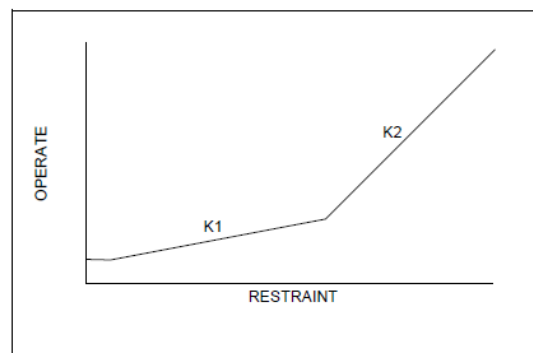


Figure 7.3 Dual Slope operating characteristics of Differential protection

7.3 Historical Development of Line Differential Relays:

According to reference [26], the foremost line differential relays utilized pilot-wires for communication using sequence voltage imposition. These relays were not reliable as the distance protection even with employment of twisted pair wires, insulating transformers, neutralizing reactors etc. However two separated scientific breakthroughs boosted the applications of these relays: Fiber-optic communication links and GPS synchronization. The studies conducted up until 2004 indicates that the accuracy of GPS synchronized line

differential relay is higher than distance protection which required adequate parameterization of protected lines; whereas employment of fiber optic links allowed these relays to be protect lines as long as 160 km without additional equipment [26 -29]. However, Fiber Optic links do cause some challenges:

- Propagation Delay (therefore data synchronization is necessary)
- Signal corruption
- Communication network (Switch N/W, Mux, bandwidth needed, Bits rate etc.)
- Hence back up protection necessary

Initially communication BW (up to 4 kHz) was limited therefore limited data could be transmitted over the distance. Therefore, the local relay converted the current waveform into its respective Fourier coefficients before transmission. The remote end would receive these coefficients and reconstruct the signal using inverse Fourier transform based on these coefficients, then it would perform differential comparison with the local signals of the second relay.

Presently, communication channel BW has increased significantly (56 to 64 kbit channels available); therefore, sampled data at a good sampling frequency can be sent over the communication channel. Hence digitized version of analysis/differential comparison can be performed. Moreover, harmonic analysis (2nd, 3rd and 5th harmonic for example) can be performed on this sampled data and sequence components can be calculated as well. Hence, complete information about both ends of the lines is present. Also because of increased BW, segregated phase protection can also be employed where each phase can be examined independently (because of larger amount of possible data transfer due to the digital communication).

7.4 Limitation of Conventional Line Differential Protection:

The conventional method of employing Line differential protection faces limitations under certain circumstances, some of which are listed below:

1. Breaker Connection in lines:
 - a. Ring connection & breaker and a half scheme: The actual line current is difficult to determine using conventional approach for these schemes. Problems associated with these schemes can be resolved by simplistic methods including

manipulating CT connections for analog relays or employing corrective measures in the algorithm for digital relays.

2. Transformer terminated lines:

- a. Inrush Current: The problems associated with transformer inrush current are resolved in digital relays by monitoring 2nd harmonic content of the current.
- b. Transformer Vector Group: The phase and amplitude correction algorithm can easily be employed in modern digital relays. Moreover, zero sequence trap based on symmetrical component calculation can resolve possible mal-operation issues due to external ground faults on grounded Y side of a D-Y transformer.

The remaining limitations require detail analysis, therefore are listed separately in the following sections.

7.4.1 High Resistance Fault on the line:

In case of high resistance faults, the fault current can be so low as compared to the restraining current that it doesn't enter the operating region of the differential relay.

This problem can be resolved by using Negative Sequence differential element. The negative sequence currents, which are generated by the fault, distribute in both sides of the line. These Negative sequence currents are compared at the two line terminals and compared by each side's relay. Moreover, the current settings for negative sequence currents can be much sharper/sensitive (as low as 0.04% therefore 10 times more sensitive than normal differential current) than positive ones because of their relative small per unit value under normal and even fault conditions [5-6]. However, this application is only applicable to unbalanced faults; therefore, three-phase fault detection cannot be performed using this method [29]

7.4.2 Capacitive charging currents:

The capacitive charging currents are prominent in cables and HV/EHV long lines. As seen in Fig. 7.4, the normal capacitive charging current I_c may seem to be internal fault current for differential protection. Therefore I_{d_min} must be set above I_c (usually 2.5 times), which can reduce the sensitivity of this protection.

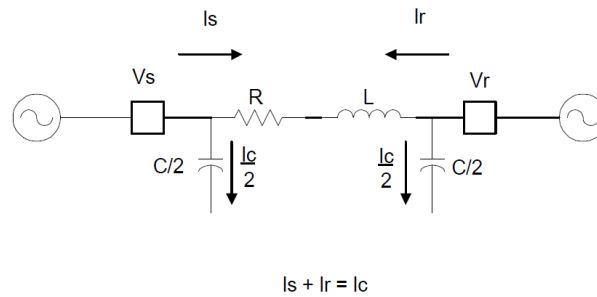


Figure 7.4 Indication of capacitive charging current in a medium length transmission line

In modern relays, the charging current can automatically be calculated by the relay as soon as the line is energized, I_{d_min} can automatically be set by the relay based on I_c . This is performed using following steps:

- a. Measure fundamental differential current under steady state conditions (i.e. no start signal, internal external fault or line energizing etc. during the measurement period)
- b. Since this differential current is the charging current of the line at steady state, therefore a bias current is added to it in order to null out the differential current.
- c. As a result the effect of charging current is nullified automatically by the relay. Hence manual compensation for charging current by setting the minimum differential current is not needed.

However, it must be noted that this method of compensating for charging current can reduce the sensitivity of line differential relays. Especially the Fault Resistance Coverage is significantly reduced in case of high resistance faults, which might be defined using Negative Sequence currents to ensure sensitive operation.

7.5 DATA Communication in Line Differential Protection

7.5.1 Communication Architecture:

Each line differential relay (installed at each terminal) can operate in two possible modes [5-6, 15]:

1. Master: In this mode, the relay receives the current information from all the associated relays and takes trip/restraint decisions for all the respective terminals based on the differential calculations performed. The logical trip/restraint commands are then transmitted to the respective relay.

2. **Slave / Remote:** In this mode, relay only transfers the complete current information to the master and awaits trip/restraint signal. The differential calculations are not performed by the relays in this mode.

As a result of this, numerous communication architectures are possible. For a 2-terminal line, 2 possible configurations are Master-Master and Master-Slave.



Figure 7.5 Two Terminal Master-Master Configuration for line differential protection

While for a three terminal line, the configuration can range from having 3 masters to only one master, as shown in figure below.

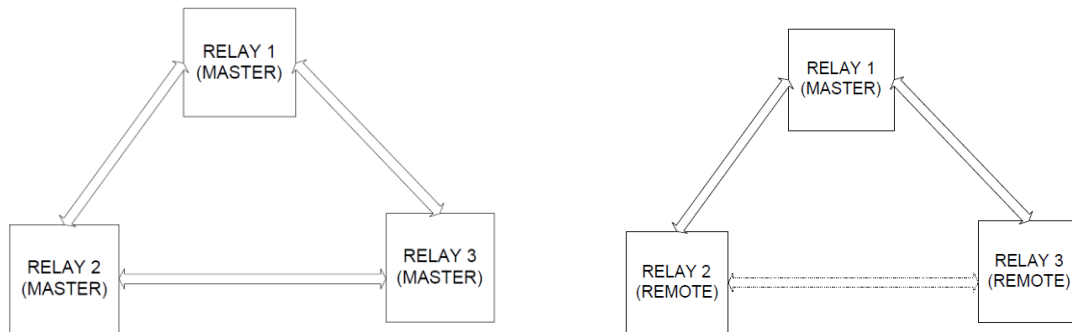


Figure 7.6 Multi terminal Configuration (Left: Master-Master), (Right: Master-Remote)

Master-Master requires all the relays to communicate with all the other relays. Therefore large amount of data and complex communication configurations are needed. Moreover provision of redundant communication paths must be ensured. Operating only one relay in Master configuration in a multi terminal line reduces the channel requirements significantly (a 5-terminal system would require 10 bidirectional communication channels in Master-Master configuration, but only 4 channels in the Master-Slave one); this, however, is not preferred for a reliable system.

7.5.2 Communication Delay Correction / Data Synchronization:

Synchronization of data is extremely important in differential protection schemes to avoid false tripping. Following popular methods of delay corrections are discussed:

- **Echo Method / Ping-Pong method:** This method is only applicable for lines where communication route is always the same. Experimentally, 1 sends data to 2 which is reflected back to 1. The time delay for data transfer between the 2 points

is determined using the principle described in figure below, where 1 sends data to 2, which delays it and then compares it with 1 to make sure the data compared are from the same instant.

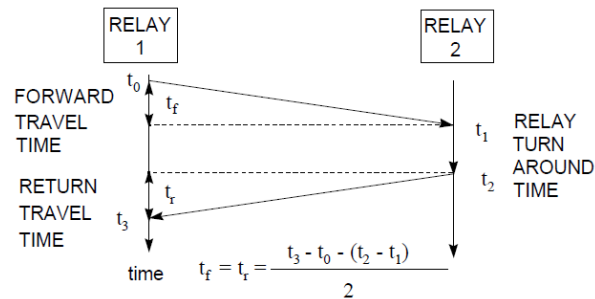


Figure 7.7 Ping-pong method for communication delay correction

This method has some practical limitations, because the channel used to transfer the data may not exactly be the same always, especially for applications such as SONET ring and switched microwave systems [15], as shown in Fig. 7.8.

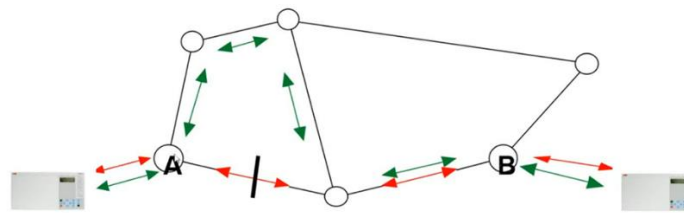


Figure 7.8 Example of Switched Microwave systems

- GPS synchronization:** Each data is time stamped with GPS time and sampled data with respective time stamps are compared by each relay. Accuracy up to 1 microsecond can be achieved using this method which is enough for line differential scheme. However, additional hardware costs and restricted availability due to military use limits the applications of this method.

7.5.3 Communication Channels

Communication channels for piloted schemes were discussed in detail in earlier chapters. However, it must be noted that the need to synchronize data is fulfilled by comparing the data with same time tags only. This requires additional processing speed, greater channel BW and complex algorithms; none of which is problematic in this day and age.

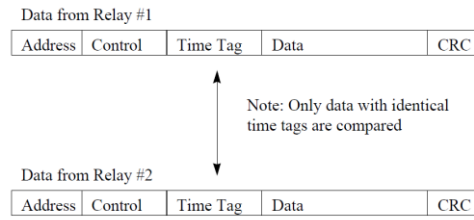


Figure 7.9 Example of Data packet transferred between local and remote relays

7.6 Alternate Approaches for Line Differential Protection:

7.6.1 Polar Plane Approach for Phasor Comparison (Schweitzer Engineering Laboratories)

Since both the remote and local currents are complex quantities, the method discussed in [29] takes a comprehensive approach and represents relay characteristics on a complex polar plane, which is defined as the ratio between Remote and Local currents, given by Eq. 7.7

$$\frac{\vec{I}_R}{\vec{I}_L} = a + jb = \vec{r} = r e^{j\theta} \quad (7.7)$$

Where,

$$a = \frac{|\vec{I}_R|}{|\vec{I}_L|} \cos \theta = r \cos \theta, \quad b = \frac{|\vec{I}_R|}{|\vec{I}_L|} \sin \theta = r \sin \theta, \quad r = \sqrt{a^2 + b^2}, \quad \theta = \arctan \frac{b}{a}$$

The shape of polar plot of this ratio depends on two quantities:

- a. Slope characteristics or operating characteristics
- b. Restraining current

The current ratio trajectory is not circular for all the characteristics as shown in Table 7-1 and Fig. 7.10. This holds true for dual slope characteristics; however, single slope characteristic with simplistic restraining current (Eq. 7.1) is used for this analysis. It should be noted that:

- Centre of the circle (-1 + j0 for given case) represents the ideal restraining characteristics for external faults and heavy load conditions.
- The region inside the circle represents restrain region, while rest is operating region. This analysis is equivalent to analyzing distance relay performance in Impedance (R-X) Plane.

Table 7-1 Differential relay characteristics in current ratio plane

Operation Equation: IOP	Restraint Quantity: IRT	Type of Characteristic	Center	Radius
KI_{RT}	$ \tilde{I}_L - \tilde{I}_R $	Circular	$-\frac{1+K^2}{1-K^2} + j0$	$\frac{2K}{1-K^2}$
	$ \tilde{I}_L + \tilde{I}_R $	Not Circular	—	—
	$\text{Max}(\tilde{I}_L , \tilde{I}_R)$	$ \tilde{I}_L > \tilde{I}_R $ Circular	$-1 + j0$	K
		$ \tilde{I}_L < \tilde{I}_R $ Circular	$-\frac{1}{1-K^2} + j0$	$\frac{K}{1-K^2}$
	$\sqrt{ \tilde{I}_L \cdot \tilde{I}_R \cos \theta}$	Circular	$-\left(1 - \frac{K^2}{2}\right) + j0$	$\frac{K}{2} \sqrt{k^2 - 4}$
$KI_{RT} + K_0$	$I_{RT} = 0$	Circular	$-1 + j0$	$\sqrt{\frac{K_0}{ \tilde{I}_L }}$
	$ \tilde{I}_L - \tilde{I}_R $	Not Circular	—	—
	$ \tilde{I}_L + \tilde{I}_R $	Not Circular	—	—
	$\text{Max}(\tilde{I}_L , \tilde{I}_R)$	$ \tilde{I}_L > \tilde{I}_R $ Circular	$-1 + j0$	$\sqrt{1 + \left(K + \frac{K_0}{ \tilde{I}_L }\right)^2}$
		$ \tilde{I}_L < \tilde{I}_R $ Not Circular	—	—
	$\sqrt{ \tilde{I}_L \cdot \tilde{I}_R \cos \theta}$	Not Circular	—	—

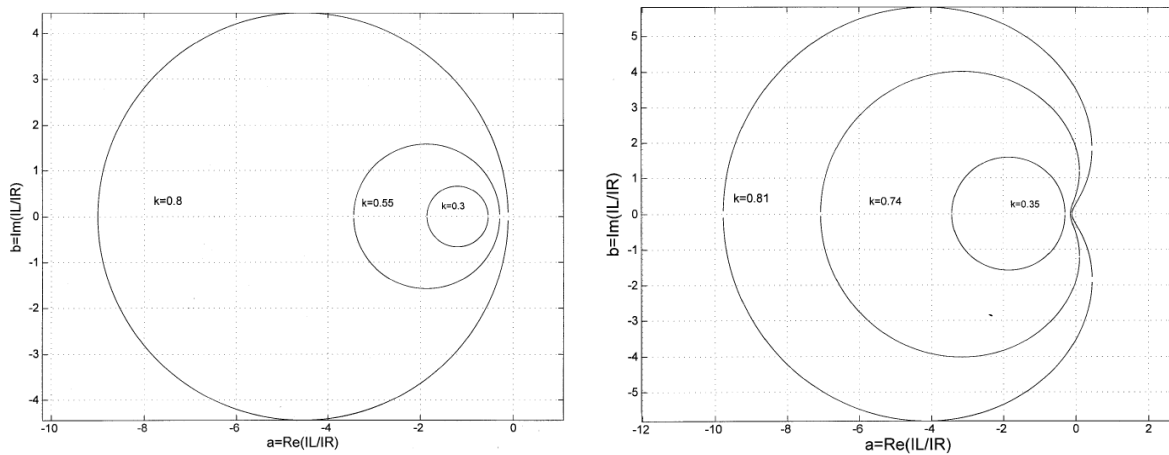


Figure 7.10 Operating trajectories in polar plane for different restraint currents
Left: Circular, Right: Not circular

The ideal trajectories of current ratios (without any uncertainty or disruptive consideration) is given in figure below. It should be noted that ideal Restraint Region is limited to a point, while operating region for internal fault with infeed and outfeeds are also shown.

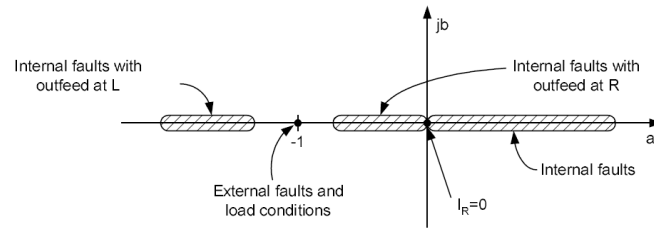


Figure 7.11 Restrain and Operating Region for Ideal conditions (Polar Plane analysis)

Reference [29] further builds upon these characteristics and introduce uncertainties due to power system angles, system impedance non-homogeneity, charging currents, channel delay and asymmetry. The combined effect of all these uncertainties is given in Fig. 7.12.

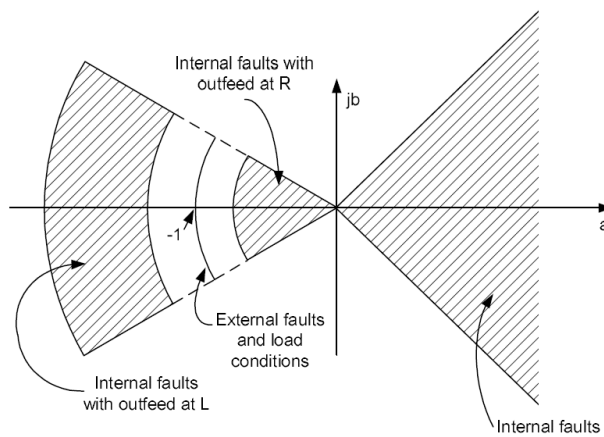


Figure 7.12 Restrain and Operating Region for Non-Ideal conditions (Polar Plane analysis)

The restrain region, as prescribed by figure above, can be defined in the polar region using dual arcs shown in Fig. 7.13. Reference [29] also prescribes that these characteristics can be set such that all the different load conditions and fault regions are accommodated along with CT saturation and low-frequency oscillations of Series Compensated lines.

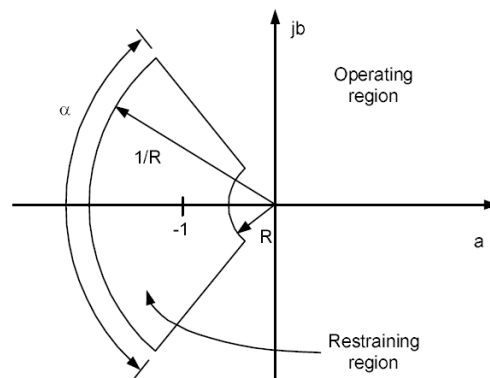


Figure 7.13 Proposed Operating Characteristics of Line Differential protection in Polar Plane

These new characteristics are definitely advantageous than previously examined circular and even non-circular characteristics, as shown in figure below, since it offers significantly large tolerance to both channel asymmetry and internal faults with outfeed.

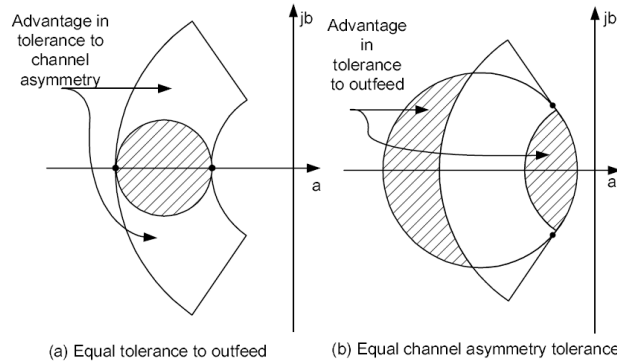


Figure 7.14 Comparison of proposed scheme with circular restrain characteristics

The performance of the proposed method for fault resistance coverage has been further evaluated in reference [29] and other options including Conventional distance protection (87L), Mho Distance and Quadrilateral Distance have been compared. The performance is **not satisfactory** for the proposed approach and provides resistive coverage only 5-10 Ohms of secondary fault resistance due to CT saturation limitation. However the fault resistance coverage improves significantly (0-125 Ohms) if the same algorithm is applied to negative sequence currents.

7.6.2 Phaselet & Variable Window Fourier Transform Approach by GE (1998):

The proposed method, discussed in [15], estimates the reduction of fault detection time which is inherently large in fixed-size sliding data window, which is equal to half or full electrical cycle. The Fourier transform performed on this window usually requires one complete cycle to estimate correct fault data, as shown in Fig. 7.15.

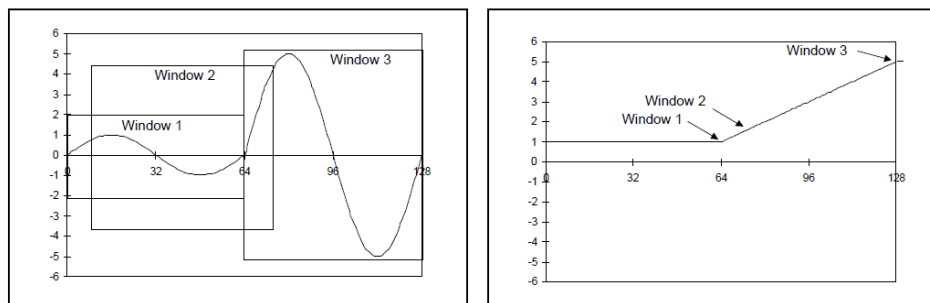


Figure 7.15 Fixed Window Approach (Left: Time varying signal) (Right: Output of fixed window integration)

This method utilizes variable window approach and estimates the actual phasor by adding a group of phaselets. These phaselets allow utilization of sampling windows considerably smaller than half cycles. During normal operation, the phaselets add up to give normal window (i.e. one cycle); however, during a disturbance the window size is dynamically reduced to the width one phaselet. This significantly increases the phasor estimation response as shown in Fig. 7.16.

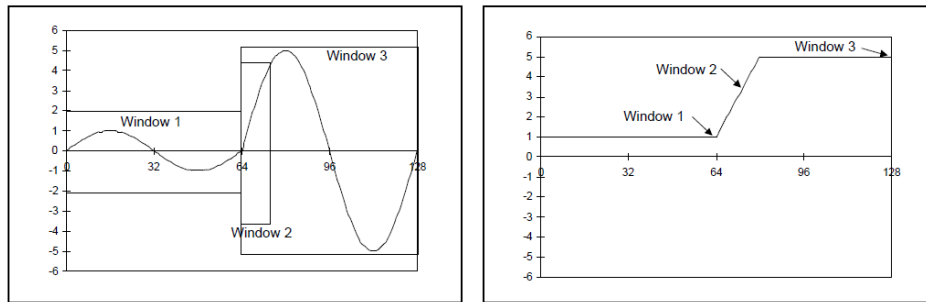


Figure 7.16 Variable Window Approach (Left: Time varying signal) (Right: Output of variable window integration)

Besides the use of phaselets and variable window size, the reconstructed sine wave is compared with the measured samples, refer to Fig. 7.17, and a least square variance is calculated for the difference between these quantities. This variance serve as the restraint signal, thereby giving rise to the adaptive nature of the proposed method. Hence in case of larger distortions due to CT saturation, fault transients etc., the restrain signal would also be large and would avoid nuisance tripping.

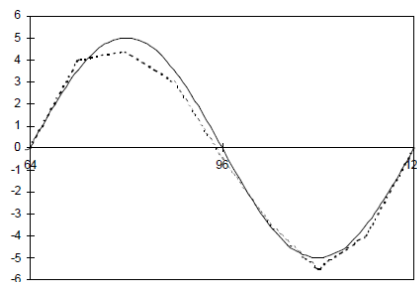


Figure 7.17 Dotted: Sample Signal, Bold: Reconstructed Sine Signal

The restrain region, when observed in the complex plane, is usually fixed and singular (as discussed in previous proposal). But this approach results in adaptive restrain signal, which is also circular if phaselet approach is not considered and whose area is significantly smaller in steady state fault conditions than the dynamic ones. The shape defined by dynamic restraint due to error variance calculation is circular for normal fixed-size sliding window but depends

on the position of phase let and results in elliptical shape as shown in Fig. 7.18. This results in a more sensitive and dependable solution.

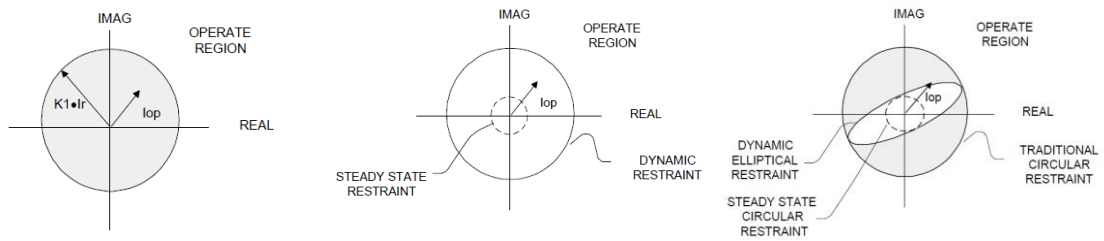


Figure 7.18 Polar Plane Analysis (Left: Static Restraint Signal, Middle: Dynamic Restraint Signal, Right: Dynamic Elliptical Restraint Signal)

Chapter 8 - Identification of Practical Constraints for Communication-based Protection and Tested Relays

This chapter reviews the common practical issues associated with communication-based protection and identifies the relevance of these issues for tested relays. The reviewed constraints include data management and handling for both directional and differential protection, data synchronization, limitations of communication channels and their application for multi-terminal systems. Finally, some miscellaneous problems are identified. Since most of these issues are customary for line differential protection schemes, therefore these schemes are the primary focus for this chapter.

8.1 Data Handling and Management

Data handling issues are a primary source of concern for line differential protection only. Piloted directional protection requires tripping supervision only, which does not require data synchronization and channel BW issues are minimal as well. A modern current-based line differential protection relay faces a major constraint from a design perspective, which is its desired compatibility with limited BW communication channels. [1, 3]

The problem has been resolved to a large extent by application of point-to-point Fiber Optic (FO) cables. FO cables allow data BW in the range of several Megabits per second (Mbps) and can be drawn in numerous channels allowing parallel data transfer, which reduces its application costs to a large extent. Most commonly, these channels are of 64 kilobits per second (kbps) BW today [16]. Although this BW might seem adequate for an untrained eye, a brief analysis is provided in Table 8-1 to determine the actual number of bits available for data transfer in each sample. The line differential relays under consideration, ABB RED 615 and Siemens SIPRTOEC 4 7SD552, have sampling frequencies of 1.6 kHz (32 samples per cycle) and 1 kHz respectively (20 samples per cycle). Therefore, the analysis is performed for both the cases.

Table 8-1 Analysis of Available Channel BW and Relay requirements

Parameter		Value
Channel BW (bits per second)		64000
Bits per electrical cycle (50 Hz)		1280
Bits per quarter of a cycle (50 Hz)		320
Bits per sample	RED 615 (1.6 kHz)	40
	SIPROTEC 4 (1 kHz)	64

The analysis reveals that for a 64 kbps channel, 40 bits are available per sample for RED 615 and 64 bits for SIPROTEC 4 7SD552. As mentioned earlier, these numbers might seem adequate but the prerequisite overhead for all data packets in communication-based protection cannot be ignored. Therefore, each packet of communicated data included an overhead and the actual payload (three phase current information for line differential protection). Data overhead is necessary to ensure the legitimacy of received data and can usually take between 60 and 80 bits in total. The usual break up of overhead is provided in Table 8-2.

Table 8-2 Structure for data packet overhead for line differential protection

Header (15 bits)	Redundancy Check (32 bits)	Data Synchronization (16 bits)	Address (4-8 bits)	Flags (4-8 bits)
----------------------------	--------------------------------------	--	------------------------------	----------------------------

Therefore, this simple analysis reveals that if the 64 kbps channel is used to send data 16 or 20 times in each electrical cycle, the overhead alone would take up the entire BW. Hence, two data related constraints are to be dealt with at the same time:

8.1.1 Protection constraints: The current data must be sent several times per cycle (16 or 20 times ideally) to ensure that fresh current information is available on disposal for relays at each end. By ensuring high rate of data transfer every cycle, minimum latency can be achieved resulting in secure and fast operation. It is necessary to mention that, if real-time current values were sent over the communication channel 20 times in each cycle, each value would be 18 electrical degrees apart from its predecessor. This can result in serious dependency on the accuracy of transmitted information. This dependency can be reduced by transmitting current phasor information instead.

8.1.2 Communication constraints: These constraints include the frequency of data transfer, encoding and protection of data; whereas, smart data packaging is also important. High rate of data transfer leaves less number of bits available for each data packet, making it almost impossible to adjust both the overhead and actual payload in one packet.

Both these constraints go hand-in-hand. A smart protection scheme based on information other than real-time current values can reduce communication constraints; while smart management of data packets can provide more room for payload. A common practice to manage both these constraints is to improve the payload-to-overhead ration by reducing the rate of data transfer (i.e. transferring data at a rate slower than sampling time), which is achieved by combining

multiple samples in one data packet. Table 8-3 gives a nominal structure for payload information if 3 samples are combined allowing the rate of data transfer to be reduced three-folds.

Table 8-3 Proposed structure for the data packet payload (with 3 samples per packet)

Phase A (samples)			Phase B (samples)			Phase C (samples)			Restraint Terms		
(k-1)th	kth	(k+1)th	(k-1)th	kth	(k+1)th	(k-1)th	kth	(k+1)th	Per Phase	Neg. Seq.	Zero Seq.

If this approach is used for both the studied cases, each data packet needs to be sent once every 3 ms for SIPROTEC 4 and every 1.875 ms for ABB RED 615. Reference [16] reveals that the payload mentioned in Table 8-3 can be squeezed within 100 – 120 bits. Therefore, the actual data packet size would be between 150 – 200 bits (overhead + payload). Referring to the worst case of 3 ms data transfer delay for a 64 kbps channel, data packets of 192 bits can easily be transferred. Data packet optimization can reduce the actual data packet size even further.

Conclusively, the data transferred is more than 6 times for SIPROTEC 4 and more than 8 times for RED 615 reducing data latency to a minimum and resulting in fast operation. The improved payload-to-overhead ratio reduces the BW requirements of the channel. Loss of one data packet results in loss of 3 ms information only, which is not a matter of concern for distribution line protection.

8.2 Data Synchronization

In case of line differential protection, besides dealing with restricted channel BW issues it is extremely critical to align remote and local current data before these signals are fed to the differential block. The synchronization of data is performed using one of the two popular techniques, including channel-based and external time reference-based synchronization.

In order to compensate for channel delays, each data packet is time stamped. The differential relays on each end of the protected line receive this time-stamped data and performs data comparison once both the local and remote currents are expressed in the same time frame. This expression is ensured by measuring the clock offset and by manipulating the received time stamps accordingly.

8.2.1 Channel-based data synchronization

This technique is extremely relevant for dedicated communication channels with almost fixed time delays. The offset time of channel is actually measured by exchanging data between local

and remote relays over a long period and by averaging the individual delays. This allows the estimated delay to be independent of data packet corruption or channel loss. This method relieves the relay of the requirement of a GPS clock or other external time reference; thereby reducing the overall cost of installation, which can be crucial for application in distribution networks.

Fig. 8.1 reveals one of the techniques for determining offset time using channel-based synchronization; whereas the calculations are mentioned in Eq. 8.1 – Eq. 8.4. It must be mentioned that t_{OFFSET} is not fixed and depends upon the average offset time of moving averaging window (i.e. the most recently recorded time delays).

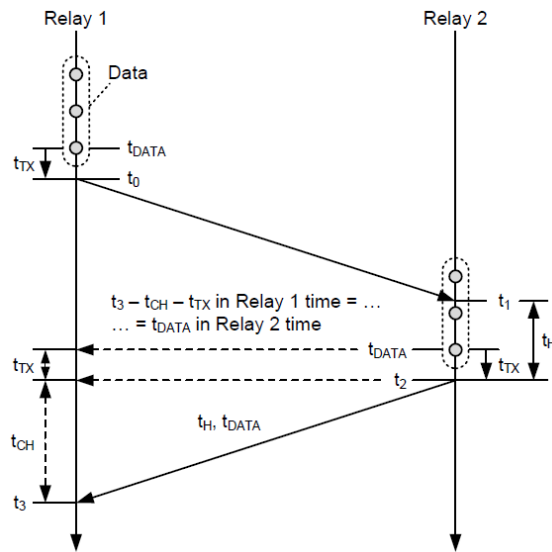


Figure 8.1 Offset time determination for Channel-base data synchronization (proposed technique)

$$t_{CH} = \frac{t_3 - t_0 - t_H}{2} \quad (8.1)$$

$$t_{DATA (Relay_2)} = t_3 - t_{CH} - t_{TX} \quad (8.2)$$

$$t_{OFFSET} = t_{DATA} - t_{DATA (Relay_2)} \quad (8.3)$$

Where,

t_{TX} = time after which sampled data is dispatched from Relay 1

t_H = Hold time of Relay 2

t_{CH} = Channel delay time (one side)

Hence, in this way the remote time stamp (time stamp of Relay 1 at Relay 2) is corrected by adding the offset time to the actual stamp once the average offset time is known from previous data packets, as shown in Eq. 8.4

$$t_{DATA (Relay_2)} = t_{DATA} + t_{OFFSET} \quad (8.4)$$

8.2.2 Data Synchronization using External Time Reference

This technique is relatively simpler and utilizes a uniform, external time reference source (like GPS) to time stamp the data packets for relays on each end. This time stamped data has zero offset because the data is sampled at the same time, which allows this technique to be employed for asymmetrical communication channels resulting in different time delays, as shown in Fig. 8.2.

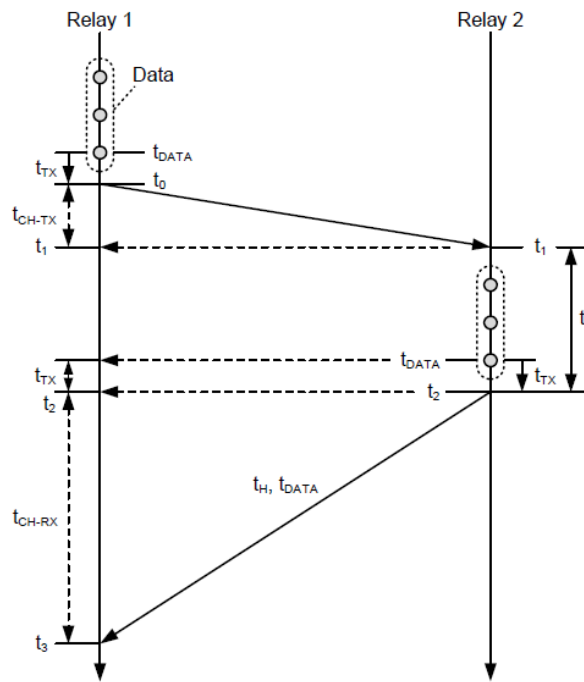


Figure 8.2 Data Synchronization using External Time Reference

The most commonly employed external time reference has been based on GPS, with a time source installed at each relay. Although a costly option, GPS based time synchronization is a widely employed technique in different military as well as civilian applications. However, loss of this reference is inevitable at certain times and several fallback strategies have been devised over the years, with SONEt system being one of the widely used wide-area time generation techniques.

8.3 Communication Channels and Multi-terminal Application:

The possibility to employ directional or differential protection for multi-terminal applications has become extremely relevant with distribution networks. Besides the challenge of dealing with multiple differential and restrain currents, which can be resolved by utilizing partial terms, the major challenges associated with these applications are linked with communication restrictions. If direct point-to-point connection technique is used for communication, following challenges would arise:

- For N terminals, each terminal's relay would require N-1 communication ports at least.
- The point-to-point connections increase drastically with the number of terminals with only 1 channel needed for 2 terminal application and as many as 10 channels for a 5 terminal system.
- Data synchronization using channel time delay approach for line differential application becomes extremely difficult in this case.

These challenges not only affect the cost and availability of protection, but the overall reliability of operation is also affected. Some methods of work-around have been explored, including changing the master-master configuration to a hybrid master-slave configuration to reduce the number of channels; however, the increased operation time cannot be ignored. A modern approach for resolving the issues related to the number of connections and data synchronization is the employment of wide-area communication systems like Synchronous Optical Networking (SONET) and Synchronous Digital Hierarchy (SDH).

The communication technique based on SONET/SDH, as shown in Fig. 8.3, utilize the deterministic communication techniques (like Ethernet) to provide not only protection functions but also a common wide-area source for time source which can be used for external time referencing independent of GPS [16]. This futuristic technique not only offers a cheaper solution to these challenges but can also improve the overall system reliability by decreasing the number of components and possible point of failures. However, the application of third-party multiplexed channels can often increase the complexity, ride-through attempts and modes of failure; therefore, the relays need to be critically designed to deal with these challenges.

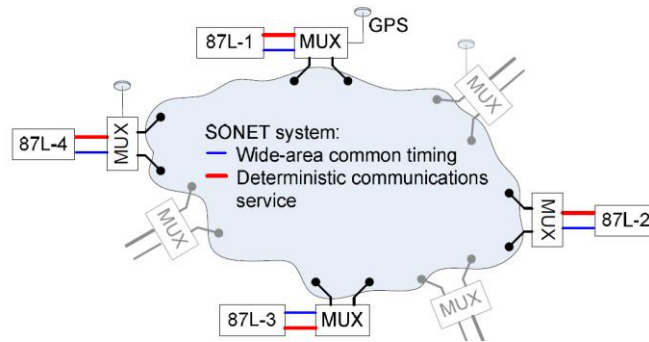


Figure 8.3 Multiplexed Communication Technique based on SONET/SDH

8.4 Miscellaneous Issues:

Some of the miscellaneous issues associated with line differential protection include the interpolation of data between sampled signals and the type of data that must be transmitted over the communication channel in order to minimize the channel requirements with minimal impact on accuracy of information. Transmitting phasors instead of real-time sampled current values increase the BW requirement of the channel, which in return reduces the rate at which the information can be exchanged over the communication channel. Henceforth, the possibility to interpolate data between sampled signals while ensuring accuracy also decrease because of decrease in sampling frequency.

Chapter 9 - Test System, Performance Parameters and Fundamental Blocks

9.1 Test Model

The system under test, presented in Fig. 9.1, is inspired by IEEE PSRC Recommended circuit [21]. The 22 kV, 50 Hz test system combines two distribution networks through a 50 km line and comprises of two distributed generation sources (DG-A and DG-B) with varying strengths located 10 km from each network. The protected line is one of the two parallel lines with a length of 30 km. Pilot Protection relays are installed at each end of the line, with the possibility to acquire both the current and voltage information or only the current information (for current-only schemes) of each end. The line and tower parameters along with source and network characteristics are summarized in APPENDIX A.

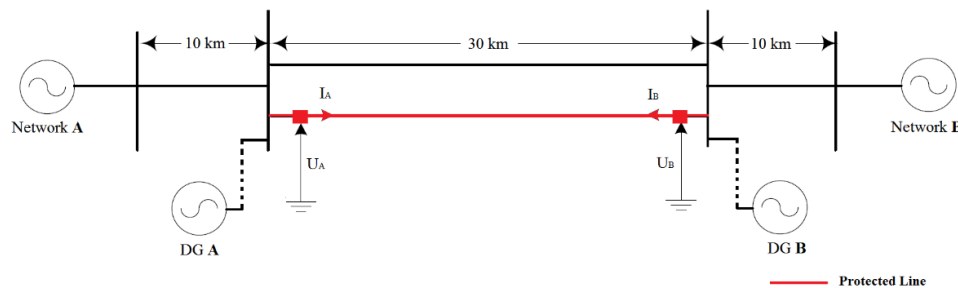


Figure 9.1 Test Power System

It must be noted that the distributed generators are represented in the PSCAD/EMTDC environment using a nominal current source (or a voltage source with large positive and zero sequence impedance).

The external and internal faults are specified in Fig. 9.2. The location of these faults is varied between 1% to 99% of the respective line lengths. The system and fault parameters necessary to assess the effectiveness of each method under consideration are discussed in the next section.

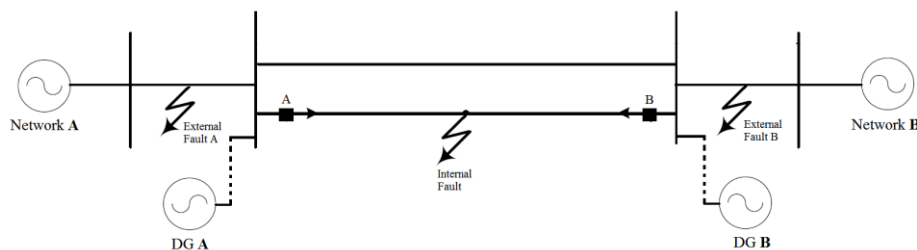


Figure 9.2 Internal and External fault condition for test system

9.2 Performance Parameters:

Following performance parameters have been devised to determine the effectiveness of different directional protection methods:

- 1) Fault Type
- 2) Fault Resistance Coverage
- 3) Bidirectional Power Flow
- 4) Load Angle Variation
- 5) Fault Inception Angle
- 6) System Grounding method and NGR size variation
- 7) Source Strength Tests
- 8) Network Complexity
- 9) Data Synchronization and Channeling issues
- 10) Hardware/Equipment limitations

The extensive tests carried out for all the modeled algorithms follow strict protocols. The diversity of each model is expressed by studying the behavior for different types of faults (L-G, L-L, L-L-L, L-L-G, L-L-L-G) associated with each phase. The sensitivity is determined by varying the fault resistance between 0.01 Ohm (Bolted Fault) and 1000 Ohms, which refers to a high resistance fault for the tested distribution network.

Since the sensitivity and performance of various directional algorithms depend extensively upon the phasor displacement of current and/or voltage, various conditions have been formulated to verify the respective impacts. Table 9-1 presents the details of tests belonging to this category. The impact of DC fault component is investigated by varying the fault inception time consequently the fault inception angle. Besides studying the impact of variation in fault inception angle, individual voltage phase angle of each end and the difference between the latter quantities (load angle), the impact of bidirectional power flow is also tested.

Table 9-1 Test Criterion for Phasor Displacement of pre-fault conditions

Quantity	Range of Test (Degrees)	Step Size (Degrees)
Sending and Receiving End Voltage Angles	-179 to 179	10
Fault Inception Angle	0 to 359	30
Load Angle	-40 to +40	5

The impact of system grounding and variation in source and network strength is also studied. As suggested in Table 9-2, the tested distribution system is either solidly grounded or the ground current is limited using a Neutral Grounding Impedance (NGR). The ground current is varied between 10 Amperes (High resistance ground – HRG) and 100 Amperes (Medium Resistance Ground) and the grounding method is chosen to be a parallel RL-based impedance. The calculations for NGR sizing take into account the limiting ground currents. As an example, for 100 Amp limit, the NGR size is calculated to be $127 \Omega \{22kV/(\sqrt{3} * 100)\}$. This is verified by imposing a bolted short circuit on the terminals of the source; the SC currents are found to be close to the ground current limits.

Similarly, as suggested in Table 9-3, the surge impedance ratio (SIR) is varied by changing the positive and zero sequence impedance of the source, consequently varying the source strength. The performance of each algorithm for an extremely strong system (SIR = 0.7) and an extremely weak distribution network (SIR=56) serves as the basis to test the impact of increasing distributed generation in the network. The source strength is either varied individually for the local or the remote end or varied collectively for both ends.

Table 9-2 Test Criterion for Test network's Grounding methods

Grounding Method	Impedance Value (Ohms)	Grounding Current Limit (Amps)
Solidly Grounded	0	No limit
Grounding through Impedance (R L)	127	100
	635	20
	1100	10

Table 9-3 Test Criterion for Test network's Strength variation

Positive Sequence		Zero Sequence	
Source Inductance (mH)	SIR	Source Impedance (Ohms)	SIR
10	0,7	127	3
50	2	635	14
200	6	1100	25
500	15		
1000	28		
2000	56		

The complexity of network is also varied by including either of the distributed generators in the network. The switching action is not taken into account for this study. Most of the network complexity tests assess the impact of local DG on the directional element (i.e. DG-A is considered to be a part of the network when assessing faults from End-A).

Data Synchronization and Channeling issues are considerable problems for line differential protection; therefore, the restrictions are discussed in Chapter 12. Hardware and equipment limitations are taken into account by employing practical signal transformation models for CTs and VTs in PSCAD. As far as the current transformers are concerned, CT Lucas model block is utilized based on the parameters of Table 9-4 [66]. Further information about the Lucas model is available in Reference [67]. Moreover, the relay hardware limitations in terms of sampling frequency is also ensured.

Table 9-4 Current Transformer Data

CT Manufacturer	ABB
Model	TPU 63.11
CT Class	10P
Transformation Ratio	1000/1
Accuracy Limit Factor - ALF	15
Nominal Burden (VA)	10

9.3 Fundamental Blocks

The generic piloted protection scheme is provided in Fig. 9.3. Although the directional block mechanism varies for each individual algorithm, but the fundamental blocks are exclusively common. All the fundamental blocks besides the Communication interface are explored in detail in this chapter.

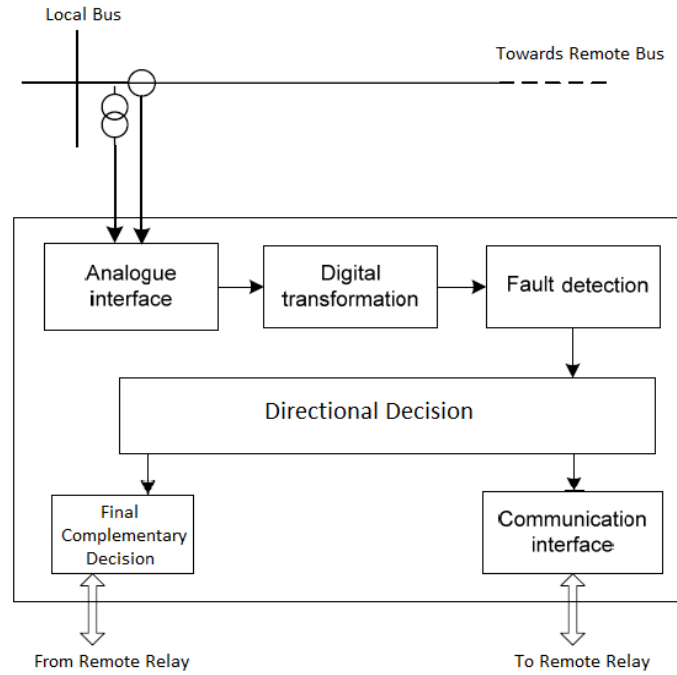


Figure 9.3 Proposed piloted protection scheme

9.3.1 Signal Processing and Filtering

The signal processing sequence used for this study is aligned with the modern numerical relays. As mentioned in Fig. 9.4, the analogue signal from the signal transducers (CTs and VTs) is fed to the relay’s signal processing block. This block includes following sub-blocks:

- Anti-aliasing Filter: 2nd Order Butterworth filter with cut-off frequency (f_c) set to 1kHz
- The Analog to Digital Converter (ADC) block samples the filtered input. This block is discussed in detail in next section.
- The Digital filter: Discrete Fourier Transform (DFT) block.

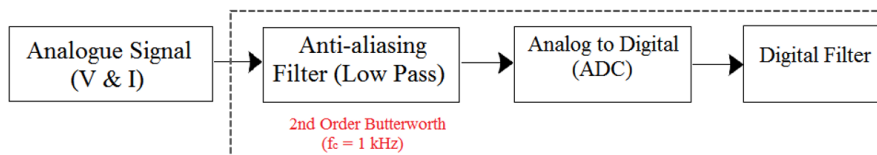


Figure 9.4 Signal Processing Sequence for Modern Numerical Relays

This is a classical chain of procession in typical numerical relays. The cut-off frequency of Anti-aliasing filter (low pass) is typically set to a few kHz aligned with the bandwidth of current and voltage transformers. This filter removes high frequency signal disturbances (Noise etc.) from the analog signal before ADC and improves the Signal to Noise Ratio (SNR). The

magnitude response of the anti-aliasing filter used for this study is provided in Fig. 9.5. Further details about the Butterworth filter design for numerical relays are available in Reference [68]

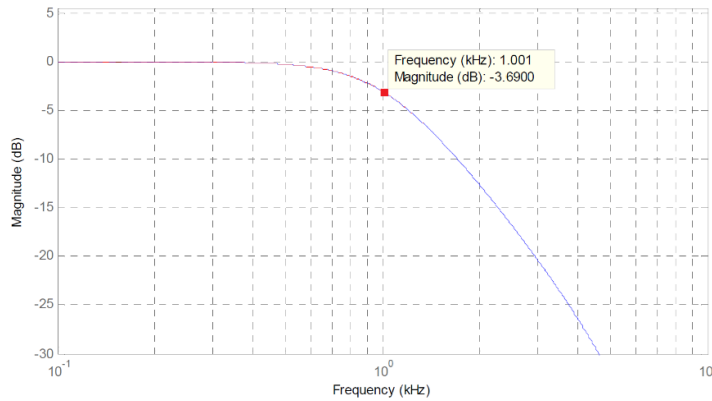


Figure 9.5 Magnitude response of Anti-aliasing filter (Butterworth - 2nd order, $f_c = 1\text{kHz}$)

The digitized version of filtered analogue signal at the output of ADC is then passed through a digital filter, which reconstructs the signal according to the fundamental frequency component. The digital filter is based on Discrete Fourier Transform, which is discussed in detail in the upcoming sections. The output of signal processing block has acceptable SNR, which improves the performance of both the transient-based and conventional directional protection. The impact of this digital filter on digitized signal is recorded in Fig 9.6. It must also be mentioned that the delta filter (to be discussed in Chapter 11) also reduces the impact of high frequency components; thereby providing additional security against high frequency noise. However, digital filters (like DFT) usually require one complete cycle's information to accurately reflect the signal; therefore, the delay associated with these filters cannot be ignored (as shown in Fig. 9.6).

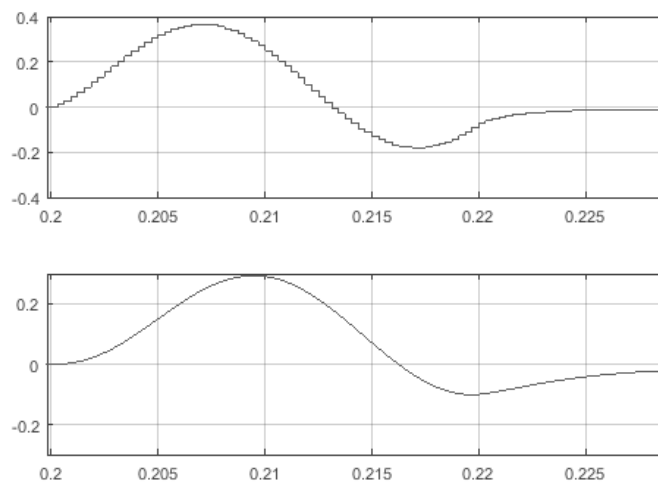


Figure 9.6 Output of Sampling Block (Top), Output of Digital Filter (Bottom)

9.3.2 Analog to Digital Conversion (ADC – Sampling Block)

ADC is an essential part of modern numerical relays. Implementation of data sampling in Matlab/Simulink based models is rather straightforward and can easily be implemented using a zero order hold (ZOH) rate transition block. However, for models implemented in EMTDC/PSCAD, the sampler block consists of numerous S/H components controlled by their periodic pulse generators, as shown in Fig 9.7. In order to interpret actual hardware restrictions of SIPROTEC 7SD552, ABB RED 670 and RED 615 relays while accounting for future hardware modifications, following sampling frequencies are tested:

- 20 samples per cycle (1 kHz)
- 32 samples per cycle (1.6 kHz)
- 64 samples per cycle (3.2 kHz)
- 80 samples per cycle (4.0 kHz)

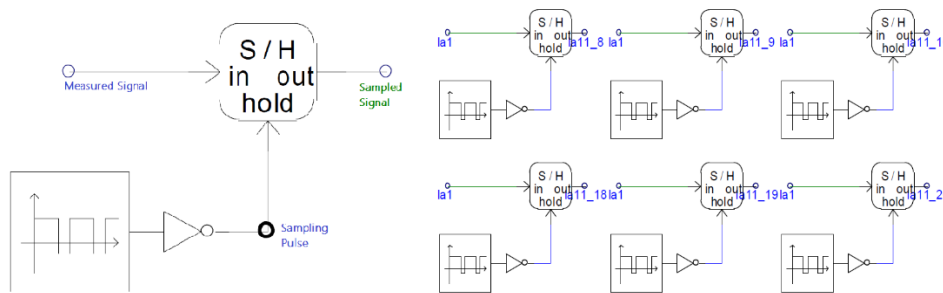


Figure 9.7 Proposed Sampling Block for PSCAD/EMTDC based models

The number of S/H components and the sampling pulse instant depend upon the tested sampling frequency. Table 9-5 reveals the pulse delay settings and other relevant information about the sampling block used in this context, while Fig. 9.8 presents a sampled waveform obtained using this approach.

Table 9-5 Parameters of sampling block

Sampling Frequency (kHz)	Samples per cycle (50 Hz signal)	No. Of S/H Blocks	Pulse Delay (μ s)	Electrical Angle Shift per pulse (Degrees)
1	20	20	1000	18
1.6	32	32	625	11.25
3.2	64	64	312.5	5.625
4.0	80	80	250	4.5

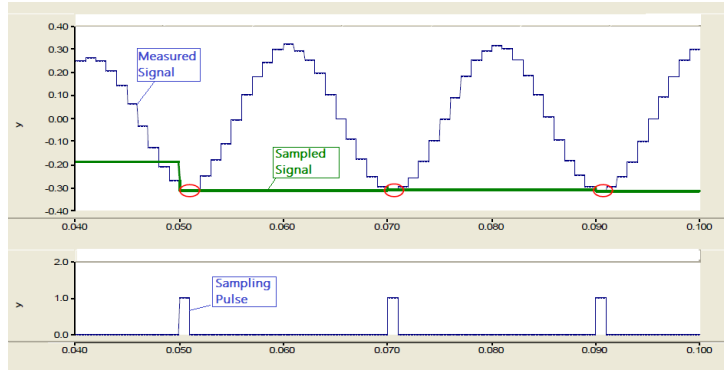


Figure 9.8 Sampled Signal (Top) and Sampling Pulse (bottom) - $f_s = 20$ samples per cycle (PSCAD/EMTDC)

9.3.3 Discrete Fourier Transform Block

In order to obtain the fundamental frequency components (both in the polar and complex planes) of the real-time signals, several filtering techniques have been examined with primary focus on Kalman Filter and Discrete Fourier Transform (DFT). The mathematical equivalent of the DFT algorithm is given in Eq. 9.1.

$$X = \frac{\sqrt{2}}{N} \left\{ \sum_{k=0}^{N-1} x_k \cdot \cos\left(\frac{2\pi}{N}k\right) - j \sum_{k=0}^{N-1} x_k \cdot \sin\left(\frac{2\pi}{N}k\right) \right\} \quad (9.1)$$

Where, N = number of samples in one fundamental cycle

k = sample number (0, 1, 2... N)

x_k = value of k^{th} sample

X = fundamental frequency component

This DFT algorithm requires one cycle of information to reconstruct the signal. Fixed sliding window approach allows appropriate phasor computation with unchanging phase for steady-state operation unless the signal is corrupted by noise or measurement errors, which is not the case in EMTDC/PSCAD Simulations [60]. The possibility to use both the recursive and non-recursive DFT computation is evaluated. Recursive DFT is chosen primarily because the tested algorithms are evaluated for practical problems including noise and frequency deviation, which significantly influences the sequence component calculation [64]. Besides approximating the fundamental-frequency component, same DFT algorithm is utilized to assess the percentage of second harmonic distortion in the signal. This evaluation is necessary for inrush restraint and negative sequence blocking in line differential and directional algorithms respectively.

9.3.4 Sequence Component Extraction

A number of directional protection schemes utilize sequence/symmetrical components of Fig. 9.9. These components are extracted by physical transformation of the three phase current and voltage quantities. Reference [69] discusses in detail the role of each of these components for different fault types (L-G, L-L, L-L-L)

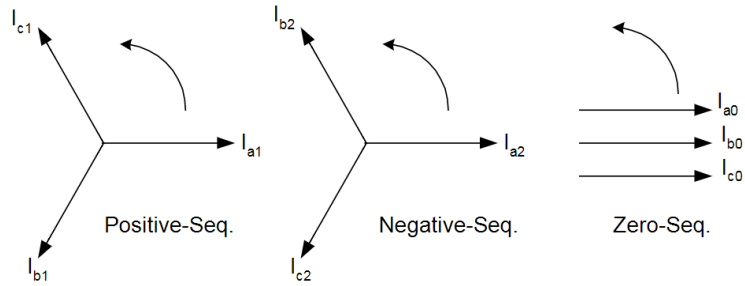


Figure 9.9 Symmetrical components for a three phase system

Chapter 10 - Conventional Directional Protection Model and Performance Evaluation

10.1 Comprehensive Model

The final comprehensive model combines the attributes of **positive, negative and zero Sequence** algorithms for reliable and sensitive operation. This approach is similar to ABB REL 670 relay's directional element mechanism but combines the attributes of SEL-321 Relay for negative sequence element. The complete description of steps to determine fault direction using combined conventional approach is mentioned in Fig. 10.1. While the snap of Simulink model along with the individual threshold settings have been provided in APPENDIX B.

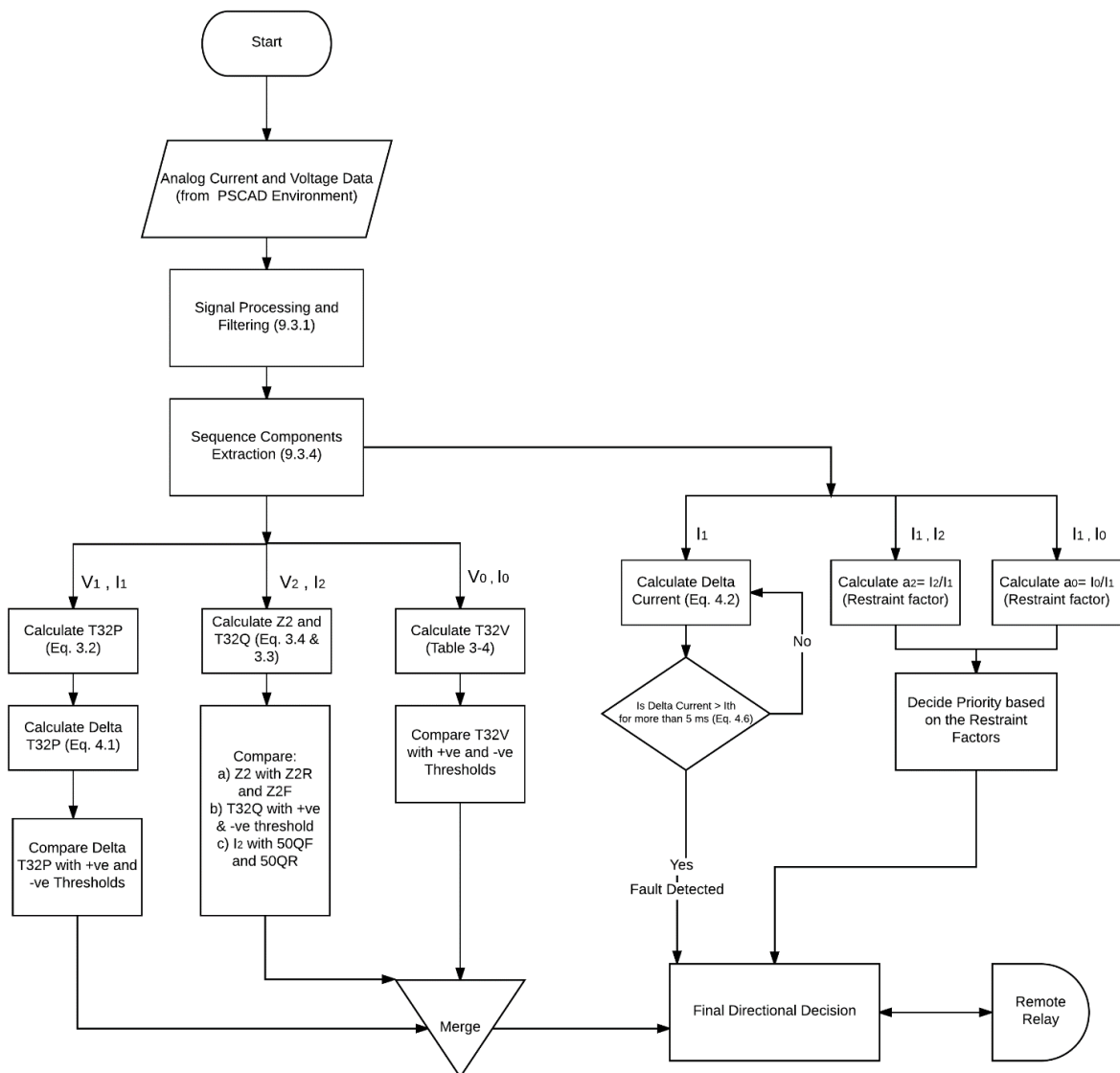


Figure 10.1 Description of steps for combined conventional directional protection

10.2 Test Results

The combined conventional model has been extensively tested. The performance of each individual element for both the unbalanced and balanced faults is discussed below.

10.2.1 Unbalanced Faults

As discussed earlier, unbalanced faults are primarily detected by the negative sequence block and zero sequence block (for ground related faults). The performance of each of the elements for L-G faults has been recorded in Fig. 10.2 and 10.3. The sudden rise in the zero and negative sequence currents beyond the set threshold allows the priority block to shift the control to either of these elements. It must be mentioned that ideally the magnitudes of all the sequence components should be same for L-G faults; however according to PSCAD simulations, slight difference is observed between the positive sequence and other sequence components. Both the Negative Sequence (Z_2 and T32Q) and Zero Sequence (T32V) blocks are aligned in terms of the directional decision during forward and reverse faults. Although the change in positive sequence torque (T32P) also suggests the correct fault direction, the priority block bases the final decision on negative and zero sequence blocks only.

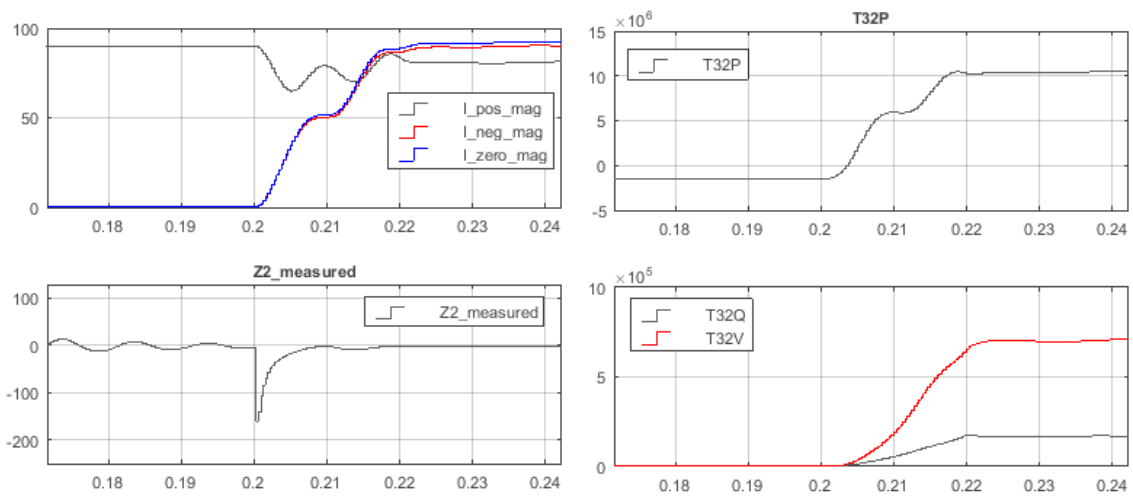


Figure 10.2 L-G Fault (Forward). Sequence Currents (top-left), Negative Sequence Impedance (bottom-left), Positive Sequence Torque (top-right), Negative and Zero Sequence Torques (bottom-right).

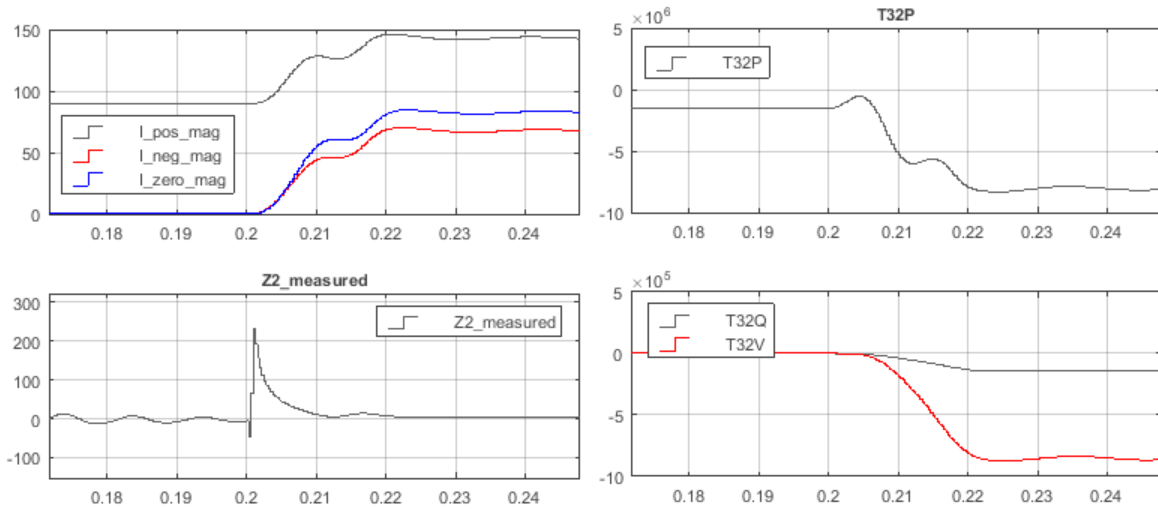


Figure 10.3 L-G Fault (Reverse). Sequence Currents (top-left), Negative Sequence Impedance (bottom-left), Positive Sequence Torque (top-right), Negative and Zero Sequence Torques (bottom-right).

It must be noted that in either of the previous cases, Z_2 crosses the forward (Z_{2F}) and reverse (Z_{2R}) thresholds respectively. Whereas, T_{32Q} and T_{32V} are well beyond the respective set thresholds as well.

During L-L faults, the control is transferred to the negative sequence block only. As shown in Fig. 10.4 and 10.5, the negative sequence impedance and torque cross the respective threshold within $1/4^{\text{th}}$ of an electrical cycle.

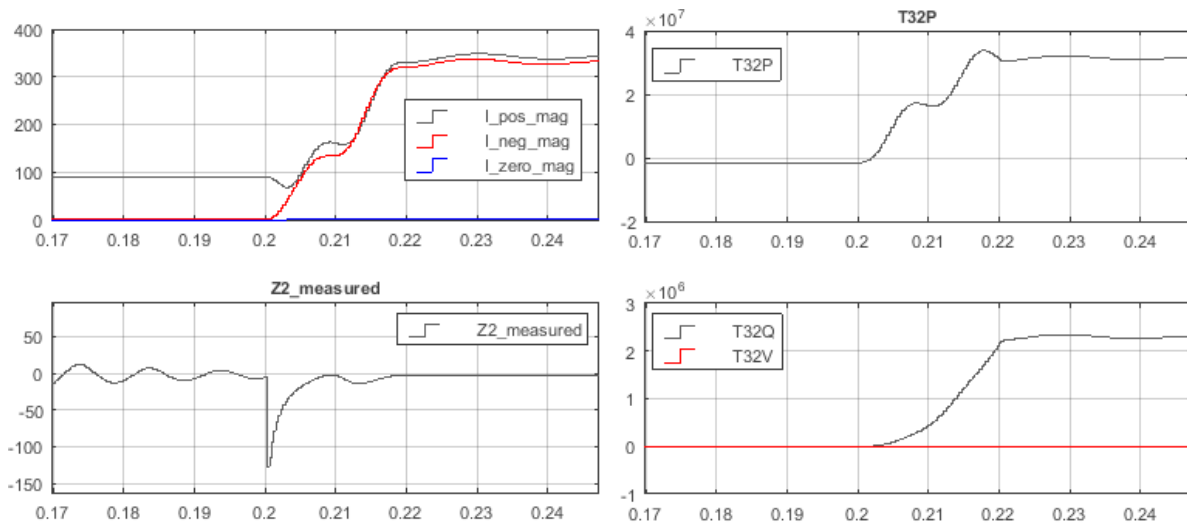


Figure 10.4 L-L Fault (Forward). Sequence Currents (top-left), Negative Sequence Impedance (bottom-left), Positive Sequence Torque (top-right), Negative and Zero Sequence Torques (bottom-right).

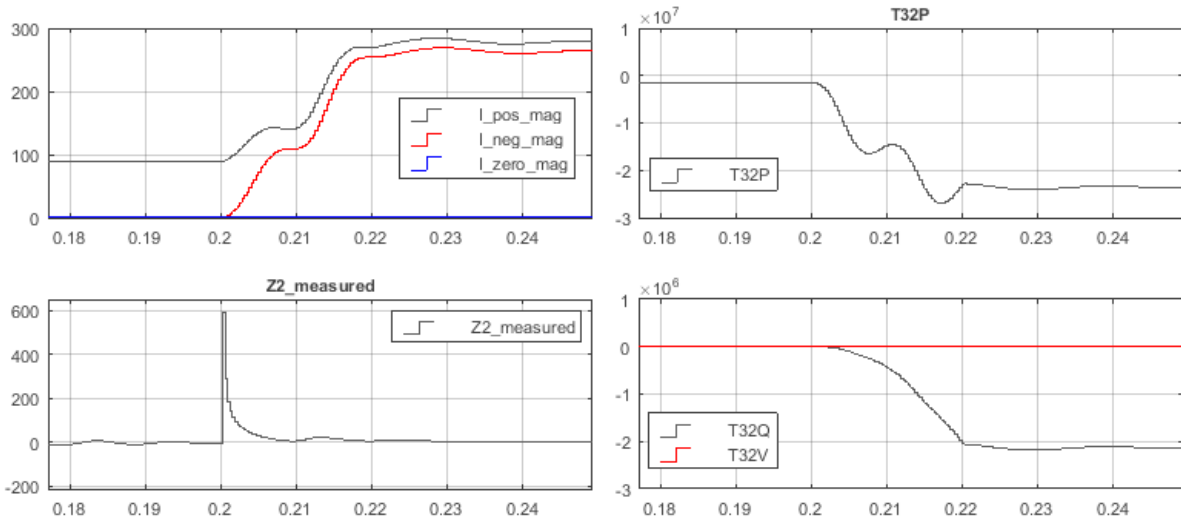


Figure 10.5 L-L Fault (Reverse). Sequence Currents (top-left), Negative Sequence Impedance (bottom-left), Positive Sequence Torque (top-right), Negative and Zero Sequence Torques (bottom-right).

10.2.2 Balanced Faults

In case of balanced faults, the negative and zero sequence currents do not cross the respective thresholds, which allows the priority block to keep the decision control with positive sequence block. Fig. 10.6 and 10.7 reveal that neither the negative and zero sequence currents nor their respective operating quantities cross the thresholds. However, positive sequence torque ($T32P$) records the fault direction in less than a half-electrical cycle.

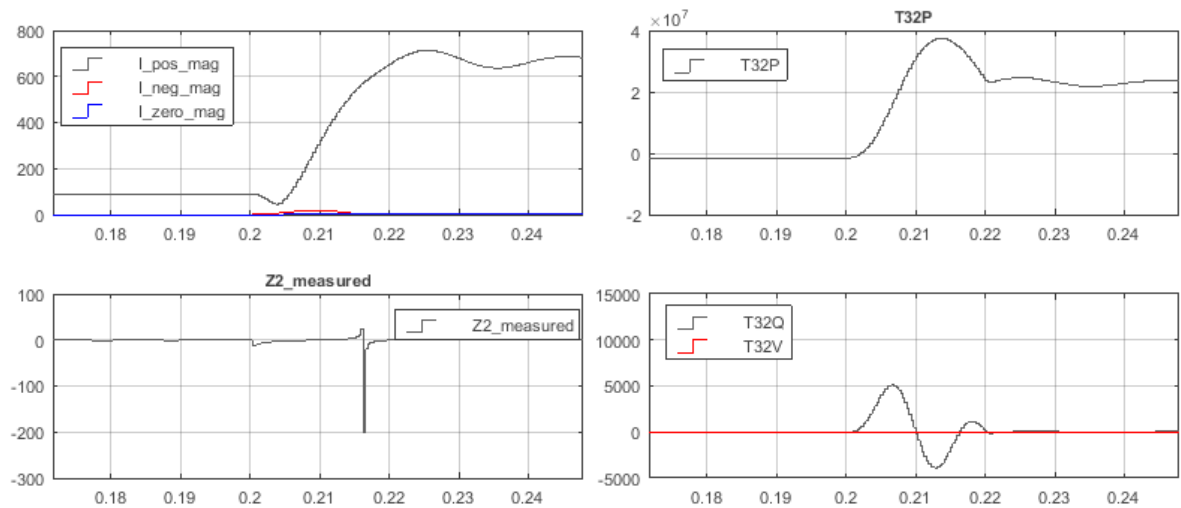


Figure 10.6 L-L-L Fault (Forward). Sequence Currents (top-left), Negative Sequence Impedance (bottom-left), Positive Sequence Torque (top-right), Negative and Zero Sequence Torques (bottom-right).

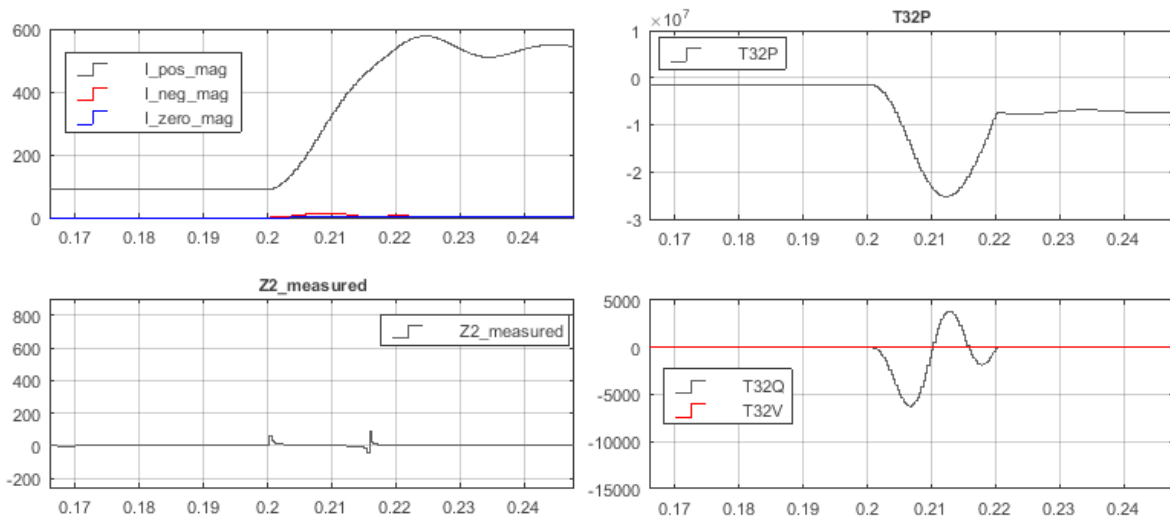


Figure 10.7 L-L Fault (Reverse). Sequence Currents (top-left), Negative Sequence Impedance (bottom-left), Positive Sequence Torque (top-right), Negative and Zero Sequence Torques (bottom-right).

10.2.3 Extensive Test Results

Referring to Table 10-1, the combined conventional directional model performs exceptionally well for all fault types tested at different locations. These tests are verified for bidirectional power flow and the maximum decision time stays within one electrical cycle, which is much quicker than the prescribed limits for an MV Distribution network. The fault resistance coverage is tested for ground faults only. The performance is satisfactory for R_f ranging between 0.01 Ohm (bolted fault) and 100 Ohm. While for faults with higher resistance (500 Ohm), the fault detection block needs to be more sensitive especially for balanced fault condition. This increase in sensitivity can result in reduced security.

Table 10-1 Test Results for combined Conventional directional protection (Fault Type, Fault Resistance, Fault Location and Bidirectional power flow)

Fault Type	Fault Resistance (Ohms)	Forward Fault Test Line length = 30 km		Reverse Fault Test Line Length = 10 km	
		Range of Fault Location	Max Decision Time	Range of Fault Location	Stable 'No Trip' Decision
A-G	0.01 - 500*	0.1 - 29.9 km	6 - 13 ms	0.1 - 9.9 km	Yes
B-G	0.01 - 500*	0.1 - 29.9 km	6 - 13 ms	0.1 - 9.9 km	Yes
C-G	-	0.1 - 29.9 km	6 - 13 ms	0.1 - 9.9 km	Yes
AB	-	0.1 - 29.9 km	6 - 13 ms	0.1 - 9.9 km	Yes
AC	-	0.1 - 29.9 km	6 - 13 ms	0.1 - 9.9 km	Yes
AB-G	0.01 - 500*	0.1 - 29.9 km	6 - 13 ms	0.1 - 9.9 km	Yes
BC-G	0.01 - 500*	0.1 - 29.9 km	6 - 13 ms	0.1 - 9.9 km	Yes
AC-G	0.01 - 500*	0.1 - 29.9 km	6 - 13 ms	0.1 - 9.9 km	Yes
ABC	-	0.1 - 29.9 km	< 15 ms	0.1 - 9.9 km	Yes
ABC-G	0.01 - 500*	0.1 - 29.9 km	< 15 ms	0.1 - 9.9 km	Yes

The ground fault tests are repeated for different ground current limits mentioned in Chapter 9. The performance is aligned with the results of Table 10-1 for ground currents ranging between 10 Amps (High Resistance) and 100 Amps (Medium Resistance). One important observation is the impact of mutual coupling of parallel lines (when both the lines are in operation) on zero sequence element during L-G fault detection. The detection is delayed and the fault resistance coverage is limited to 100 Ohms.

The impact of distributed energy resources is tested by varying the positive sequence source impedance of DG-A and DG-B of Fig. 9.1, thereby affecting the Surge Impedance Ratio of the network. Extensive tests reveal that the fault detection and direction determination of the model are exemplary for strong distribution network ($SIR < 10$) but the directional decision is corrupted once the SIR increases beyond the 15 mark for the tested system, especially in case of L-L faults because the negative sequence block suggests incorrect fault direction. Similarly, for L-G faults with low NGR impedance, the directional decision is inaccurate for faults close to the relay location due to voltage collapse.

The impact of power swings on the model is also investigated and the poor performance of conventional directional protection during frequency mismatch between the remote and local buses resulting in power swings is discussed in APPENDIX B.

Chapter 11 - Transient-based Directional Protection Models and Performance Evaluation

The directional algorithms based on the traveling wave principle also called transient-based or delta component directional protection strictly follow a similar order. The Simulink block diagram presented in Fig. 11.1 determines this order.

1. The **Data Extraction Blocks** are common for all the algorithms tested in this chapter. These blocks include **Data Import**^(1a) and **Data Sampling**^(1b) which imports relevant signals from the PSCAD/EMTDC Environment and samples the acquired data according to hardware specifications of the tested relays as specified in Chapter 09. These signals include both the current and voltage information of local end for all the algorithms with the exception of Current-Only transient-based methods.
2. The **Signal Processing Blocks** perform several method-specific functions including **Signal Filtering** to improve SNR, reconstruction of fundamental-frequency component using **Discrete Fourier Transform** and determination of **sequence components**. More importantly, the delta components of all the relevant signals are extracted by the **Delta Filter Block**^(2b). The functionality of each of these blocks is based on discussions of Chapter 04 and 09. Whereas the performance of delta filter block is mentioned later in this chapter.
3. Adaptive threshold based **Fault Detection Block** is common for all the algorithms presented in this chapter, with the exception of Average Window based approach. This block serves as the trigger for Directional Element and the final trip decision is taken if the output of this block and the directional element decision of both the local and remote relays are in cohesion, which is usually the case for piloted protection. The extensive performance review of the fault detection block is later presented.
4. The **Directional Element** is unique for each of the tested method. The performance of each of these methods is evaluated based on the criteria defined in Chapter 9.

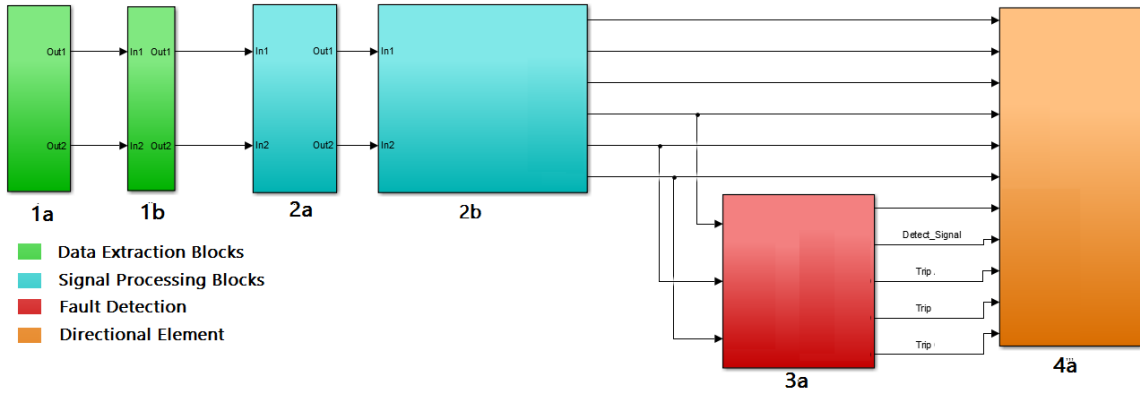


Figure 11.1 Simulink Block Diagram for Transient-based directional protection

11.1 Fundamental Blocks

11.1.1 Delta Filter

The voltage and current delta components are obtained using Equation (11.1). The reason to use a double window approach to acquire the fault components is to reduce the influence of load variation, switching and other disturbances. The output of delta filter is zero during steady state operation but changes to a non-zero value during a disturbance. The performance of delta filter is shown in Fig. 11.2 for an L-G fault, while the impact of a three phase to ground fault is recorded in APPENDIX C.

$$\Delta X = ||x_k - x_{k-N}| - |x_{k-N} - x_{k-2N}|| \tag{11.1}$$

Where x, k and N correspond to the definitions of Eq. 9.1

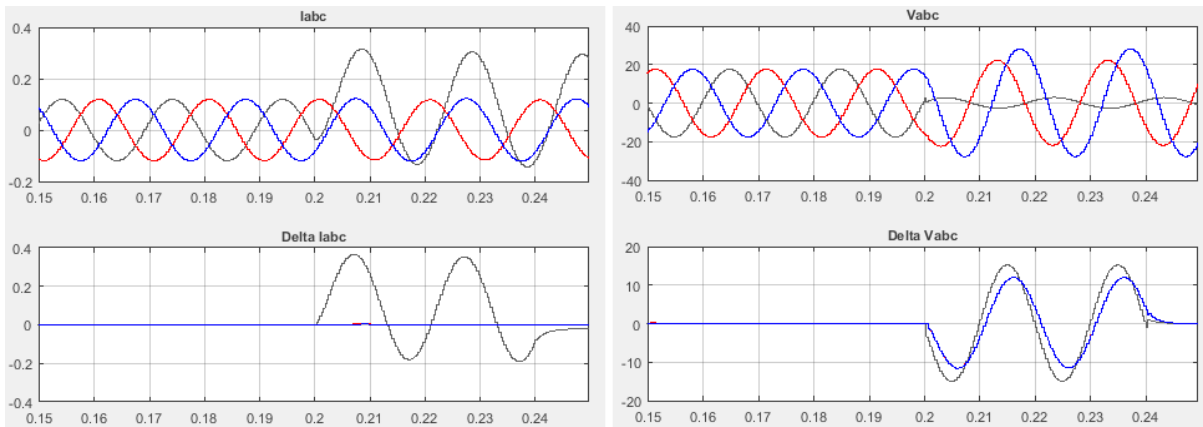


Figure 11.2 L-G Fault (Top: Three phase signals) (Bottom: Three Phase Delta quantities)
Fault Incepted at 0.2 seconds

In order to evaluate the impact of practical system disturbances, power swings have been induced by using the source frequency mismatch method. The frequency of either the remote end source or the local end source is varied between 48 Hz and 52 Hz. Fig. 11.3 presents the

influence of power swings on current and voltage recorded by the local relay when the remote end frequency is set to 48 Hz. Similarly, Fig. 11.4 describes the situation when an L-G fault is recorded during power swings. It is important to note that pre-fault delta components are non-zero in this case therefore may result in maloperation of fault detection block.

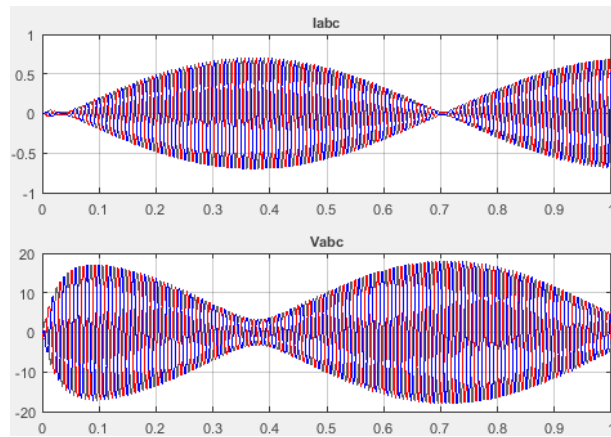


Figure 11.3 Impact of Power Swings on Three phase Current (top) and Three phase Voltage (bottom)

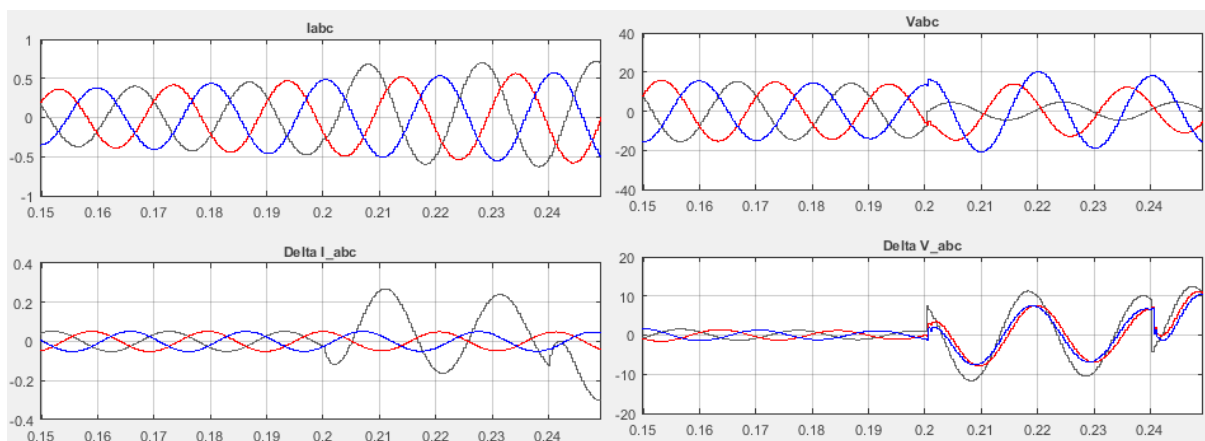


Figure 11.4 L-G Fault with Power swings
(Top: Three phase signals) (Bottom: Three Phase Delta quantities)

11.1.2 Fault Detection Block

The adaptive threshold technique explained in **Chapter 4** is used to detect fault condition. The difference between the real time delta component of the current (either phase-to-phase or positive sequence) and its equivalent adaptive threshold value is monitored. The fault detect signal is set to ‘High’ when this difference becomes greater than zero for more than 5 milliseconds, as shown in Fig. 11.5. This prevents the initiation of fault detect signal due to unfiltered noise and unhostile system disturbances.

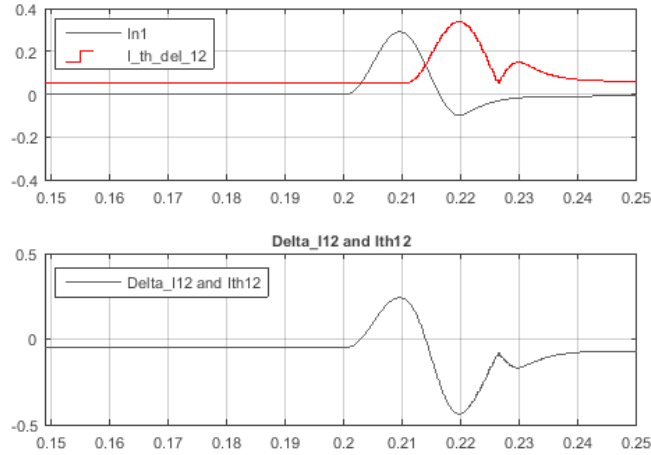


Figure 11.5 L-G Fault (Top: Real time current and Threshold current)
(Bottom: Difference between threshold and real-time current)

The parameters setting for adaptive threshold (Eq. 4.6) is rather straightforward. The current I_N is set in its p.u. form ranging between 0.1 and 10, where ‘1’ would define the nominal system current. While the weighing factors K and A vary between 0.01 and 1. These factors determine the sensitivity of the adaptive threshold. Higher the value of K lesser the sensitivity but greater the security. However, the decrease in sensitivity results in reduced fault resistance coverage affecting the block’s dependability. Another important parameter to be set is the time delay ‘ T ’, which inadvertently improves dependability of fault detection block during power swings. Some of the conventional settings are mentioned in Table 11-1. The power swings restraint is targeted for frequency mismatch between 48 and 52 Hz, with steps of 0.5 Hz.

Table 11-1 Performance of different Time Delay settings for Adaptive Threshold

Time Delay	Performance
1/4 cycle	Poor
1/2 cycle	Fast and accurate
1 cycle	Fast and accurate

The performance of adaptive-threshold fault detection block is recorded in Fig. 11.6 and 11.7. It is evident that the difference doesn’t cross the ‘zero’ mark during power swings if the weigh factors and time delay settings are accurate; while fault disturbances are detected accurately. The sensitivity of fault detection block is contrary to the security because of its vulnerability to mal-operate during system disturbances. Another important point to note is the speed of fault detection block, the decision is taken within an electrical half-cycle (<10ms). Speed might not be the primary requirement for protection of distribution networks, but it plays an important role in piloted protection based on traveling waves.

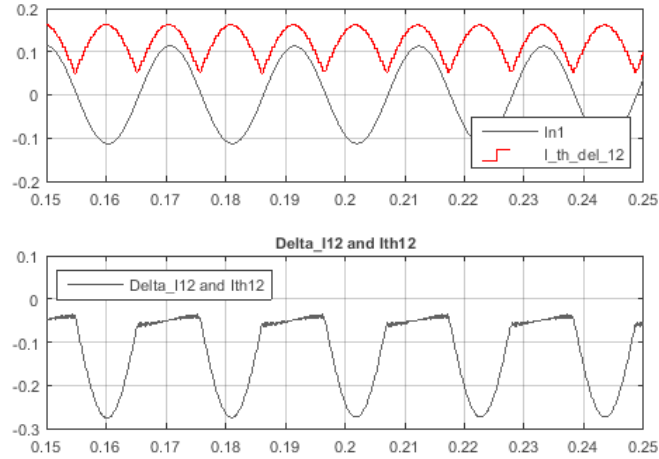


Figure 11.6 Power Swings, No Fault (Top: Real time current and Threshold current)
(Bottom: Difference between threshold and real-time current)

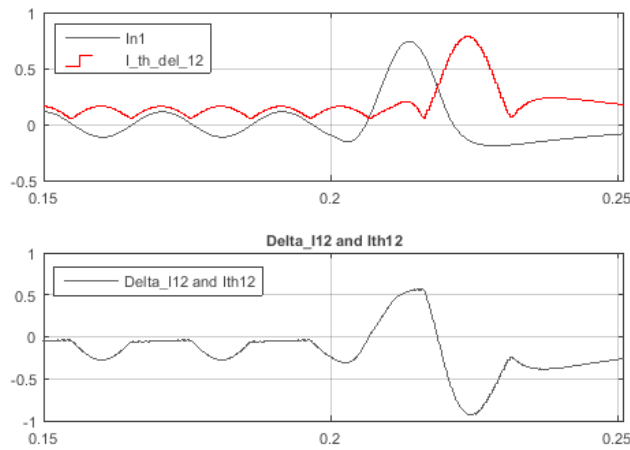


Figure 11.7 Power Swings, L-G Fault (Top: Real time current and Threshold current)
(Bottom: Difference between threshold and real-time current)

11.2 Directional Element

The transient-based directional algorithms mentioned in Chapter 05 are extensively tested in this section. The performance of each of these methods is evaluated for predefined performance parameters mentioned in Chapter 09.

11.2.1 Energy-based Algorithm (ASEA-RALDA)

The directional algorithm based on transient energy is inspired by the functionality of ASEA RALDA relay. Fig. 11.8 presents the series of steps deployed in the Simulink model. The output of Delta filter block includes fault components for phase-to-phase quantities. The product of individual fault components of current and voltage for all the phases are then summed and the discrete time integrator accumulates the transient energy over time. However, the integrator block is triggered by the fault detect signal which allows the accumulation of post-fault transient energy only. As mentioned in Chapter 05, the accumulated energy is supposed to be positive for reverse faults and negative for forward faults.

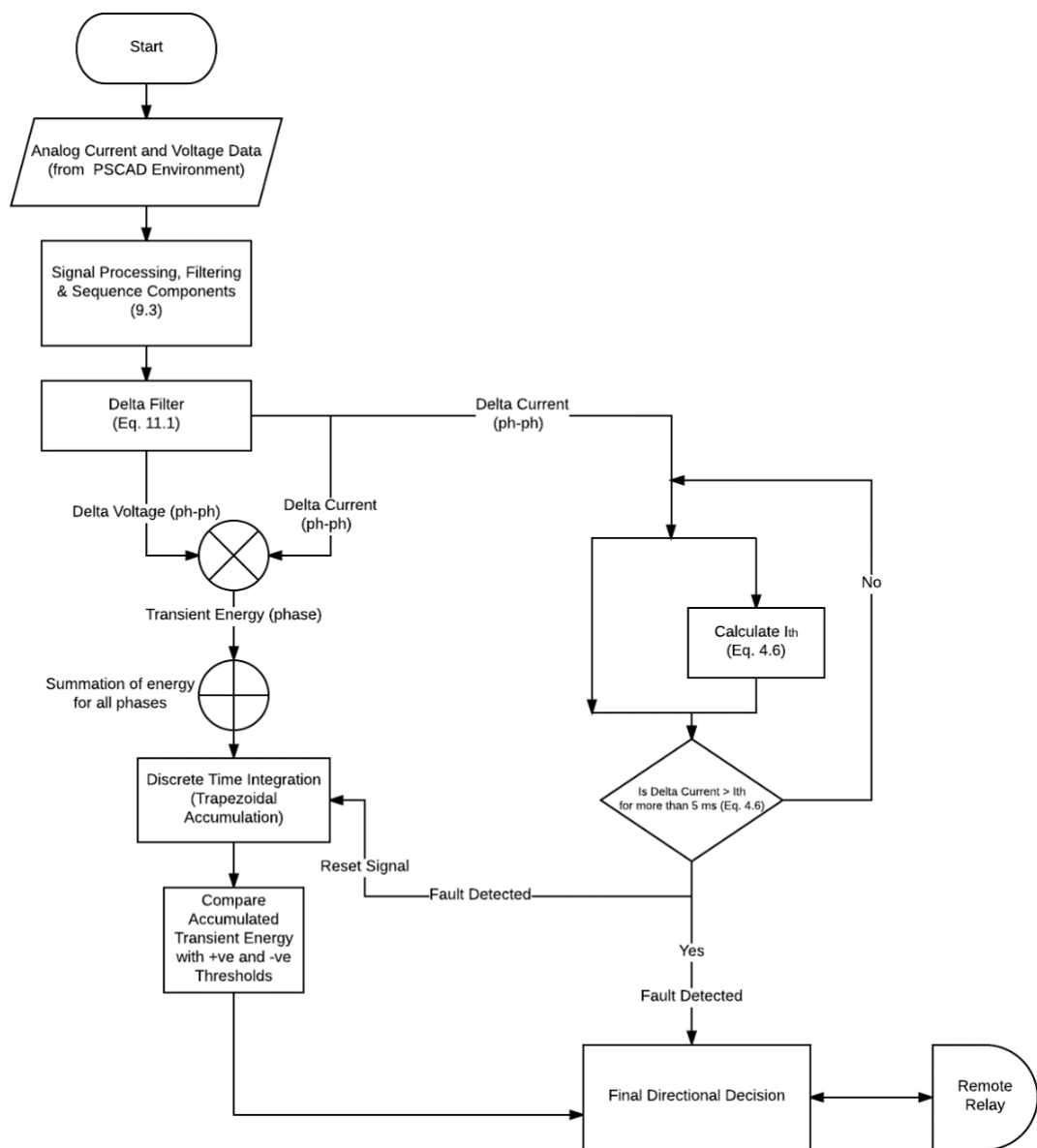


Figure 11.8 Proposed algorithm for Transient Energy based method

Fig. 11.9 presents output of Integration block for forward and reverse L-G faults. The fault is triggered at 0.2 seconds and the accumulation begins as soon as the fault is detected. The speed of fault detection and directional decision, as seen in Fig. 11.9 results in an extremely fast and accurate decision. These attributes are the primary advantages of this approach when compared with conventional directional methods.

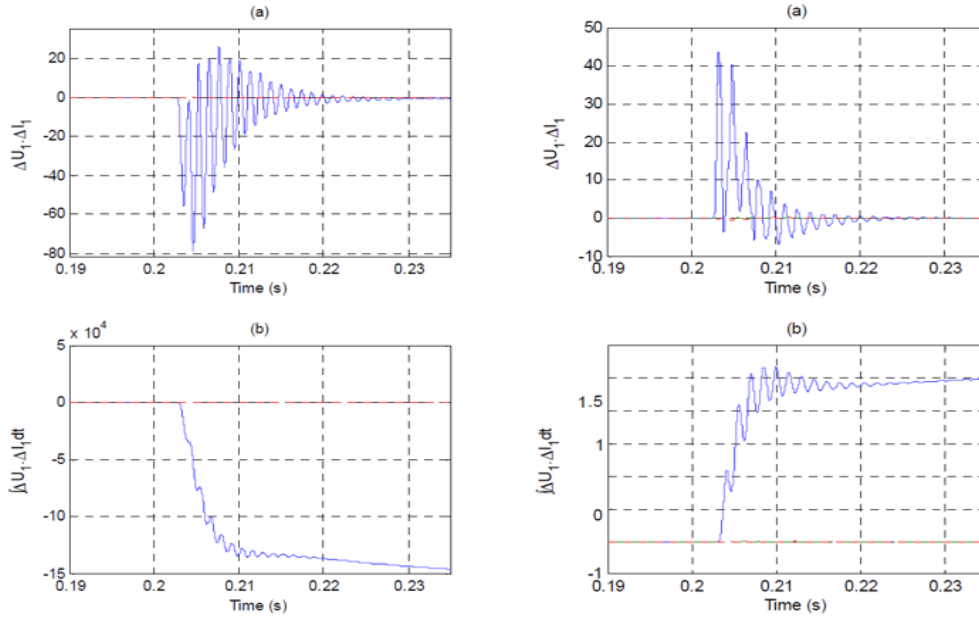


Figure 11.9 L-G Fault (Left: Forward Fault) (Right: Reverse Fault)

Extensive testing reveals that the transient energy based directional protection exhibits an outstanding performance in terms of accuracy, speed and security for all types of faults. As suggested in Table 11-2, the fault resistance coverage is twice as better as the conventional directional protection. However, sensitivity of fault detection block has to be increased for fault resistance close to 1000 Ohms; but the directional decision remains intact. Another important feature to note is the speed of operation, because all the tested faults are detected and their directions are accurately determined within half the electrical cycle (10 ms).

Table 11-2 Extensive Test Results for Transient Energy-based method (Fault Type, Fault Resistance, power flow direction)

Fault Type	Fault Resistance (Ohms)	Forward Fault Test Line length = 30 km		Reverse Fault Test Line Length = 10 km	
		Range of Fault Location	Max Decision Time	Range of Fault Location	Stable 'No Trip' Decision
A-G	0.01 - 1000*	0.1 - 29.9 km	6 - 9 ms	0.1 - 9.9 km	Yes
B-G	0.01 - 1000*	0.1 - 29.9 km	6 - 9 ms	0.1 - 9.9 km	Yes
C-G	0.01 - 1000*	0.1 - 29.9 km	6 - 9 ms	0.1 - 9.9 km	Yes
AB	-	0.1 - 29.9 km	6 - 9 ms	0.1 - 9.9 km	Yes
BC	-	0.1 - 29.9 km	6 - 9 ms	0.1 - 9.9 km	Yes
AC	-	0.1 - 29.9 km	6 - 9 ms	0.1 - 9.9 km	Yes
AB-G	0.01 - 1000*	0.1 - 29.9 km	6 - 9 ms	0.1 - 9.9 km	Yes
BC-G	0.01 - 1000*	0.1 - 29.9 km	6 - 9 ms	0.1 - 9.9 km	Yes
AC-G	0.01 - 1000*	0.1 - 29.9 km	6 - 9 ms	0.1 - 9.9 km	Yes
ABC	-	0.1 - 29.9 km	6 - 9 ms	0.1 - 9.9 km	Yes
ABC-G	0.01 - 1000*	0.1 - 29.9 km	6 - 9 ms	0.1 - 9.9 km	Yes

The results tabulated above are verified for bidirectional power flow and the ground faults are repeatedly checked for different ground current limits. The directional decision remains intact for both the conditions. The variation in fault inception instant does not affect the directional decision. The only impact is seen on the detection time, which increases by a few ms at worst.

The complexity of network is also varied by switching the distributed generator 'DG-B' into the network and by varying the positive sequence impedance of Network B. This not only allows the algorithm to be tested for weak local source but the directional decision of relay at point A verifies the results for weak remote source as well. The performance is satisfactory for SIR = 28 but the algorithm fails to detect L-L faults if strength of the source feeding the fault is reduced beyond this value.

11.2.2 Replica Impedance and Compensated Current Model (SEL & Siemens)

This approach is frequently used by SEL and Siemens. The direction of fault is determined by comparing the compensated delta current with delta voltage. Primarily, the correct voltage and current information is acquired by ensuring that the equivalent delta impedance corresponds

with the negative of positive sequence impedance of the source behind the relay. The relevant voltage and currents fulfilling this criterion vary from fault to fault. The transient impedances which are equal to the $-Z_{s1}$ for different faults have been listed in Table 5-3, which suggests that the phase-phase transient quantities would fulfill this requirement.

The flowchart defining the sequence of steps has already been provided in Fig. 5.5. The Simulink model follows this approach and utilizes a discrete time integrator triggered by fault detection reset. This integration block also performs the function of Stabilization Integral of Fig. 5.3 and 5.4. The tested algorithm utilizes phase-to-phase delta voltages and currents. Therefore the directional decision is phase-separated, which is not a primary requirement for distribution network protection.

The performance of Integral for the AB phase in case of A-G fault is recorded in Fig. 11.10 for both the forward and reverse faults. Fault is incepted at 0.2 seconds and the integral sign is opposite to the one that is discussed in References [19] and [30] which is mentioned in Chapter 05. Therefore, positive post-fault integral means reverse fault and negative integral means forward fault.

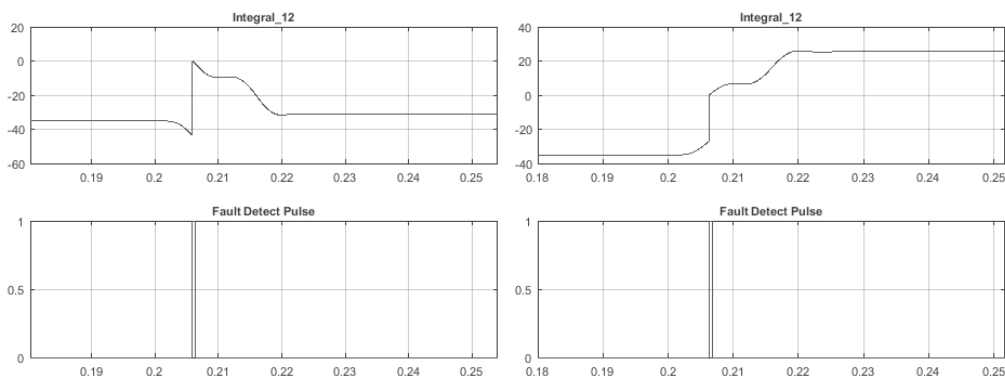


*Figure 11.10 Output of Discrete Time Integrator (Top)
Left: Forward Fault, Right: Reverse Fault*

The time domain integration is performed using Discrete-Time Integrator based on Trapezoidal Accumulation method for integration [65]. It is important to note that the output of this integrator is only taken into account once the fault detection block sends the relevant fault detect pulse, as shown in Fig. 11.10. Moreover, the integrator output does not have zero pre-fault value but the fault detection interlocking allows for correct fault direction determination once the post fault data starts accumulating. The absolute value of this output must cross a threshold before the directional decision is processed in order to minimize the impacts of noise and measurement errors. [30] suggests that this threshold should be set equal to $0.16 \cdot V(n) \cdot I(n)$

The impacts of power swings is recorded in Fig. 11.11, which suggests that the incurrence of pre-fault system disturbances does not affect the directional decision.

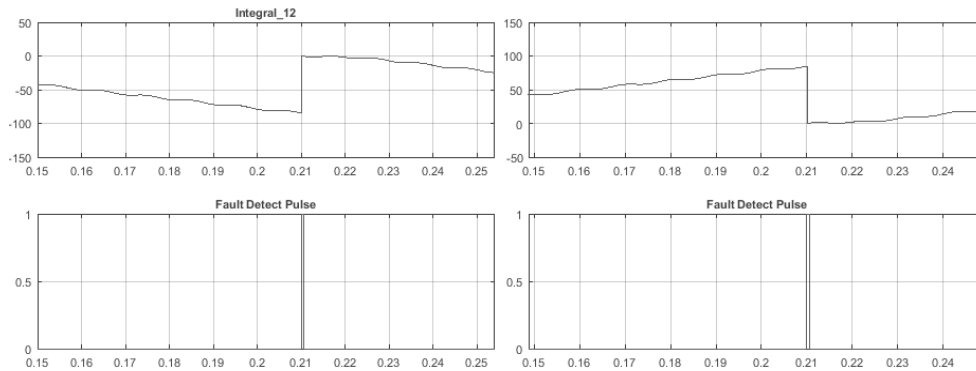


Figure 11.11 Output of Discrete Time Integrator during power swings (Top)
Left: Forward L-G Fault, Right: Reverse L-G Fault

Table 11-3 summarizes the performance of replica impedance method for several parameters including fault types, fault location, fault resistance coverage and speed of operation. One of the prominent observations is the increased decision time as compared to the transient energy based method. The fault detection block is the major culprit and the directional decision is rather quick, as seen in Fig. 11.11 earlier. Moreover, the delay is not a matter of concern for protection of distribution network.

Table 11-3 Extensive Test Results for MIMIC Filter (Replica Impedance) based method (Fault Type, Fault Resistance, power flow direction)

Fault Type	Fault Resistance (Ohms)	Forward Fault Test Line length = 25 km		Reverse Fault Test Line Length = 10 km	
		Range of Fault Location	Max Decision Time	Range of Fault Location	Stable 'No Trip' Decision
A-G	0.01 - 500	0.1 - 24.9 km	< 20 ms	0.1 - 9.9 km	Yes
B-G	0.01 - 500	0.1 - 24.9 km	< 20 ms	0.1 - 9.9 km	Yes
C-G	0.01 - 500	0.1 - 24.9 km	< 20 ms	0.1 - 9.9 km	Yes
AB	0.1	0.1 - 24.9 km	< 12 ms	0.1 - 9.9 km	Yes
BC	0.1	0.1 - 24.9 km	< 12 ms	0.1 - 9.9 km	Yes
AC	0.1	0.1 - 24.9 km	< 12 ms	0.1 - 9.9 km	Yes
AB-G	0.1	0.1 - 24.9 km	< 15 ms	0.1 - 9.9 km	Yes
BC-G	0.1	0.1 - 24.9 km	< 15 ms	0.1 - 9.9 km	Yes
AC-G	0.1	0.1 - 24.9 km	< 15 ms	0.1 - 9.9 km	Yes
ABC	0.1	0.1 - 24.9 km	< 12 ms	0.1 - 9.9 km	Yes
ABC-G	0.1	0.1 - 24.9 km	< 12 ms	0.1 - 9.9 km	Yes

Network complexity or bidirectional power flow does not affect the directional decision for Replica Impedance based method. The results of Table 11-3 are verified for both these conditions, where performance for complex networks is assessed by introducing local and remote DGs for both the internal and external fault conditions. Similarly, the ground current limits do not affect the directional decision but the fault detection block requires higher sensitivity for 10 Ampere grounding current limit in case of ground faults. Extensive tests reveal that impact of variation in network strength is similar to the transient-energy based algorithm.

It must be mentioned at this point that the presence of a parallel line does not affect the directional decision of either of the transient energy and replica impedance based method, which satisfies the claims made in References [18] and [30]; however double circuit lines can negatively influence the directional decision of these methods due to involuntary current reversal. The impact of series compensation behind or in front of the relay on either of these methods is understood to adversely affect the directional decision but is not investigated in this study.

11.2.3 Positive Sequence Transient Impedance (ΔZ_1) Model

This method is based on the sequence of steps mentioned in Fig. 5.10. The positive sequence components of delta currents and voltages are obtained after digital filtration (DFT). The ratio between positive sequence delta voltage and current is equivalent to Positive Sequence Transient Impedance (ΔZ_1). The phase angle of ΔZ_1 determines fault direction according to Fig. 5.9. The block angle is set to 15 degrees for this particular model.

The phase angle of ΔZ_1 recorded for forward and reverse L-G faults are presented in Fig. 11.12. The phase angle is found to be negative and less than block angle (-15 degrees) for forward fault; while it is positive and greater than block angle (+15 degrees) for reverse faults. The decision is delayed because the DFT block and sequence component extraction takes one complete cycle to accurately reflect the fault direction.

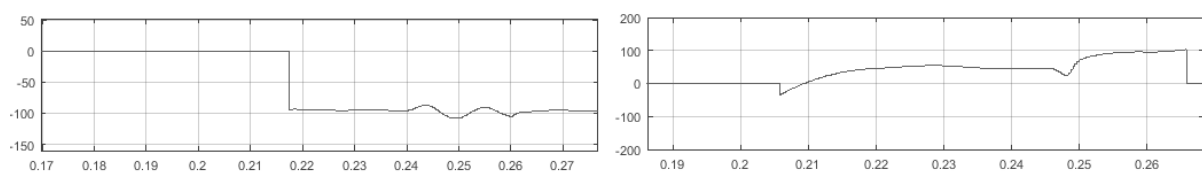


Figure 11.12 Phase angle of ΔZ_1 for L-G Fault (Left: Forward Fault) (Right: Reverse Fault)

The extensive test results presented in Table 11-4 for this method reveal certain limitations including limited fault resistance coverage and delayed directional decision. High resistance faults result in sensitivity issues for both the fault detection and directional decision block which fails to cross the block region (± 15 degrees) under certain conditions. Although the directional decision is delayed but the final phase angle is held stable to a certain value after first electrical cycle for the complete fault period (Fig. 11.12) which accounts for the reliability of this approach.

The location of faults does not affect the directional decision, especially for close-in faults (< 1km from the relay point) in case of strong sources on either ends; thereby eliminating the possibility of voltage dead-zones for close-in faults. Similarly, fault direction is accurately determined for all types of faults.

*Table 11-4 Extensive Test Results for Pos. Seq. Transient Impedance based method
(Fault Type, Fault Resistance, power flow direction)*

Fault Type	Fault Resistance (Ohms)	Forward Fault Test Line length = 30 km		Reverse Fault Test Line Length = 10 km	
		Range of Fault Location	Max Decision Time	Range of Fault Location	Stable 'No Trip' Decision
A-G	0.01 - 100	0.1 - 29.9 km	< 22 ms	0.1 - 9.9 km	Yes
B-G	0.01 - 100	0.1 - 29.9 km	< 22 ms	0.1 - 9.9 km	Yes
C-G	0.01 - 100	0.1 - 29.9 km	< 22 ms	0.1 - 9.9 km	Yes
AB	0.01	0.1 - 29.9 km	< 15 ms	0.1 - 9.9 km	Yes
BC	0.01	0.1 - 29.9 km	< 15 ms	0.1 - 9.9 km	Yes
AC	0.01	0.1 - 29.9 km	< 15 ms	0.1 - 9.9 km	Yes
AB-G	0.01	0.1 - 29.9 km	< 15 ms	0.1 - 9.9 km	Yes
BC-G	0.01	0.1 - 29.9 km	< 15 ms	0.1 - 9.9 km	Yes
AC-G	0.01	0.1 - 29.9 km	< 15 ms	0.1 - 9.9 km	Yes
ABC	0.01	0.1 - 29.9 km	< 12 ms	0.1 - 9.9 km	Yes
ABC-G	0.01	0.1 - 29.9 km	< 12 ms	0.1 - 9.9 km	Yes

The variation of fault inception angle is also investigated according to Table 9-1 and no significant impact of DC component of fault quantities is observed. In order to verify the dependence on load condition and bidirectional power flow due to involvement of positive sequence components, load angle is varied between -40 degrees and +40 degrees with the step

size of 5 degrees for L-G faults. The directional decision is found to be independent of either of these conditions. However, light load conditions ($-5 \text{ degrees} < \text{load angle} < +5 \text{ degrees}$) does affect the fault detection block.

One important observation is the dependence of positive sequence fault components (voltage and current) on source strength. For weak local source ($\text{SIR} \geq 28$), faults located further from the local end seldom result in inaccurate direction especially for high resistance condition ($R_f \geq 100 \text{ Ohm}$). This inaccuracy arises due to insignificance of positive sequence fault components for currents. Similar observations are noted for strong local sources ($\text{SIR} \leq 6$) and remote end faults ($> 25\text{km}$) due to insignificant voltage positive sequence fault components.

11.2.4 Average of Superimposed Quantities (sliding window method)

According to Reference [21], this abstract method is rather unique and require considerable number of tests and a comprehensive analysis. Since the ‘Delta Filter’ used for this method utilizes a sliding window of length of one electrical cycle to determine transient components, a comparison is provided in Fig. 11.14 and 11.15. These figures replicate a nominal line energization scenario and an ABC fault condition respectively. The transient components are calculated using conventional delta filter and sliding window based delta filter.

Although the outputs of each of the compared techniques are not exactly similar but the initial polarity variation of conventional transient-components of each phase seem to align with their sliding window counterparts. This property would be used to determine fault direction. The impact of power swings is on this approach is recorded in APPENDIX C.

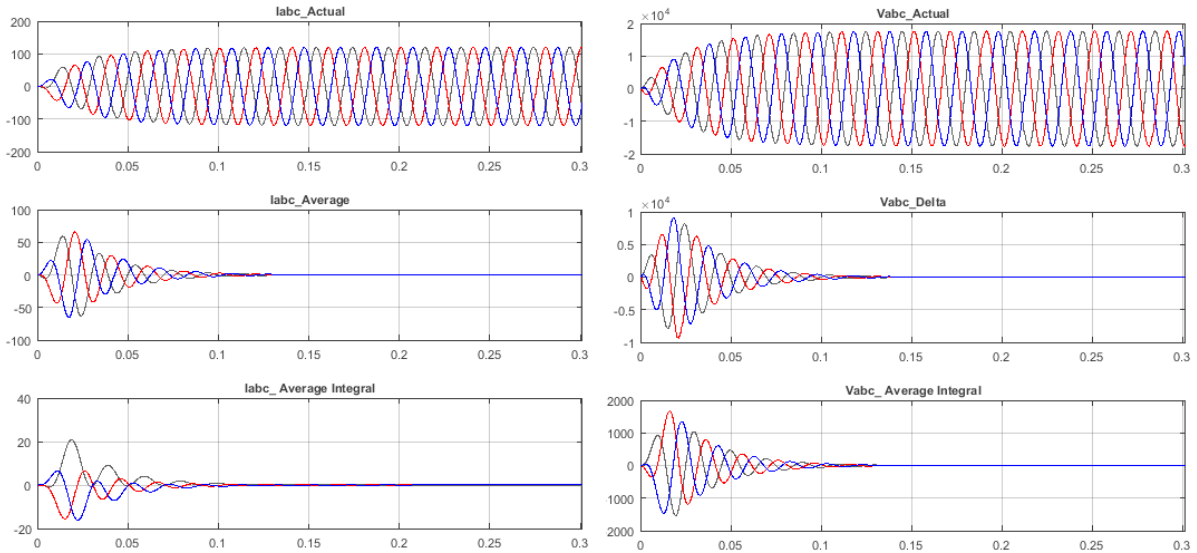


*Figure 11.13 Comparison of Delta Filter output with Average Integral filter output (Line Energization, No Fault)
Top: 3-phase quantities, Middle: 3-phase Conventional Delta Filter output, Bottom: 3-phase Average Integral filter Output*

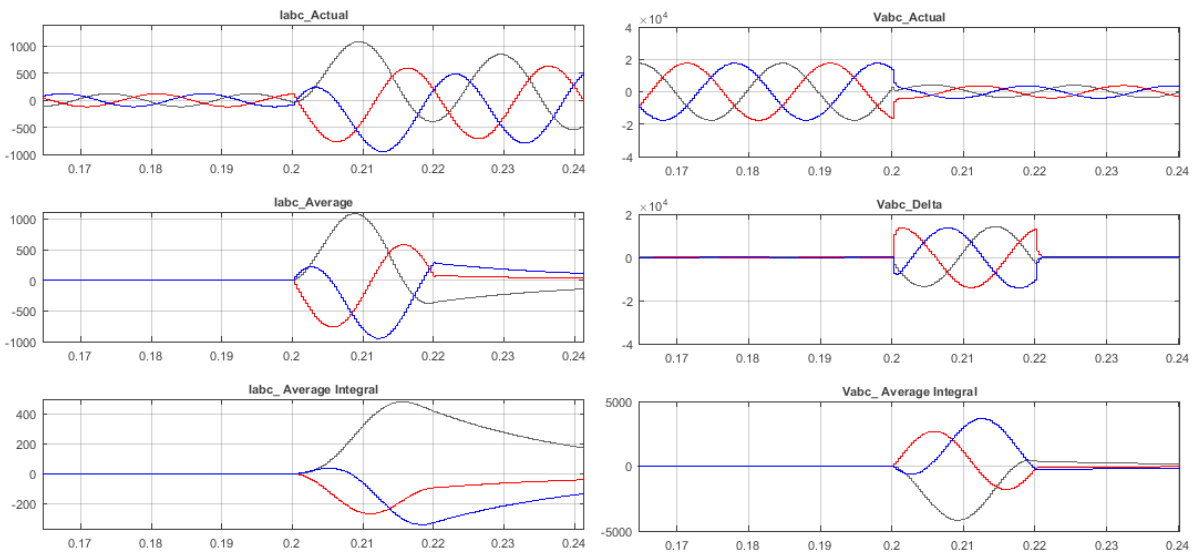


*Figure 11.14 Comparison of Delta Filter output with Average Integral filter output (L-L-L Fault)
Top: 3-phase quantities, Middle: 3-phase Conventional Delta Filter output, Bottom: 3-phase Average Integral filter Output*

As suggested in Reference [21], the current and voltage pickup thresholds are set to 25% and 10% of the variation in nominal values respectively. The performance of this approach, especially in case of power swings and high resistance faults, can further be improved by employing adaptive threshold technique suggested earlier. The cumulative integral C_r is determined by averaging the cumulative products of voltage and current average integrals over a moving window whose size is $1/8^{\text{th}}$ the size of one cycle (i.e. 8 samples for sampling

frequency of 64 samples per cycle). The polarity of this cumulative integral determines fault direction, as mentioned in Chapter 05.

The output of cumulative integral (Cr) is presented in Fig. 11.15, along with the average window outputs for current and voltage of all the three phases. The abrupt change in Cr in the negative and positive direction for forward and reverse L-G faults respectively suggests that directional decision fulfills the speed requirement like previously discussed algorithms.

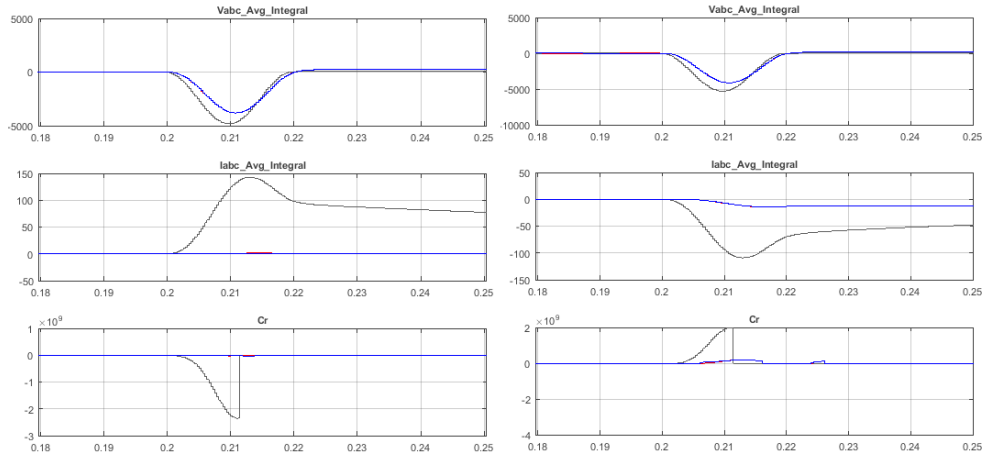


Figure 11.15 L-G Fault (Left: Forward fault, Right: Reverse fault)

Top: 3-phase Voltage Average, Middle: 3-phase Current Average, Bottom: Cr (Product of post-fault average qty.)

The fault detection and directional decision blocks of this approach perform exceptionally well for all types of faults and the location of fault does not affect the directional decision or decision time. Similar attributes are recorded for high resistance faults (up to 1 kΩ) without the need to increase threshold settings for either of these blocks. This proves the efficiency of average window method for less complex faults. Alternatively, extensive testing has also revealed that the variation of source neutral grounding type and grounding current limits for either the local or remote source or even both, according to Table 9-2, does not affect the directional decision for all the ground related faults. The network strength and complexity is also carried for all the cases specified in Table 9-3 by varying the source impedance and switching either of the distributed generators in the network. The directional decision is observed to be accurate for the faults including ungrounded ones. Both these revelations prove the effectiveness of Average-Window method for complex distribution networks with large scale DG integration.

Table 11-5 Extensive Test Results for Pos. Seq. Transient Impedance based method
(Fault Type, Fault Resistance, power flow direction)

Fault Type	Fault Resistance (Ohms)	Forward Fault Test Line length = 30 km		Reverse Fault Test Line Length = 10 km	
		Range of Fault Location	Max Decision Time	Range of Fault Location	Stable 'No Trip' Decision
A-G	0.01 - 1000	0.1 - 29.9 km	< 12 ms	0.1 - 9.9 km	Yes
B-G	0.01 - 1000	0.1 - 29.9 km	< 12 ms	0.1 - 9.9 km	Yes
C-G	0.01 - 1000	0.1 - 29.9 km	< 12 ms	0.1 - 9.9 km	Yes
AB	0.01	0.1 - 29.9 km	< 10 ms	0.1 - 9.9 km	Yes
BC	0.01	0.1 - 29.9 km	< 10 ms	0.1 - 9.9 km	Yes
AC	0.01	0.1 - 29.9 km	< 10 ms	0.1 - 9.9 km	Yes
AB-G	0.01	0.1 - 29.9 km	< 12 ms	0.1 - 9.9 km	Yes
BC-G	0.01	0.1 - 29.9 km	< 12 ms	0.1 - 9.9 km	Yes
AC-G	0.01	0.1 - 29.9 km	< 12 ms	0.1 - 9.9 km	Yes
ABC	0.01	0.1 - 29.9 km	< 10 ms	0.1 - 9.9 km	Yes
ABC-G	0.01	0.1 - 29.9 km	< 10 ms	0.1 - 9.9 km	Yes

Besides the positive attributes, certain limitations have also been recorded for the tested algorithm. The fault detection block is found to be extremely sensitive to Power Swings. This sensitivity can be reduced by permanently modifying the pickup settings, which would inadvertently reduce the fault resistance coverage and affect the performance for weak local sources. A comprehensive review of the problem suggests that these limitations can be moderated by either employing power-swing-blocking feature, which is quite common in distance protection or by using adaptive pickup settings like adaptive threshold method used in previous methods.

One more point to note is the impact of fault inception angle on the directional decision. Since the DC component of the fault current during the first half-cycle period is dependent on the fault inception angle, this could delay the directional decision. However, this particular method uses a sliding window approach to accurately determine the average of delta components; one complete cycle's information is needed before the DC component is accurately reflected. Therefore, even in case of zero DC component, the calculated average rises to a non-zero value and goes back to zero after one cycle as shown in Fig. 11.16.

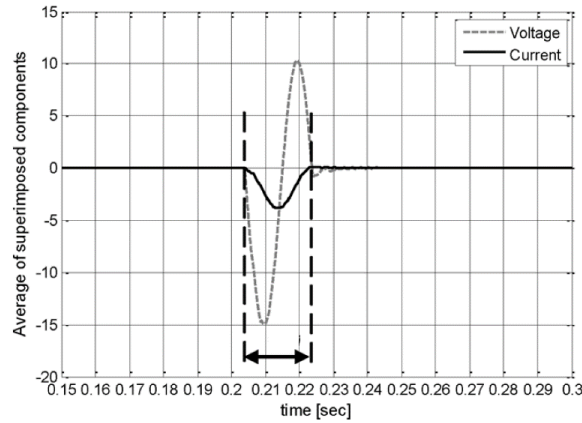


Figure 11.16 Average of Superimposed Components for zero DC fault component

11.2.5 Current-only Directional Algorithms

I. Delta Phase Angle of individual Phase Currents or Positive Sequence Current

The algorithm of Fig. 6.3 when compared with the block diagram of Fig. 11.1 reveals that the directional element for this approach is extremely simple and utilizes comparator blocks to determine fault direction. The delta phase angle of current is monitored continuously, as shown in Fig. 11.17 (bottom). A positive delta value suggests that the fault is opposite to the direction of pre-fault power flow, while negative delta suggests otherwise.

As discussed in chapter 06, this method is only applicable for protection of radial distribution networks with unidirectional power flow. The observations recorded in Fig. 11.17 and 11.18 reveal that the directional definitions change with change in direction of power flow. The phase angle change is not always equal (or close to) 90 degrees. It varies with phase angle of the individual bus voltage, fault location, fault resistance, positive sequence impedance of source and line impedance. It has also been observed that positive seq. component of current exhibits less phase variation than individual phase and is also observed to be slower because of the digital filtering involved.

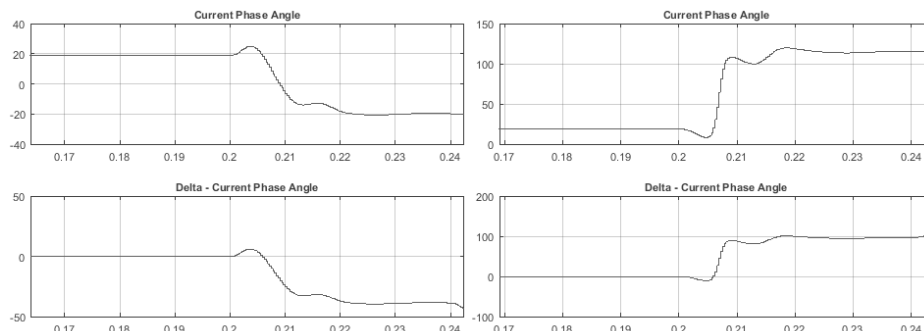


Figure 11.17 Variation in current phase angle - Forward power flow w.r.t Local Relay (Left: Forward fault) (Right: Reverse fault)

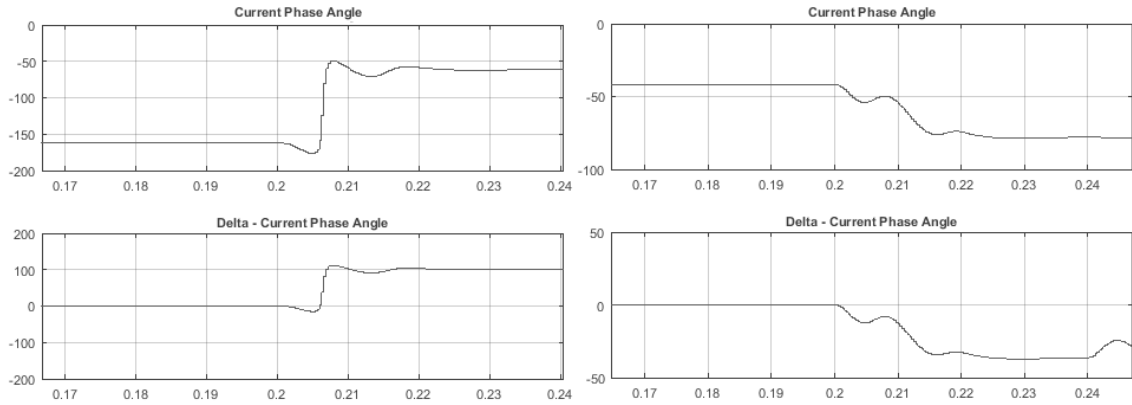


Figure 11.18 Variation in current phase angle - Reverse powerflow w.r.t Local Relay (Left: Forward fault) (Right: Reverse fault)

One important observation that several literatures fail to cover is the impact of $+\pi < \theta < -\pi$ window for phase angle of current. Hence, referring to Fig. 11.19 (left), in case of pre-fault phase angle close to $-\pi$ with negative post-fault phase change, the window allows the phase angle to enter through the $+\pi$ region allowing the phase angle change to become positive when it shouldn't. However, the maximum phase shift during faults can be $\pm\pi/2$ therefore the $\Delta\theta$ would be beyond the $+\pi$ mark in this case.

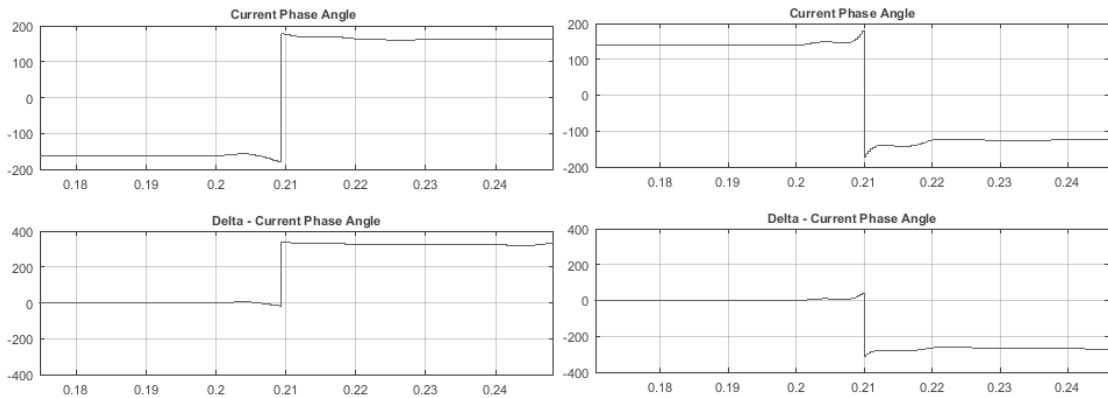


Figure 11.19 Impact of ± 180 degree limit on Variation of current phase angle - Forward powerflow w.r.t Local Relay (Left: Forward fault) (Right: Reverse fault)

This algorithm has been extensively tested and the performance goes hand-in-hand with its voltage-based counterparts. The maximum fault resistance tested for L-G faults is similar to the average-window method, with slight changing of fault detection settings. The slowness of directional decision is in response to the high resistance faults.

The impact of neutral grounding and source strength are comprehensively tested as well. Decreasing the ground current limit to 10 Ampere doesn't affect the directional decision.

Whereas this approach accurately determines the fault direction even when the SIR of DG-B is reduced to 56, which replicates an extremely weak source. Both the grounding methods and source strengths are varied for either of the local or remote source without any impact on the directional decision.

Table 11-6 Extensive Test Results for Pos. Seq. Transient Impedance based method (Fault Type, Fault Resistance, power flow direction)

Fault Type	Fault Resistance (Ohms)	Forward Fault Test Line length = 30 km		Reverse Fault Test Line Length = 10 km	
		Range of Fault Location	Max Decision Time	Range of Fault Location	Stable 'No Trip' Decision
A-G	0.01 - 1000*	0.1 - 29.9 km	< 30 ms*	0.1 - 9.9 km	Yes
B-G	0.01 - 1000*	0.1 - 29.9 km	< 30 ms*	0.1 - 9.9 km	Yes
C-G	0.01 - 1000*	0.1 - 29.9 km	< 30 ms*	0.1 - 9.9 km	Yes
AB	0.01	0.1 - 29.9 km	< 12 ms	0.1 - 9.9 km	Yes
AC	0.01	0.1 - 29.9 km	< 12 ms	0.1 - 9.9 km	Yes
AB-G	0.01	0.1 - 29.9 km	< 15 ms	0.1 - 9.9 km	Yes
BC-G	0.01	0.1 - 29.9 km	< 15 ms	0.1 - 9.9 km	Yes
AC-G	0.01	0.1 - 29.9 km	< 15 ms	0.1 - 9.9 km	Yes
ABC	0.01	0.1 - 29.9 km	< 12 ms	0.1 - 9.9 km	Yes
ABC-G	0.01	0.1 - 29.9 km	< 12 ms	0.1 - 9.9 km	Yes

II. Delta Phase Angle ($\Delta\theta$) comparison of Local and Remote Ends:

Based on the suggestions of Reference [61], the impact of power flow direction on phase change is resolved by communicating the current phase change of each ends. For internal faults the phase change is observed to be opposite for the local and remote end; whereas for internal faults, the phase change is similar. These observations are recorded in Fig. 11.20 and 11.21 for forward and reverse power flow respectively.

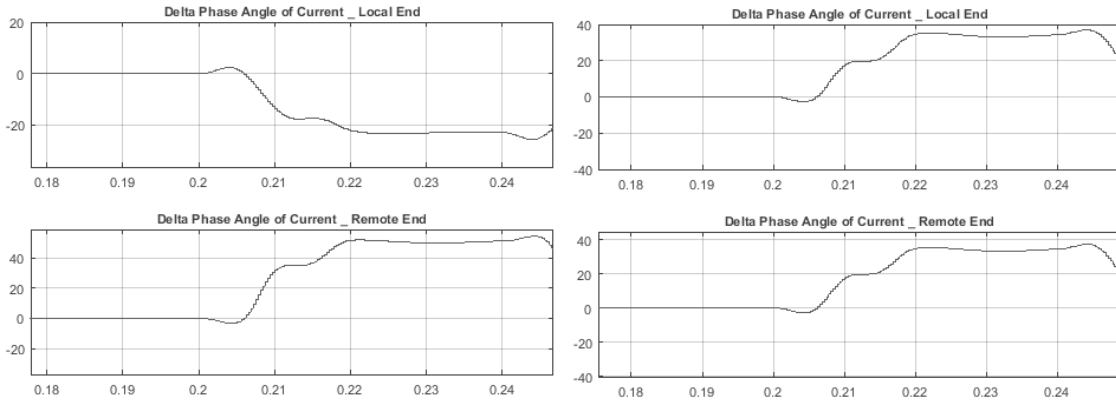


Figure 11.20 Forward Power flow w.r.t Local Relay (Left: Internal fault) (Right: External fault)

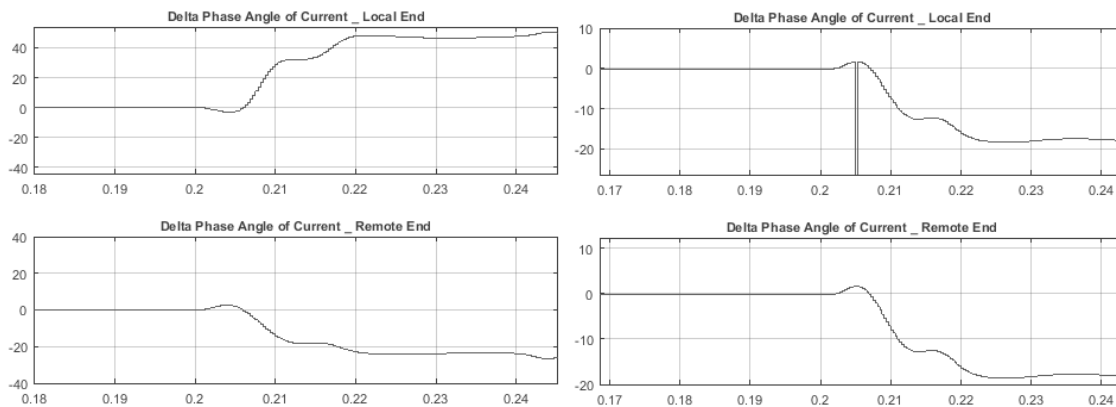


Figure 11.21 Reverse Power flow w.r.t Local Relay (Left: Internal fault) (Right: External fault)'

The comprehensive test results discussed in previous section are relevant for this approach. This is true because both these methods are based on the exact same principle with the addition of communication. The impact of $+\pi < \theta < -\pi$ is also relevant for this method.

III. Post-fault current based algorithm

The last transient-based method of reference [57] resolves the dependence on power flow direction by basing the directional decision on post fault current and its positive and negative derivatives. The $\pm\pi/2$ phase shift for positive and negative derivatives are visible in Fig. 11.22. The inception of fault takes place at 0.2 seconds; the post-fault variation in delta angle (bottom) settles down to a stable value after one complete cycle in each case. The correct directional decision is therefore only determined after one cycle of fault inception. It is visible in Fig. 11.22 and 11.23 that the reversal of pre-fault power flow does not commend change in directional definition, which contradicts the principle of previous current-only methods. The abrupt change of delta angle to -90 degrees for reverse faults and +90 degrees for forward faults proves the effectiveness of this method.

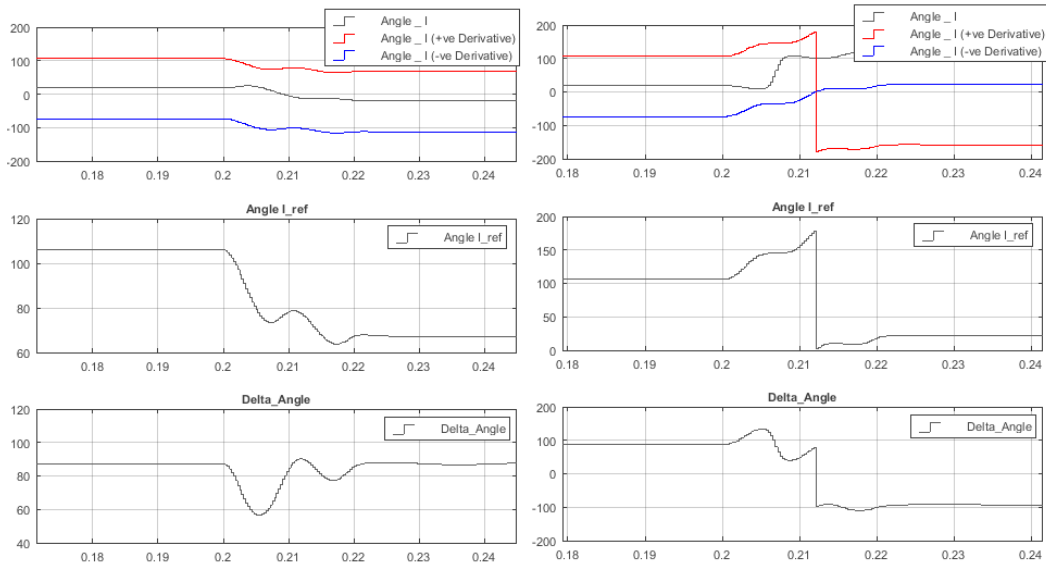


Figure 11.22 Forward power flow (left: Forward fault) (right: Reverse fault)
 Top: Phase Angles, Middle: Phase Angle of I_{ref} , Bottom: Delta Angle

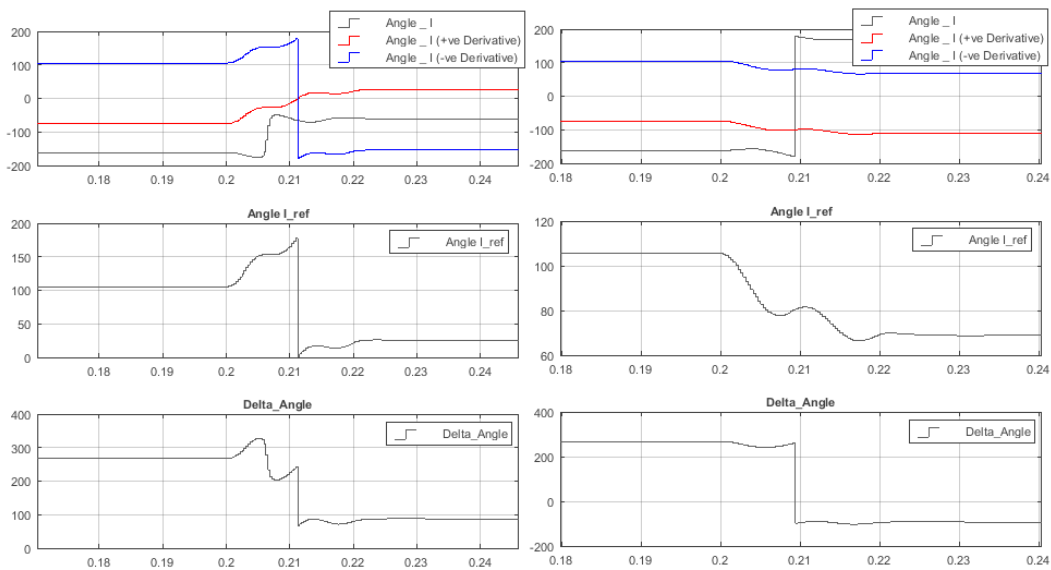


Figure 11.23 Reverse power flow (left: Forward fault) (right: Reverse fault)
 Top: Phase Angles, Middle: Phase Angle of I_{ref} , Bottom: Delta Angle

Reference [57] fails to address the vulnerability of this approach for varying load conditions. The method fails to accurately determine fault direction under certain conditions. Some of the observed dependencies include load angle (difference between voltage phase angles of both ends), individual voltage phase angle of local bus for forward faults and strength of the source feeding the fault. Moreover, the fault resistance coverage is also limited. The impact of power swings has also been studied and seldom failures to determine fault direction are observed. These limitations have been resolved by providing power-flow-direction supervision, which is beyond the scope of this report.

Chapter 12 - Line Differential Protection Models and Verification

In order to assess the performance of line differential protection (87L), operating mechanism of two of the well renowned differential relays have been investigated:

1. SIPROTEC 4 7SD522 by Siemens
2. RED 670/615 by ABB

The relays under discussion are primarily employed for HV transmission lines protection, but the operating mechanisms of their counterparts for distribution lines protection are same. Besides analyzing the operating principle in time domain, a simplistic polar plane analysis has also been performed later in this chapter.

12.1 PSCAD/EMTDC Model

In order to review the performance of both the relays, certain assumptions have been made to allow simplicity and to meet time restrictions for the project. These assumptions include:

- Prevention of inrush cross blocking from different phases by allowing ‘Inrush Restraint’ to be active for all the three phases.
- Secondly, a mono-mode fiber optic cable is used for communication of current phasors between remote and local relays; which allows fixed channel time delay and reduces data synchronization complexity. Moreover, channel BW and data packet issues are ignored.
- The omission of ‘Charge Comparison’ technique, which allows the final decision to be based on ‘Phasor Comparison’ only. This is especially important for a simplified SIPROTEC 4 Relay.
- Finally, the circuit is supposed to be energized and pre-energization differential and inrush current settings are not needed.

Fig. 12.1 determines the generic model developed in PSCAD/EMTDC; while Fig. 12.2 gives a brief flowchart of operation including communication between the local and remote relays. The model has been divided in three blocks, as mentioned in the figure.

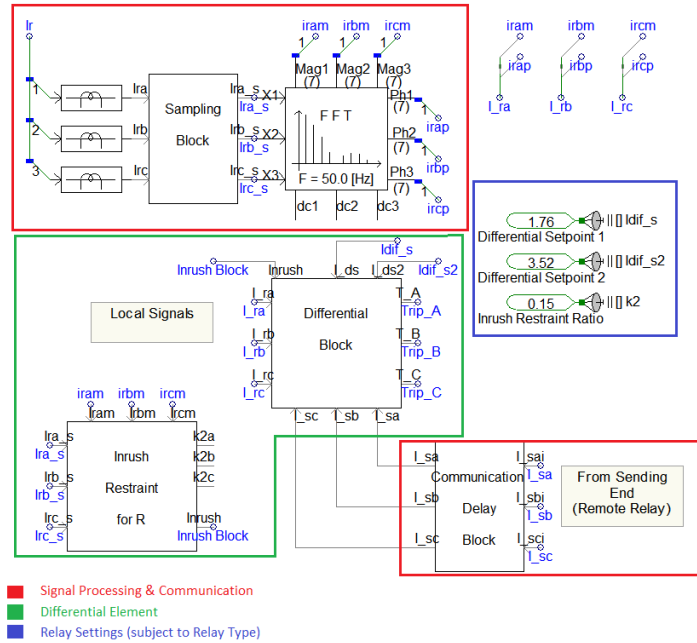


Figure 12.1 Classification of blocks in PSCAD/EMTDC Model for Line Differential Protection

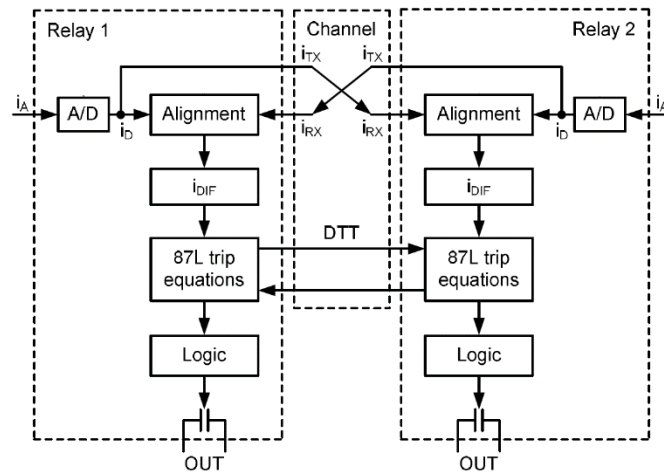


Figure 12.2 Steps of operation for the tested PSCAD/EMTDC Model

12.1.1 Signal Processing & Communication

This block extracts the local three phase current signal using current transformers, passes it through an anti-aliasing filter, digitizes the improved SNR data and reconstructs the fundamental signal using a digital filter (FFT). All these steps have been explicitly explained in Chapter 9.

In contrast to commonly employed methods, mono-mode fiber optic (FO) cables with a dedicated 64 kbps channels have been employed over the 30 km length for communication.

The data transfer speed of each of the tested relay is assumed to be equal to the bandwidth speed of the FO cable (which is 512 kbits/s) for this study. As carefully calculated in Chapter 08, the sampling frequency of SIPROTEC 4 7SD552, which is 1 kHz (20 samples per electrical cycle of 50 Hz) is considered for determining the size of each data packet. This does not constitute the worst case because ABB RED 615 offers more number of samples per cycle and will have a smaller available BW as compared to its counterpart. The results have now been summarized in Table 12-1, along with technical data of the mono-mode FO cable [14].

Table 12-1 Data Management Results and FO Cable Data

Symbol	Parameter	Value
Sampling Data		
fs	Sampling Frequency (kHz)	1
n	Samples per cycle	20
T	Time for each sample for 50 Hz (ms)	1
Data Handling Results		
T_d	Fixed Time between transferred data packets (ms)	3
n_a	Size of data packet for 3 samples of data (bits)	100
n_o	Expected Overhead size (bits)	50 - 80
n_p	Max. Total data packet size : n _p = n _o + n _a (bits)	180
n_{BW}	BW @ 3 ms packet delay and 64 kbps channel (bits)	192
n_F	Fixed frame length for data packet (bits)	200
FO Cable data		
v_{BW}	Bandwidth Speed (kbits/s)	512
L_C	Length of cable (km)	30
c_{FO}	Speed of light for FO Cable (km/s)	200000

As explained in chapter 08, the channel-based synchronization requires the calculation of t_{OFFSET} , which represents the channel time delay. This calculation allows the data to be aligned at each relay, as shown in Fig. 12.3, where instantaneous remote and local current data packets are aligned before the data can be analyzed by the differential block. The fixed channel latency (t_{OFFSET}) is calculated using Eq. 12.1 and found to be 0.931 ms.

$$t_{OFFSET} = T_L + T_C + T_R \quad (12.1)$$

Where,

$$T_L = \text{Sending delay for local relay} = \frac{n_F}{v_{BW}}$$

$$T_C = \text{Transmission delay through FO cable} = \frac{L_C}{c_{FO}}$$

$$T_R = \text{Receiving delay for remote relay} = \frac{n_F}{v_{BW}}$$

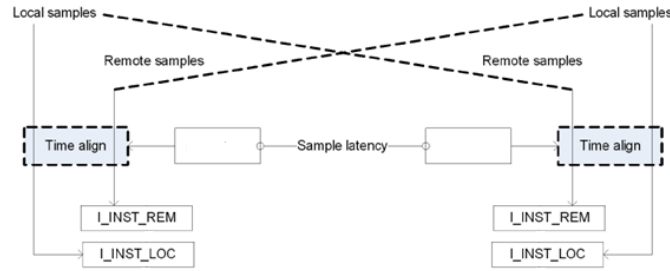


Figure 12.3 Mechanism of Data Transmission for tested relays

It must be acknowledged that this is a rather simple technique used for data synchronization and is based on fixed time delays, which is usually the case with dedicated channels in FO cables, but well versed real-time techniques like pingpong/echo methods should be used for actual channel delay calculation. Moreover, practical issues like data packet loss, signal attenuation due to cable length and all the relevant problems related to data handling and synchronization mentioned in Chapter 8 must be taken into account for practical implementation of the communication block.

12.1.2 Differential and Inrush Restraint Blocks

These blocks are relay-specific and depend upon the individual operating principle. The RED 615 relays use a dual slope method and base their operation on Eq. 7.1, 7.2 and 7.6, as shown in Fig. 12.4.

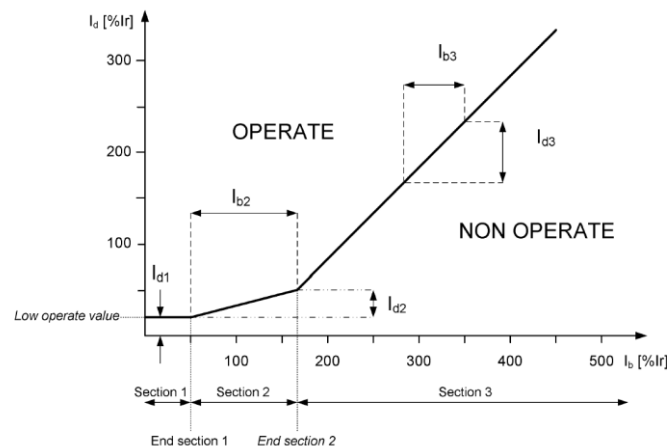


Figure 12.4 Tested operating characteristics of ABB RED 615/670 relay

Whereas, the restraint phasor for SIPROTEC has been retrieved from Ref [70] and is given in Eq. 12.2. The operating principle is rather straightforward ($I_{OP} > I_{RES}$) while the operating

current (I_{OP}) calculation is same as Eq. 7.6. APPENDIX D can be referred for the PSCAD/EMTDC differential block model of SIPROTEC 4 7SD52

$$I_{RES} = I_{dif_s} + \begin{cases} A2 \cdot |I_1| : |I_1| \leq A1 \\ A3 \cdot |I_1| : |I_1| > A1 \end{cases} + \begin{cases} A2 \cdot |I_2| : |I_2| \leq A1 \\ A3 \cdot |I_2| : |I_2| > A1 \end{cases} \quad (12.2)$$

The inrush restraint block is common for both the tested algorithms. The second harmonic current phasors are extracted using the Fast Fourier Transform digital filter tuned to 100 Hz. The algorithm continuously monitors the ratio between the magnitudes of second and first harmonic current phasors. Tripping signal is blocked if this ratio crosses the ‘Inrush Restraint Ratio’ threshold setting (k_{2_set}), as shown in Eq. 12.3

$$\frac{|I_2|}{|I_1|} > k_{2_set} \quad (12.3)$$

12.2 Relay Settings

These settings are subject to the type of relay under test. Fig. 12.1 refers to the I_{dif_s} and inrush restraint settings for SIPROTEC relay. Moreover, the A1, A2 and A3 relay parameters for determining correct restrain current are determined by following the procedure explained in [70]. Moreover, the dual slope settings for ABB RED 615 and RED 670 have been set for Section 2 and 3 of Fig. 12.4 only. The basic differential current setting (I_{S1}) has been set to 3.75 A while the slope representing the section 2 percentage bias setting (K_1) has been set to 30%. For large through current condition represented by section 3, the restrain current threshold (I_{S2}) is set to 0.25 kA and the higher percentage bias setting (K_1) is set to 150%.

It must be noted that the capacitive charging current (I_c) for the protected OHL line is found to be 1.2 A, which dictates the settings for I_{S1} . The current I_c is approximated using the Eq. 12.4 and verified by measuring the differential current during steady-state operation.

$$I_c = 3.63 \times 10^6 U_N f_N C_{OP} L \quad (12.4)$$

Where,

U_N = Nominal Line-Line Voltage in kV

f_N = Nominal system frequency (Hz)

C_{OP} = Line per-phase capacitance in nF/km (8 nF/km for the OHL)

L = Length of line in km

12.3 Test Results and Discussion

The slight difference in operating principle of either of these relays does not reflect the same in their performance. Extensive tests have revealed that the operating time, fault resistance, fault type and fault location coverage are very similar. The results, summarized in Table 12-2, reveal that the line differential algorithms fulfill all the requirements for protection of distribution lines. The ability to detect bolted faults extremely close to the relay location independent of the strength of source feeding the fault is one of these advantages, verified in the table. Another important feature is the fault resistance coverage of up to 200 Ohm for the tested network. However, the operating time is slightly on the higher side when compared with transient-based directional protection. This apparent delay in operation is introduced because of communication and data alignment delays. It should be noted that similar delays would exist for the piloted transient-based directional protection as well.

The differential and restraint (bias) currents for each phase are recorded in Fig. 12.5 and Fig. 12.6 for internal and external faults respectively. It can be seen that the I_{diff} crosses the relevant I_{bias} within 10-15 ms of fault inception in case of internal faults. However, for external faults the through current increases only and so significant deviation is observed for differential currents.

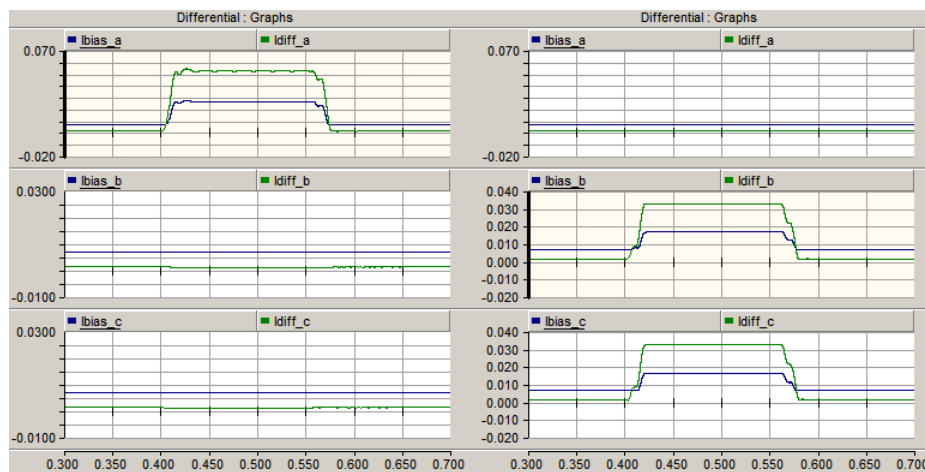


Figure 12.5 Three Phase Differential and Restrain Currents for Internal Faults (Left: A-G fault, Right: B-C fault)

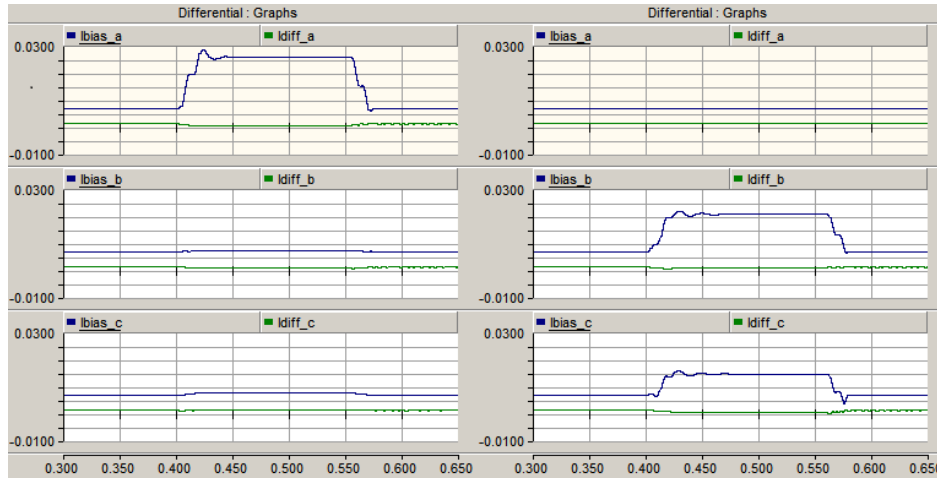


Figure 12.6 Three Phase Differential and Restrain Currents for External Faults (Left: A-G fault, Right: B-C fault)

Another important observation is the impact of fault resistance on both the differential and restraint currents, as shown in Fig. 12.7. The change in both I_{diff} and I_{bias} is significantly less for 200 Ohms fault resistance than the previous internal fault case but both show similar reduction, which allows the differential current to cross the restraint one easily. This proves the effectiveness of this scheme for high resistance faults.

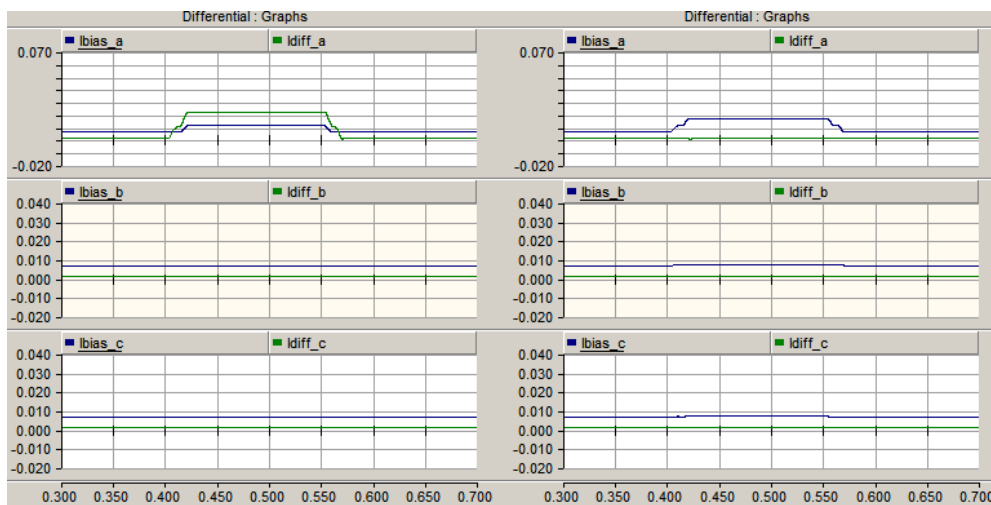


Figure 12.7 Three Phase Differential and Restrain Currents for 200 Ohm A-G Faults (Left: Internal, Right: External)

After exhaustive testing, it is observed that the line differential protection successfully operates for all types of faults and the decision is taken within two electrical cycles for the tested system in worst case. This satisfies the critical fault clearing time requirements of current distribution networks. The results have been summarized in Table 12-2 and it can be seen that maximum fault resistance resulting in accurate operate is limited 200 Ohms only, which proves the substantial susceptibility to fault resistance. Unlike current-only transient based methods, pre-

fault power flow direction does not influence the fault decision (internal and external). The prefault load condition and the fault inception angle do not influence the decision; however, the decision time varies between 14 – 30 ms for different fault inception instants. Whereas, as far as source strength and network grounding mechanism are concerned, the performance exactly corresponds with the performance of current-only transient based directional protection.

Table 12-2 Extensive test results for line differential protection

Fault Type	Fault Resistance (Ohms)	Internal Fault Test Line length = 30 km		External Fault Test Line Length = 10 km	
		Range of Fault Location	Max Decision Time	Range of Fault Location	Stable 'No Trip' Decision
A-G	0.01 - 200	0.1 - 29.9 km	< 28 ms*	0.1 - 9.9 km	Yes
B-G	0.01 - 200	0.1 - 29.9 km	< 28 ms*	0.1 - 9.9 km	Yes
C-G	0.01 - 200	0.1 - 29.9 km	< 28 ms*	0.1 - 9.9 km	Yes
AB	0.01 - 200	0.1 - 29.9 km	< 20 ms	0.1 - 9.9 km	Yes
BC	0.01 - 200	0.1 - 29.9 km	< 20 ms	0.1 - 9.9 km	Yes
AC	0.01 - 200	0.1 - 29.9 km	< 20 ms	0.1 - 9.9 km	Yes
AB-G	0.01 - 200	0.1 - 29.9 km	< 25 ms	0.1 - 9.9 km	Yes
BC-G	0.01 - 200	0.1 - 29.9 km	< 25 ms	0.1 - 9.9 km	Yes
AC-G	0.01 - 200	0.1 - 29.9 km	< 25 ms	0.1 - 9.9 km	Yes
ABC	0.01 - 200	0.1 - 29.9 km	< 20 ms	0.1 - 9.9 km	Yes
ABC-G	0.01 - 200	0.1 - 29.9 km	< 20 ms	0.1 - 9.9 km	Yes

12.4 Polar Plane Analysis and Discussion

The operating characteristics of line differential protection are also explored on the polar current diagram. This diagram represents the ratio between remote and local current phasors, with horizontal axis representing the real component of the ratio and vertical axis representing the imaginary part. The characteristics of ABB RED 615/670 are reciprocated only to avoid

complication. As mentioned in [29], the dual slope characteristics represented by Eq. 7.1 ($I_{OP} \geq K \cdot I_{RT} + K_0$) and Eq. 7.2 ($I_{RT} = k |I_L - I_R|$) does not result in circular characteristics on the polar plane which makes the analysis difficult. The analysis is simplified by using the single slope characteristic ($I_{OP} \geq K \cdot I_{RT}$) for second section only and the tests are repeated for heavy load condition (large prefault restraint current) only. Polar plane circular characteristics are parameterized according to the first row of Table 7-1; therefore, the radius and center of the circle is found to be 2.6 units and ‘-1.2 + j0’ units respectively for slope settings of 0.71. This can be reviewed in Fig. 12.9 and it must be noted that as long as the measured locus stays within this region, trip command is not generated by the relay.

The locus of current phasors ratio for nominal load variation is presented in Fig. 12.8 This includes the voltage buildup and line charging period as well. It can be seen that the locus is confined in a very small region and stays within the ‘No Trip’ region at all times. The tests are repeated for various load conditions by varying the load angle between the two networks and no significant deviations are observed.

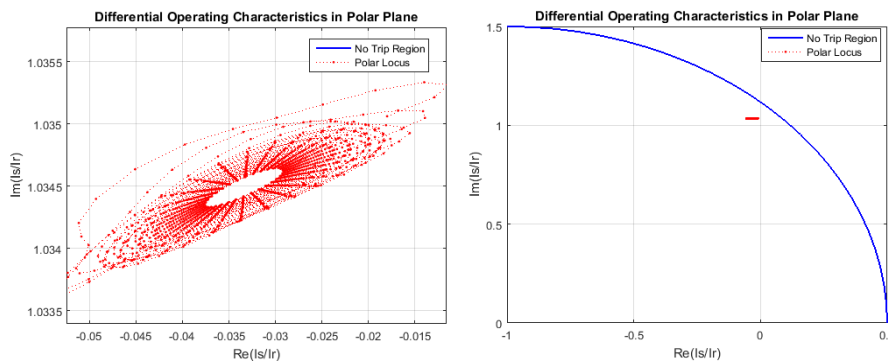


Figure 12.8 Nominal load condition including voltage buildup period (Left: Magnified View, Right: Overview)

The analysis is repeated for external faults (A-G and A-B-C) and the locus is only plotted for fault duration (Fig. 12.9) and for Phase-A only. It can be observed that the locus is no longer centralized to a small region and significant variation as compared to nominal load condition is recorded. However, the ‘No Trip’ region is never violated and the locus fails to initiate trip command, which fulfills the protection requirements.

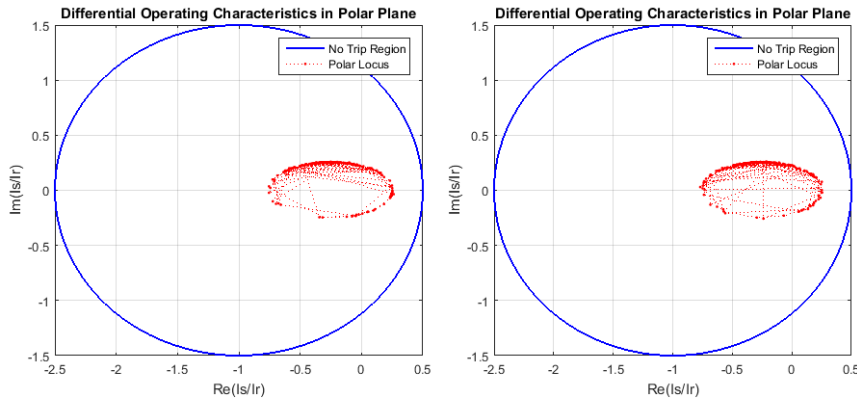


Figure 12.9 External Fault Trajectory in the Polar Plane (Left: L-G Fault, Right: L-L-L Fault)

The tests are repeated for several fault resistances between 0.01 Ohm and 200 Ohm along with variation in fault location in order to verify the performance for maximum and minimum fault currents. The trajectory changes slightly between each of these conditions but the locus never crosses the set operating characteristics boundary.

In case of internal faults, the polar trajectory changes significantly. Fig. 12.10 reveals that the loci enters the trip region numerous times for both the faults. Extensive repetition of tests suggests that the fault resistance coverage is adequate and location of fault does not affect the decision. Moreover, no significant impact of ground current limit and source strength is observed either.

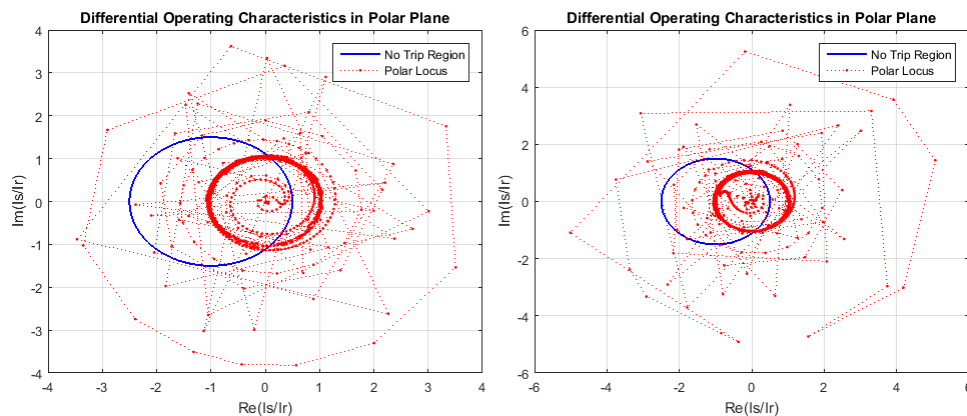


Figure 12.10 Internal Fault Trajectory in the Polar Plane (Left: L-G Fault, Right: L-L-L Fault)

Another important analysis that can be made using the polar plane approach is the impact of sampling rate on secure operation. The sampling frequency and communication channel BW are two important constraints that must be dealt with for line differential protection. Since the information transmitted across the channel in this case is not real-time but reconstructed current phasors, the requirement of high sampling frequency is reduced. As shown in Fig. 12.11, the 0.5 kHz sampling rate (left) results in 10 samples per cycle and the trajectory in less elaborate;

whereas, the sampling frequency when gradually increased to 4.0 kHz (right) resulting in 80 samples per cycle reveals the nominal shape of trajectory during nominal load condition. It must be noted that although the trajectory may not be ideal for low sampling frequencies, the loci is still concentrated in the same region. The tests are repeated for different sampling frequencies for internal and external fault conditions as well and similar observations are recorded; which implicates the impact of this technique.

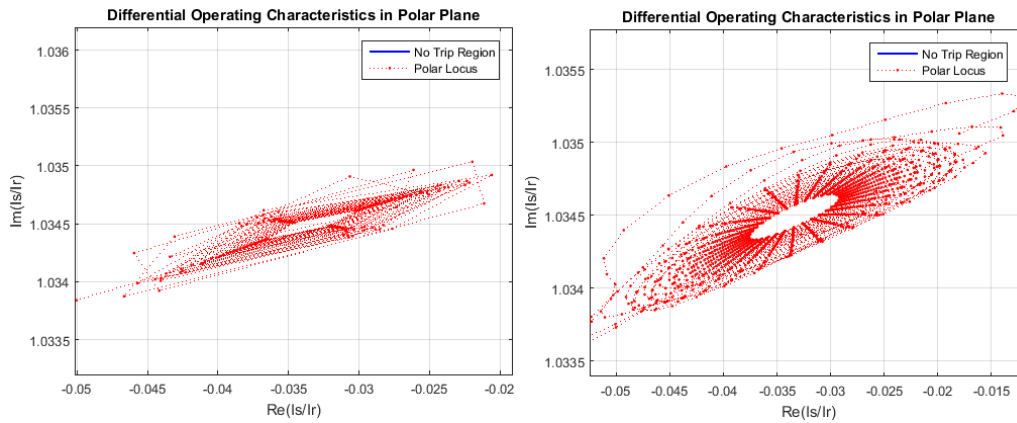


Figure 12.11 Nominal load condition including voltage buildup period (Left: $f_s = 0.5$ kHz, Right: $f_s = 4$ kHz)

Chapter 13 – Discussion and Performance Comparison of Pilot Protection Schemes (Line Differential, Conventional and Transient-based Directional Protection)

The discussion of Chapter 8 – 12 is summarized in this section and a brief comparison is provided to assess the performance and relevance of each of the tested algorithms for the protection of future distribution networks.

13.1 Practicality of implementation (Current and Voltage information)

Trusted directional protection algorithms (both conventional and transient-based) require both the local current and voltage information to accurately determine fault direction. This would require wide scale employment of voltage transformers in the distribution network, which increases the cost of implementation drastically. Whereas, all the proven differential algorithms use either the current-phasor comparison method or the charge comparison technique to determine whether the fault is internal to the protected region or external.

This practical hindrance is extremely important in terms of economy for application in distribution networks, because voltage transformers are usually not installed on both the MV and LV distribution systems across Europe. However, these considerations are set to change with implementation of microgrids and wide area monitoring and protection systems. Power systems including distribution networks are expected to go through some extensive revamping in the next decade and installation of voltage transformers across the system might be considered in order to provide additional control to the system operators.

Another important point to mention regarding transient-based directional protection is the investigation of current-only schemes. The methods discussed in Chapters 6 and 11 prove the effectiveness of current-only schemes along with the relevant restrictions. The original method developed during this study uses only the current information to accurately determine fault direction and the limitations associated with other current-only schemes are not observed in this case. This original method has been filed as an invention disclosure case with ABB and is currently under review.

13.2 Communication Channel:

The communication channel requirements are sterner for line differential protection because real-time current information has to be transmitted over the channel while maintaining high rate of data exchange. Therefore, line differential protection usually requires a 56 or 64 kbps

dedicated channel in case of point-to-point connections. Whereas, the communication speed as low as 9 kbps would be sufficient for transient-based and conventional directional protection.

13.3 Data Management and Synchronization:

As suggested by the discussion in Chapter 8, line differential protection is fundamentally built upon data management and synchronization. This requires a meticulous effort during planning and design phase because managing relevant data is just as important as the effectiveness of protection algorithm itself. The requirements of data synchronization and management are listed in reference [16], including data packet structuring techniques, overhead to payload management, data alignment accuracy and time referencing (internal or external). These considerations are extremely important, primarily because protection engineers have limited access to data channeling and related equipment.

Data synchronization is not as crucial for piloted directional protection. Almost all the tested algorithms can hold the trip signal stably for a certain period, which allows the transfer tripping scheme to perform effectively well. Moreover, since the actual current or voltage data is not transmitted over the communication channel there is no need to align the remote end's data with the local one.

Data management becomes relatively simple for directional protection because limited communication channel BW is less influential during the relay design phase because only the tripping supervision signal is to be transferred instead of actual data and also because the rate of data transfer does not have to be as high as for line differential protection.

13.4 Data Transmission Delay:

The unexpected communication delay encountered in case of routed communication channels severely affects the performance of line differential protection, but neither the transient-based directional schemes nor the conventional ones are sensitive to such delays.

13.5 Parallel and Double Circuit Lines:

Neither the mutual coupling due to double circuit lines nor due to parallel lines affect the decision of line differential protection. The performance is found to be satisfactory for faults when parallel line is in operation. However, the conventional directional protection are strongly impacted by the inductive coupling with lines within close proximity of the protected line. The zero sequence element fails to detect high resistance faults ($R_f > 100$ Ohms) when the parallel line is switched for the studied case. The transient-based directional schemes (including

RALDA principle and MIMIC filter approach) are found to be more prone to double circuit lines as compared to line differential protection, because of current reversal during faults, which results in inaccurate fault direction.

13.6 Series Compensated Lines:

The current and voltage reversal phenomena associated with series compensated lines make both the directional schemes ineffective. However, the line differential protection performs exceptionally well in such case. Nevertheless, this problem is not a matter of concern for distribution network and is more applicable to HV transmission lines.

13.7 High Impedance Faults:

The transient-based directional algorithms are found to be extremely sensitive to high impedance faults, with accurate and fast fault direction detection of fault resistances up to 1000 Ohms for the tested system. Conventional schemes offer fault resistance coverage up to 500 Ohms but the zero sequence mutual coupling to parallel lines can reduce the maximum fault resistance. Line differential protection is found to have sensitivity issues with fault impedance. The maximum R_f that can be detected in case of internal L-G faults is recorded to be 200 Ohms for the tested system. As shown in Fig. 12.7, the operating current reduces drastically with increasing fault resistance.

13.8 Charging Current and Phase Shift Correction:

The charging currents associated with transformer and/or cable terminated lines are a source of concern for line differential protection, but both the directional schemes are not affected by this current. This observation has been discussed in detail in previous chapters. Moreover, additional efforts with phase shift correction and compensation of CT ratio are required with line differential protection in most cases.

13.9 Saturation of Current Transformers:

The directional decision of the tested transient-based schemes is extremely fast and utilizes the information of several fault components (DC, fundamental and high frequency), therefore the saturation of CTs does not affect this decision. Therefore, CTs with lower accuracy limit factor or protection class can be used. While, line differential protection is highly susceptible to this saturation and often require critical CT design to overcome this restriction.

13.10 Impact of Source Strength (DG integration) and fault locations:

Extensive testing has revealed that both the conventional and transient-based directional algorithms are susceptible to source/network strength for different fault locations because of its dependence on voltage information. The directional decision is accurate for conventional schemes for SIR up to 15. While all the transient-based algorithms work accurately for weak sources with network SIR up to 28, with the exception of positive sequence based method which fails to detect fault direction for strong sources as well (for remote faults).

It must be mentioned that the current-only transient algorithms offer best results in terms of source strength tests. The SIR of the network is varied up to 56 (extremely weak network) and the recorded results claim that all the current-only schemes successfully determine fault direction. This was partially expected because source strength has adverse impacts on voltage of relay location (especially for bolted close-in faults), but these schemes do not use this information to determine fault location.

Lastly, the extensive testing of line differential protection reveals the same results as current-only transient-based scheme. The source strength doesn't affect the decision which proves the effectiveness of this scheme for protection of a distribution network with integrated DERs.

13.11 Impacts of System Grounding:

The performance of line differential protection is not influenced by the system grounding current limit. The decision holds valid for both high resistance ground networks (< 10 Ampere) and medium resistance ground network (10 – 100 Amperes). However, directional protection algorithms results in mixed response. The directional decision for conventional methods is often inaccurate for low resistance ground networks (>100 Amperes) when the fault is located close to the relay. Whereas some of the transient based methods (including MIMIC filter and replica impedance approaches) exhibit sensitivity issues for high grounding resistance networks.

Conclusive Remarks

The protection requirements of modern distribution networks with large-scale integration of DERs can be met by the piloted schemes assessed in this study. With the advent of communication methodologies over the last decade, these piloted schemes offer distinctive advantages over overcurrent protection with directional supervision.

However, as far as the directional protection is concerned, the conventional schemes would result in insecure operation if the faults are close to these distributed weak sources. Moreover, vulnerability of these methods to system frequency unbalance would also be a matter of concern.

In contrast, the tested transient-based directional algorithms base their decisions on fault components and the use of adaptive threshold for fault detection make these methods less susceptible to both these vulnerabilities. All the tested algorithms with the exception of positive sequence method offer high-speed performance, which allows the additional requirement of limited CCT to be met. The transient energy and replica impedance methods have already proven their worth in the transmission network, but the average window method is relatively new and seems to be more defenseless against high fault resistance and system frequency unbalance than its predecessors are. By combining both the conventional directional protection and transient-based direction protection, it is proved that a secure pilot protection system could be formulated with certain advantages. One important limitation that all the directional schemes face is the requirement of voltage information to determine fault direction, which can be practically irrelevant for distribution networks because of the involved costs.

Although the performance of the tested line differential protection relays has proven to be exemplary for modern distribution networks, the customary limitations associated with this technique including data synchronization and saturation of current transformers are the restricting factors for its wide scale implementation. Moreover, the costs and technology associated with laying a dedicated communication network also limit its application.

The transient-based directional protection scheme based on current information only would prove to be the ultimate solution for such networks because of its exceptional performance in weak networks and its autonomy over communication-based limitations associated with line differential protection. The problem associated with the impact of pre-fault power flow direction on fault directional decision can be eliminated using the technique proposed in the associated invention disclosure.

Future Work

As a matter of fact, the test conditions do not corroborate real world issues yet which includes CT saturation, inaccuracies in measuring instruments, impact of harmonics and system capacitive current etc. because of limited time scheme for the thesis work. Although the Lucas model for current transformers in PSCAD should fulfill the saturation and inaccuracy requirements for most algorithms, but the impact of white noise and other relevant disturbances, which are prominent in communication-based protection have not been taken into consideration. Moreover, the combination of OHLs and cable terminations can be impactful on transient-based directional algorithms but these circumstances are not taken into account,

These limitations can be improved by developing either a practical test bed or using Omicron in order to test the real-time performance of each of these algorithms. This can also assist in validating the performance of all the tested methods. As far as the current system model is concerned, following improvements can be made in the future:

- Accurate modeling of distributed generators (like small wind farms) on PSCAD to assess the fault contribution of these units. Currently this is done by reducing the source strength (i.e. limiting the current contribution and increasing the source impedance).
- The inclusion of inline transformers and multi terminal networks inspired by IEEE PSRC recommended test networks would allow a more comprehensive analysis.
- Several differential protection methodologies including the ones based on phase locked loops and active current extraction can be investigated. These algorithms reduce the communication channel limitations; therefore, can be fruitful for distribution network protection.
- Similarly, the analysis of polar plane method for differential protection can also be helpful.
- Incorporate communication delays, packet loss and synchronization challenges using PSCAD communication blocks.

References

- [1] *IEEE C37.113 Guide for Protective Relay Applications to Transmission Lines*
- [2] IEEE Power System Relaying Committee Report, "Line protection design trends in the USA and Canada," *IEEE Transactions on Power Delivery*, Vol. 3, No 4, October 1988, pp. 1530-1535
- [3] Application guide on protection of complex transmission network configurations: *CIGRE materials, CIGRE SC-34 WG 34.04*, Nov. 1991.
- [4] Power System protection Principles by Alstom, Chapter 11 (Distance Protection)
- [5] G. Ziegler, Numerical Differential Protection: Principles and Applications, *Nuremberg, Germany: Siemens AG, Jul. 2005*
- [6] P.M. Anderson, Power System Protection, McGraw-Hill /IEEE Press, New York, NY, 1999.
- [7] J. Tan, D. Tholomier, G. Bin, and W. Hua, "Sensitivity and stability of superimposed component based directional comparison protection," in *Proc. Can. Conf. Elect. Comput. Eng.*, 2007, pp. 280–283.
- [8] H. Gao and P. A. Crossley, "Design and evaluation of a directional algorithm for transmission-line protection based on positive sequence fault components," in *Proc. Inst. Elect. Eng., Gen. Transm. Distrib.*, Nov. 2006, vol. 153, no. 6, pp. 711–718.
- [9] W. Chen, O. P. Malik, X. Yin, D. Chen, and Z. Zhang, "A wavelet based ultra-high speed superimposed voltage directional protection," in *Proc. PowerCon*, 2002, vol. 1, pp. 300–303.
- [10] S. Guorong, "A new directional relay based on the variation of power frequency components," *Autom. Elect. Power Syst.*, vol. 11, no. 1, pp. 28–38, Jan. 1983.
- [11] Horowitz S.H., Phadke A.G., and Thorp J.S., 1988. Adaptive transmission system relaying, *IEEE Trans. Power Del.*, vol.3, no.4, pp.1436-1445.
- [12] G. Benmouyal, "Amplitude-independent comparators for UHS directional relays," *Developments in Power System Protection*, Conference Publication IEE, no. 434, pp. 78-82, 25-27th March 1997.
- [13] S. Zhu, *Theory and Technology of HV Network Protective Relaying* (in Chinese). Beijing, China: China Electricity Press.
- [14] M. Szykiel, C. Leth Bak 'Line Differential Protection Scheme Modelling for Underground 420 kV Cable Systems'
- [15] M. G. Adamiak, Dr. W. Premerlani, G. E. Alexander, 'A New Approach to Current Differential Protection for Transmission Lines' *Electric council of new England protective relaying committee meeting october 22-23, 1998 portsmouth, nh*
- [16] H. Miller, J. Burger, N. Fischer B. Kasztenny 'Modern Line Current Differential Protection Solutions', *Line Current Differential Protection: A Collection of Technical Papers Representing Modern Solutions, 2014*
- [17] X. Deng, R. Yuan, 'A Novel Current Differential Protection Scheme for Transmission Lines using Fast Active Current Extraction'
- [18] J. Blumschein, C. Dzienis, M. Kereit, 'Directional Comparison based on High-Speed-Distance Protection using Delta Quantities' *Siemens AG, Infrastructure & Cities Sector*
- [19] C. Dzienis, M. Kereit, 'An Experimental Analysis of High-Speed-Distance Protection' *October 2010 Source: IEEE Xplore*
- [20] M. Chamia, S. Liberman, 'Ultra High Speed Relay for EHV/UHV Transmission Line – Development, Design and Application' *IEEE Transactions on Power Apparatus and Systems*, Vol. OAS – 97, No. 6, Nov/Dec 1978, pp 2104-2113
- [21] S. M. Hashemi, M. Tarafdar Hagh 'Transmission-Line Protection: A Directional Comparison Scheme Using the Average of Superimposed Components' *IEEE transactions on power delivery*, vol. 28, no. 2, April 2013 pp 955-962
- [22] D. W. P. Thomas M.S. Jones C. Christopoulos, 'Phase selection based on superimposed components', *IEE Pvoc.-Gener. Transm Distrib.* Vol 143, No. 3, May 1996 pp. 295 - 299

- [23] X. Dong, W. Kong, T. Cui, 'Fault Classification and Faulted-Phase Selection Based on the Initial Current Traveling Wave' *IEEE transactions on power delivery*, vol. 24, no. 2, APRIL 2009, pp – 552 - 55
- [24] Z. Li, X. Lin 'Efforts on Improving the Performance of Superimposed-Based Distance Protection', *IEEE transactions on power delivery*, vol. 27, no. 1, JANUARY 2012 pp- 186 - 195
- [25] E. Vázquez, J. Castruita, O. L. Chacón, 'A New Approach Traveling-Wave Distance Protection—Part I: Algorithm' *IEEE transactions on power delivery*, vol. 22, no. 2, APRIL 2007, pp. 795 - 801
- [26] K. V. Babu, M. Tripathy, A. K. Singh 'Recent techniques used in transmission line protection: a review' *International Journal of Engineering, Science and Technology* Vol. 3, No. 3, 2011, pp. 1-8
- [27] G. G. Karady, P. mandave, 'Pilot directional protection using negative sequence directional element' *Power Systems Conference (PSC), 2014 Clemson University March, 2014*
- [28] J. Roberts, A. Guzmán, 'Directional Element Design and Evaluation' *49th Annual Georgia Tech Protective Relaying Conference, May 1995 and revised edition released August 2006*
- [29] J. Roberts, D. Tziouvaras, G. Benmouyal, 'The Effect of Multiprinciple Line Protection on Dependability and Security' *55th Annual Georgia Tech Protective Relaying Conference, May 2001,*
- [30] G. benmouyal, J. Roberts, 'Superimposed Quantities: their true nature and application in relays' *presented at the 26th Annual Western Protective Relay Conference, Spokane Washington, Oct 26-28 1999*
- [31] L. Zhenkun, j. Hui, F. Yang, 'Fast Distance Protection for proximal fault of EHV transmission lines' *Telkommika*, Vol. 11, No. 2, Feb 2013, pp. 615-622
- [32] K. Zimmerman, D. Costello, 'Fundamentals and Improvements for Directional Relays' *37th Annual Western Protective Relay Conference, October 2010*
- [33] B. Fleming, 'Negative-sequence impedance directional element' *Copyright © SEL 1998 www.selinc.com*
- [34] N. Sharma, G. Karady, 'Pilot Directional protection scheme using wireless communication', *International Journal of Computer, Electrical and IT*, Vol 09, No. 7, 2015
- [35] D. Jones, J. J. Kumm, 'Future Distribution Feeder Protection Using Directional Overcurrent Elements' *IEEE transactions on industry applications*, vol. 50, no. 2 pp 1385-1391, march/april 2014
- [36] A. Hooshyar, M. Abdelkhalek, 'Three-Phase Fault Direction Identification for Distribution Systems With DFIG-Based Wind DG', *IEEE transactions on sustainable energy*, vol. 5, no. 3 pp-747-757, July 2014
- [37] Lin, H., Liu, C., Guerrero, J. M., & Quintero, J. C. V. (2015). Distance Protection for Microgrids in Distribution System. In *Proceedings of the 41th Annual Conference of IEEE Industrial Electronics Society, IECON 2015* (pp. 000731-000736). IEEE Press. DOI: 10.1109/IECON.2015.7392186
- [38] I. Xyngi, 'An Intelligent algorithm for smart grid protection applications' *Wohrmann print service, zutphen, ISBN 978-94-6186-014-9*
- [39] Seethalekshmi K., S.N. Singh, 'Wide-Area Protection and Control: Present Status and Key Challenges' *Fifteenth National Power Systems Conference (NPSC), IIT Bombay*, pp 169-175 December 2008
- [40] Z. Fan, G. Song, C. Wang, 'Study on Distance Protection Based on Wide Area Information' *2016 China International Conference on Electricity Distribution (CICED 2016) Xi'an*, 10-13 Aug. 2016 Paper No. CP0694
- [41] A. Oudalova, A. Fidigattib, 'Adaptive network protection in microgrids' *ABB Switzerland Ltd., Corporate Research, Segelhof 1, CH-5405 Dättwil, Switzerland*

- [42] D. Williston, D. Turcotte, A. Sinclair, 'Area EPS and Distributed Resources Protection Best Practices', Power and Energy Society General Meeting (PES), 21-25 July 2013
- [43] S. Voima, H Laaksonen, K Kauhaniemi, 'Adaptive Protection Scheme for Smart Grids' Developments in Power System Protection (DPSP 2014), 12th IET International Conference on, April 2014
- [44] M. Delfanti, M. Merlo, G. Monfredini, 'Hosting Dispersed Generation on Italian MV networks: towards smart grids' Harmonics and Quality of Power (ICHQP), 2010 14th International Conference
- [45] I. Xyngi, M. Popov, 'Smart Protection in Dutch Medium Voltage Distributed Generation Systems', Innovative Smart Grid Technologies Conference Europe (ISGT Europe), 2010 IEEE PES
- [46] I. Xyngi, M. Popov, E. J. C. 'short circuit behavior of distribution grids with a large share of distributed generation units' CIRED - 21st International Conference on Electricity Distribution, Frankfurt, 6-9 June 2011, Paper 0432
- [47] I. Xyngi, M. Popov, 'Transient Based Protection Scheme for Distribution Grids Supplied with Distributed Generation' Universities Power Engineering Conference (UPEC), 2009 Proceedings of the 44th International
- [48] I. Xyngi, M. Popov, 'An Intelligent Algorithm for the Protection of Smart Power Systems', IEEE transactions on smart grid, vol. 4, no. 3, September 2013, pp 1541-1549
- [49] W. K. Sonnemann, "A Study of Directional Element Connections for Phase Relays," AIEE Transactions, 1950, Volume 69, pp 1438–1451.
- [50] SEL-321 instruction manual, Schweitzer Engineering Laboratories Inc. (<http://www.selinc.com>)
- [51] Global Status Report for Renewables 2016, REN21, Renewable Energy Policy Network for the 21st Century
- [52] N. Hatziargyriou, 'Book: Microgrids Architectures and Control' *IEEE Press*
- [53] P. Kundur, 'Book: Power System Stability and Control', McGraw-Hill Inc.
- [54] M. Biswal, S. Biswal, 'A positive-sequence current based directional relaying approach for CCVT subsidence transient condition' *Protection and Control of Modern Power Systems (2017) 2:8 DOI 10.1186/s41601-017-0038-0*
- [55] Y. Li, B. Su, 'Method for identifying fault direction without voltage measurement information and directional element thereof' *Patent: WO2013106985 A1, ABB Research Ltd.*
- [56] A. K. Pradhan, A. Routray, S. Madhan 'Fault Direction Estimation in Radial Distribution System Using Phase Change in Sequence Current' *IEEE Transactions On Power Delivery, Vol. 22, No. 4, October 2007 pp: 2065 - 2072*
- [57] A. Jalilian, M. Tarafdar Hagh, S. M. Hashemi 'An Innovative Directional Relaying Scheme Based on Postfault Current' *IEEE Transactions On Power Delivery, Vol. 29, No. 6, December 2014 pp: 2640 – 2647*
- [58] A. Ukil, B. Deck, V. H. Shah, 'Current-Only Directional Overcurrent Relay' *IEEE sensors journal, vol. 11, no. 6, June 2011pp: 1403-1404*
- [59] A. Ukil 'Detection of Direction Change in Prefault Current in Current-Only Directional Overcurrent Protection' *Industrial Electronics Society, IECON 2016 - 42nd Annual Conference of the IEEE 23-26 Oct. 2016 pp: 3829-3833*
- [60] A. Ukil, B. Deck, V. H. Shah 'Smart Distribution Protection Using Current-Only Directional Overcurrent Relay' *Innovative Smart Grid Technologies Conference Europe (ISGT Europe), 2010 IEEE PES*

- [61] X. Si, Q. Chen, L. Wang ‘Protection of distribution systems with distributed generation using current phase variation’ *Developments in Power System Protection (DPSP 2014), 12th IET International Conference*
- [62] A. Ukil, B. Deck, V. H. Shah ‘Current-Only Directional Overcurrent Protection for Distribution Automation: Challenges and Solutions’ *IEEE Transactions On Smart Grid, Vol. 3, No. 4, December 2012 pp: 1687-1694*
- [63] V. Cook, Analysis of Distance Protection, *Research Study Press Ltd, John Wiley & Sons Inc., 1985*
- [64] A.G. Phadke, J.S. Thorp, Synchronized Phasor Measurements and their applications, *Springer, New York, 2008.*
- [65] Simulink Mathworks library. <https://se.mathworks.com/help/simulink/slref/>
- [66] ABB: Indoor Supporting Current Transformers for MV System (TPU 6x.xx) <https://library.e.abb.com/.../TPU>
- [67] J. Rohan Lucas, “Representation of Magnetisation Curves over a wide region using a non-integer power series,” *IJEEE: Manchester Univ. Press, vol. 25, No 4, pp. 335-340, Oct. 1988.*
- [68] Power System Protection. Volume 4: Digital Protection and Signaling, *The Electricity Training Association, Institution of Electrical Engineers, U.K., 1995.*
- [69] E. O. Schweitzer, and Stanley E. Zocholl, ‘Introduction to Symmetrical Components’ Schweitzer Engineering Laboratories, Inc. *8th Annual Georgia Tech Protective Relaying Conference, April 2004*
- [70] *SIPROTEC 4 Differential Protection 7SD52 v4.1 Manual*, Siemens AG, Nuremberg, Germany, Sep. 2009.
- [71] J. Roberts and E. O. Schweitzer, ‘Limits to the Sensitivity of Ground Directional and Distance Protection.’ Schweitzer Engineering Laboratories, Inc., *Spring Meeting of the Pennsylvania Electric Association Relay Committee Allentown, Pennsylvania May 15–16, 1997*

APPENDIX A

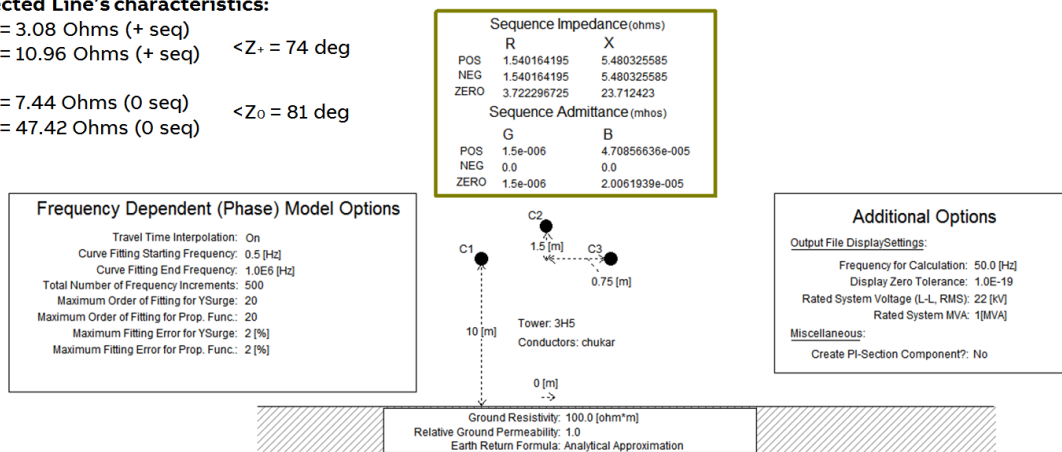
A.1 - Distribution Line Characteristics

The frequency dependent model based on distributed PLC traveling wave principle is available in PSCAD/EMTDC. Since the transient-based method utilizes the traveling waves information to correctly determine fault location, therefore the accuracy and robustness of PSCAD’s model is extremely relevant for this study.

Protected Line’s characteristics:

- R = 3.08 Ohms (+ seq)
- X = 10.96 Ohms (+ seq) $Z_+ = 74 \text{ deg}$

- R = 7.44 Ohms (0 seq)
- X = 47.42 Ohms (0 seq) $Z_0 = 81 \text{ deg}$



A.1 - Source Characteristics

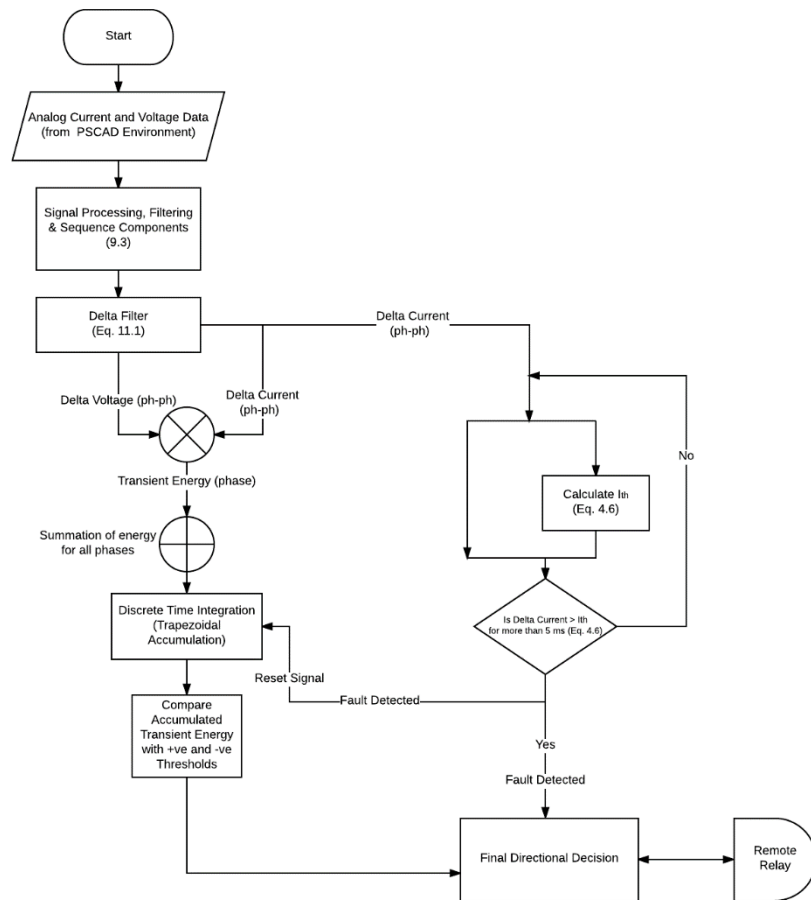
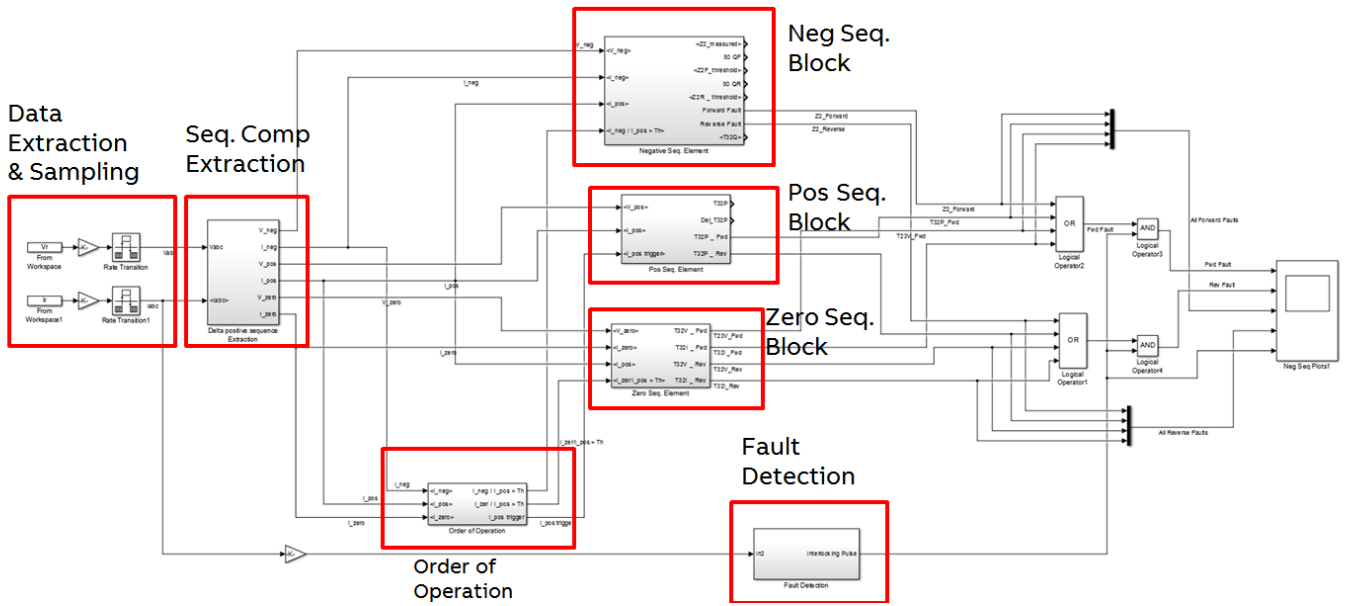
Network Characteristics	
Source Impedance Type	R - R L
MVA	100
L-L Voltage	22.0 kV
Frequency	50 Hz
Positive Seq. Impedance	15.732 < 86.3 *
Zero Seq. Impedance	127 < 20 *

DG Characteristics	
Source Impedance Type	R - R L
MVA	100
L-L Voltage	22.0 kV
Frequency	50 Hz
Positive Seq. Impedance	15.732 < 86.3 *
Zero Seq. Impedance	127 < 20 *

* These characteristics represent a strong source for the test system. Table 9-3 can be referred for variation in these characteristics for source strength tests.

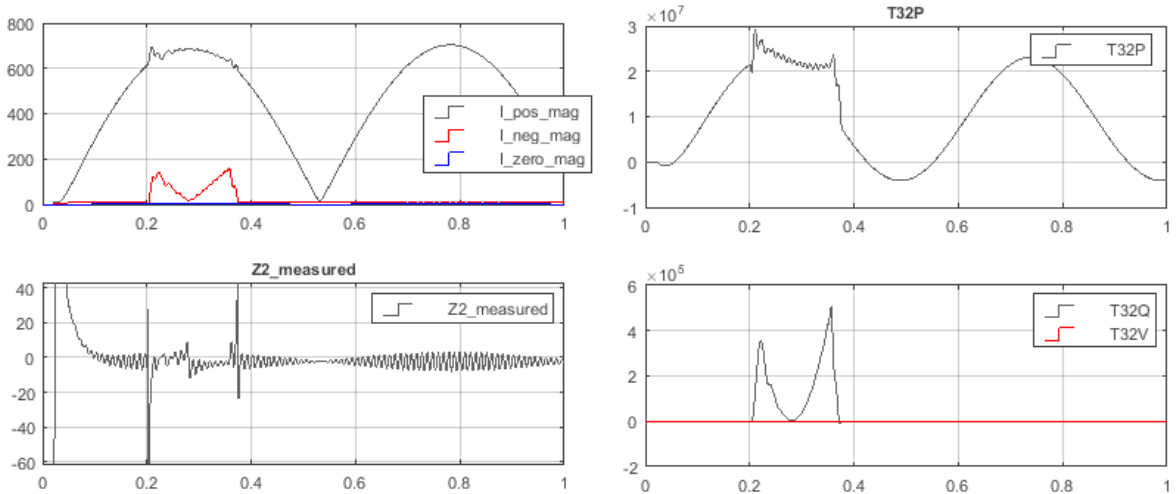
APPENDIX B

Simulink Block Diagram and Flowchart for Combined Conventional Directional Model



Impact of Power Swings on Combined conventional directional protection

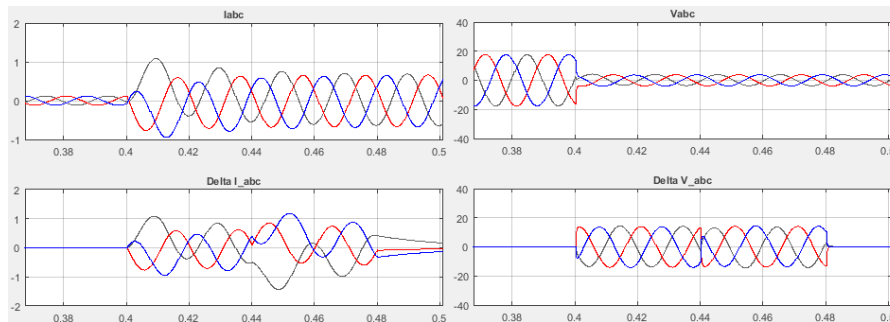
L-G Fault at 0.2 seconds - Sequence Currents (top-left), Negative Sequence Impedance (bottom-left), Positive Sequence Torque (top-right), Negative and Zero Sequence Torques (bottom-right).



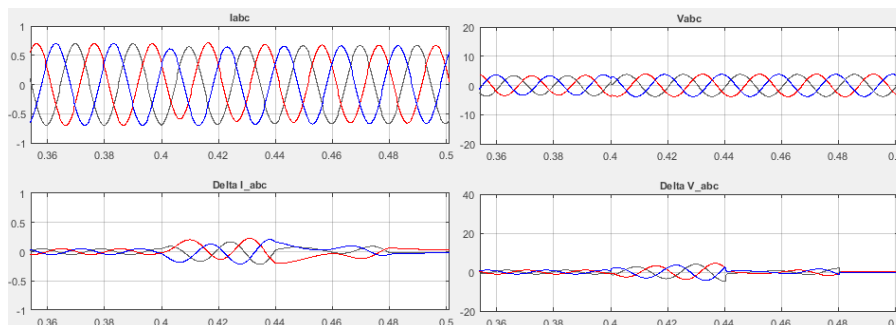
APPENDIX C

Delta Filter's Response for 3-phase faults

L-L-L Fault (Top: Three phase signals) (Bottom: Three Phase Delta quantities). Fault Incepted at 0.2 seconds

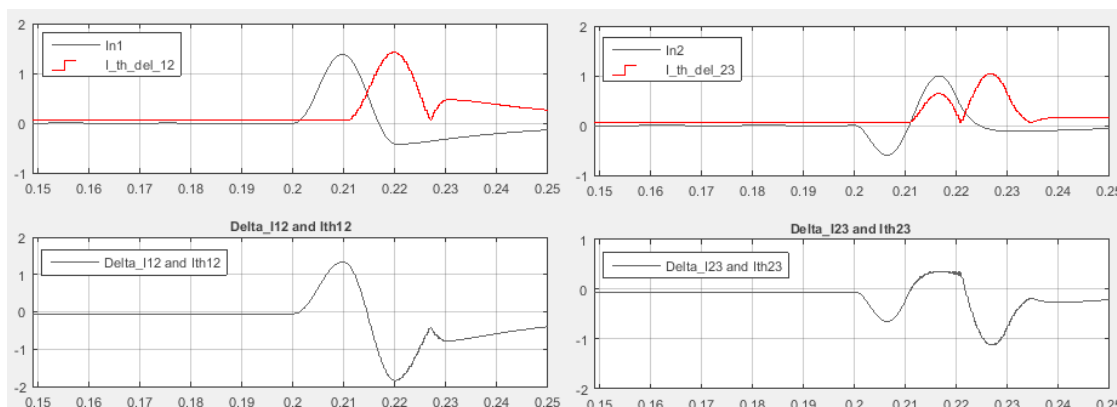


L-L-L Fault during Power swings (Top: Three phase signals) (Bottom: Three Phase Delta quantities). Fault Incepted at 0.2 seconds

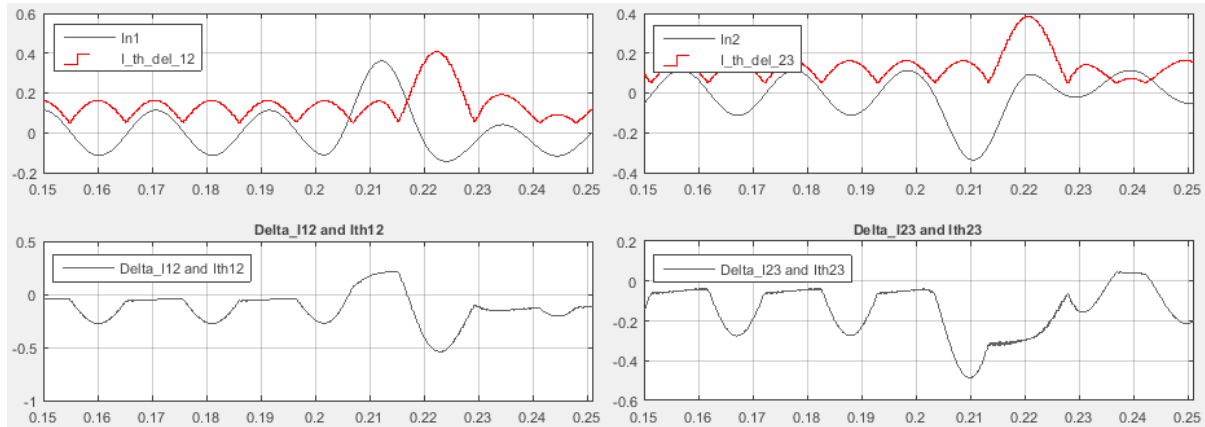


Adaptive Fault Detector's Response for 3-phase faults

L-L-L Fault (Top: Real time current and Threshold current) (Bottom: Difference between threshold and real-time current) Left: Phase A, Right: Phase B



L-L-L Fault with Power Swings (Top: Real time current and Threshold current) (Bottom: Difference between threshold and real-time current) Left: Phase A, Right: Phase B



Response of Average-window to power swings

Comparison of Delta Filter output with Average Integral filter output (Line Energization, No Fault)

Top: 3-phase quantities, Middle: 3-phase Conventional Delta Filter output, Bottom: 3-phase Average Integral filter Output

